HYDRAULIC CONDUCTIVITY OF ARTERIAL ENDOTHELIAL CELL AND SMOOTH MUSCLE CELL COCULTURES

by

RISHI A. MATHURA

A dissertation submitted to the Graduate Faculty in Biomedical Engineering in partial fulfillment of the requirements for the degree of Doctor of Philosophy, The City University of New York

2012

This manuscript has been read and accepted for the
Graduate Faculty in Biomedical Engineering in satisfaction of the
dissertation requirement for the degree of Doctor of Philosophy.

John M. Tarbell

_____ _____

Chair of Examining Committee Date

Thesis Adviser

CUNY and Wallace Coulter Distinguished Professor of Biomedical Engineering

Biomedical Engineering Department Chair

City College of New York/CUNY

Ardie D. Walser

_____ _____

Executive Officer Date

Dean of Graduate Studies

Bingmei Fu, Ph.D., Professor of Biomedical Engineering, CCNY

Sihong Wang, Ph.D., Assistant Professor of Biomedical Engineering, CCNY

Luis Cardoso, Ph.D., Associate Professor of Biomedical Engineering, CCNY

Supervisory Committee

THE CITY UNIVERSITY OF NEW YORK

ABSTRACT

HYDRAULIC CONDUCTIVITY OF ARTERIAL ENDOTHELIAL CELL AND SMOOTH MUSCLE CELL COCULTURES

by

Rishi A. Mathura

Adviser: John M. Tarbell, Ph.D.

This research investigates the hydraulic conductivity (L_p) of cocultured arterial endothelial cells (ECs) and smooth muscle cells (SMCs) exposed to pressure-driven transmural flow. Homotypic and heterotypic cellular interactions are explored through monoculturing and coculturing of bovine aortic ECs and SMCs. It is hypothesized that cocultured ECs and SMCs will have significantly different transport properties than ECs alone. This thesis is the first to examine L_p of arterial cocultures in the presence of physiological convective transmural flow.

Chapter 1 provides a general introduction to the arterial wall and reviews previous work on endothelial transport. Chapter 1 also provides a review of various EC-SMC coculture constructs and concludes with a description of specific aims that are proposed for the study of arterial coculture L_p.

Chapter 2 reports on the L_p of EC-initiated cocultures that were constructed on porous membranes. Hydraulic conductivities of these cocultures were lower than the L_p of monocultured ECs. Monoculture resistances-in-series modeled coculture L_p values were also compared to actual coculture L_p values to distinguish the presence of heterotypic interactions in coculture. Immunofluorescence staining of VE-cadherin and morphometric analysis of these

images revealed that ECs in the EC-initiated cocultures can have an elongated morphology compared to ECs in monoculture. Serum content in media was also shown to have a significant influence on EC L_p. EC-initiated cocultures on opposing sides of the porous membrane were used to mimic the EC-SMC arrangement in a normal vessel wall and produced one of the lowest L_p values that is reported in the literature.

Chapter 3 reports on the L_p of several SMC-initiated cocultures that were constructed on porous membranes. Hydraulic conductivities of these cocultures tended to be higher than the L_p of monocultured ECs. Monoculture resistances-in-series modeled coculture L_p values were also compared to actual coculture L_p values to distinguish the presence of heterotypic interactions in coculture. Immunofluorescence staining of VE-cadherin and morphometric analysis of these images revealed that ECs in the SMC-initiated cocultures can have a rounded morphology compared to ECs in monoculture. SMC-initiated cocultures that were configured on the luminal side of the porous membrane mimic the arrangement of ECs and SMCs in diseased states, such as intimal hyperplasia and atherogenesis, and produced a significantly higher L_p than ECs alone.

Chapter 4 reports on L_p of ECs in monoculture and coculture formats that have been exposed to transmural media flow. A transmural media flow apparatus was developed to interface with cultures on porous membranes. Endothelial cells in monoculture and shared-media cocultures with SMCs were exposed to 48 hours of transmural flow. Hydraulic conductivity of ECs that were exposed to transmural flow produced a higher L_p, which was not significant, compared to the L_p of ECs that were cultured in static media. Also, L_p of ECs derived from cocultures that were exposed to 48 hours of transmural flow was similar to the L_p of ECs from cocultures in static media.

Arterial coculture configurations have produced a wide range of L_p values. Hydraulic conductivity in cocultures which mimic the EC-SMC arrangement in normal vasculature is lower than EC alone while the L_p in cocultures modeling the EC-SMC arrangement in diseased states can be higher than EC alone. These variations in L_p are linked to the methods of coculturing that were used, and indicate the importance of serum content, inoculation order, culture time, and the proximity between ECs and SMCs. In general, EC-SMC coculturing produces more realistic arterial wall environments for the study of arterial transport.

ACKNOWLEDGEMENTS

I would like to thank Dr. Tarbell for his consistent mentorship throughout this research endeavor. I would like to thank Jeffery Garanich for his invaluable contributions to teaching me the fundamentals of culturing vascular cells. I would like to thank Limary Cancel for teaching me how to culture and immunostain endothelial cells, and how to operate the bubble tracking apparatus and tracking software used to calculate water flux and hydraulic conductivity. I would like to thank Severine Mouraud for her assistance with hydraulic conductivity experiments that involved shared-media cocultures. I would also like to thank my fellow graduate research assistants for their general support in the Cardiovascular Dynamics and Biomolecular Transport Laboratory. Funding for this work was provided by National Heart, Lung, and Blood Institute Grant HL57093. On a much more personal note, I would like to thank my mother, Patsy Mathura, for her loving support and invaluable words of wisdom. I would like to thank my father, Awadh Mathura, for his love and inspiration. I would also like to thank my siblings Avinash, Nalini, and Shiva Mathura for their encouragement. Finally, I would like to thank my wife, Crystal Mathura, for her unconditional love and support throughout this chapter in our lives.

TABLE OF CONTENTS

LIST OF TABLES

LIST OF FIGURES

CHAPTER 1

GENERAL INTRODUCTION

The endothelium is a dynamic multi-functioning monolayer that forms the blood-tissue interface throughout the vascular network. Endothelial cells are actively involved in vasoreactivity, inflammatory responses, resistance to clot formation, permeability function, the oxidation of LDL and much more[17]. These endothelial functions contribute to overall blood vessel health. Endothelial cells serve as key regulators of vessel function by coordinating multiple endocrine, paracrine, autocrine, and hemodynamic stimuli.

The vascular wall is exposed to a range of hemodynamic forces, which include fluid shear stress, transmural pressure, and circumferential wall strain. Local vascular structure can dictate variations in hemodynamic forces, which influence the function of normal and diseased endothelium. Both the embryologic origin of endothelial cells and local environmental stimuli (Figure 1.1), such as fluid forces, give rise to variations in endothelial cell phenotype[26].

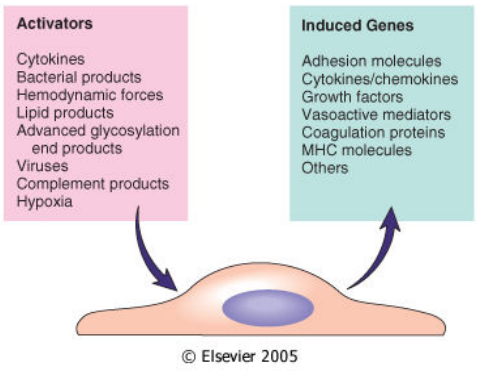

Figure 1.1. Endothelial cell gene expression is influenced by a variety of environmental stimuli[17].

Garcia-Cardena et al.[13] exposed cultured human umbilical vein endothelial cells to laminar or disturbed flow shear stress and found that endothelial gene expression was altered. Up-regulation and down-regulation of the transcriptional activity of 11,397 genes was unique for endothelial cells exposed to either 10 dyn/cm^2 of steady laminar fluid shear stress or disturbed flow shear stress. This demonstrates that endothelial cell phenotype is influenced by changes in fluid shear stress.

Endothelium-regulated vasoreactivity reveals one way that hemodynamic forces and heterotypic interactions between endothelial cells and underlying smooth muscle cells are linked. Endothelial cells secrete nitric oxide (NO) through a cascade of molecular interactions in response to stimuli such as acetylcholine, cytokines, and fluid shear stress. In turn, nitric oxide can stimulate smooth muscle cells to relax, which leads to vessel dilation.

Endothelial-regulated vasoreactivity is essential for blood vessel function and illustrates the endothelial tissue response to local fluid forces and heterotypic interaction with smooth muscle cells. Alterations in fluid shear stress at the vessel wall can also indicate disease-prone regions of the vasculature.

Low wall shear stress can alter endothelial function and promote atherosclerosis in sections of the vascular wall. Curved and branched regions of arterial vessels such as the aortic arch, carotid arteries, and coronary arteries are typical atherosclerotic sites. In particular, atherosclerosis originates along the outer region of the branched vessel (Figure 1.2) where the wall shear stress is low compared to inner wall regions[7].

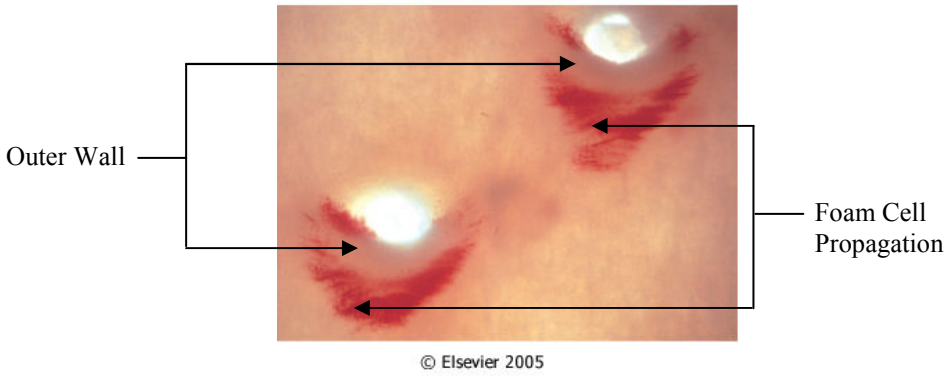

Figure 1.2. Fatty streaks in the aorta of an experimental hypercholesterolemic rabbit. Flow is from bottom to top. Foam cells are shown to propagate in the outer portion of branched vessel ostia[17].

Atherosclerosis is a dynamic and progressive disease affecting large arteries (Figure 1.3). During atherosclerotic development, increased endothelial permeability allows for LDL uptake, followed by leukocyte extravasations and the transport of growth factors such as platelet-derived growth factor (PDGF) and fibroblast growth factor (FGF) into the vascular wall. Subsequently, smooth muscle cells migrate and proliferate from the medial layer into the intima and contribute to vascular wall remodeling. In particular, altered endothelial permeability is coupled with heterotypic rearrangements of endothelial cells and smooth muscle cells during this disease process.

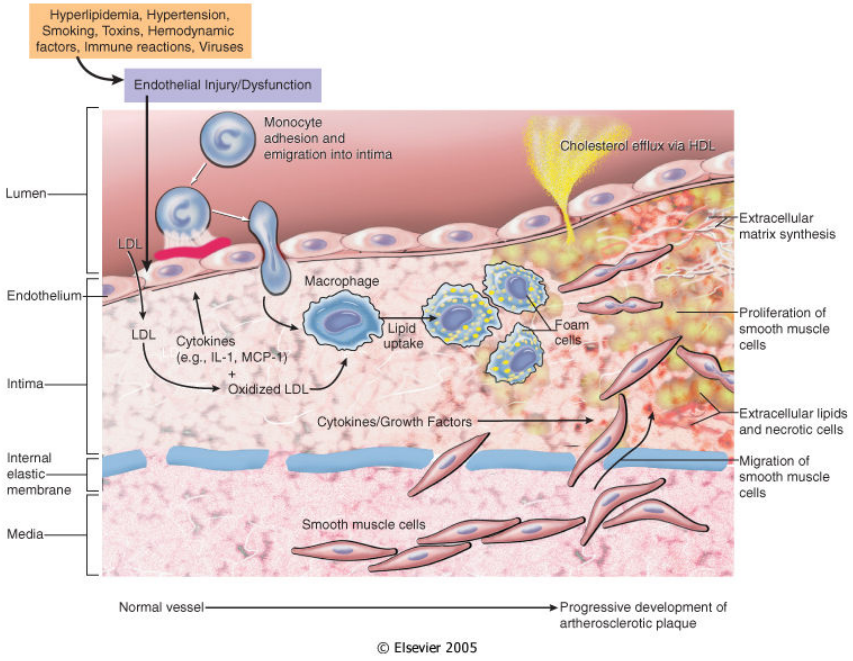

Figure 1.3. Sequence of cellular interactions during the pathogenesis of atherosclerosis[17].

Smooth muscle cells form a fibrous cap (Figure 1.4) directly below the endothelium, and both white blood cells and smooth muscle cells oxidize low density lipoprotein. The lesion progresses to form a thick intimal layer, which limits the diffusion of nutrients to subintimal tissue. In this case of a fibrous cap formation, endothelial cells and smooth muscle cells are in close proximity to each other and the influence that this direct heterotypic interaction has on arterial permeability function remains unclear.

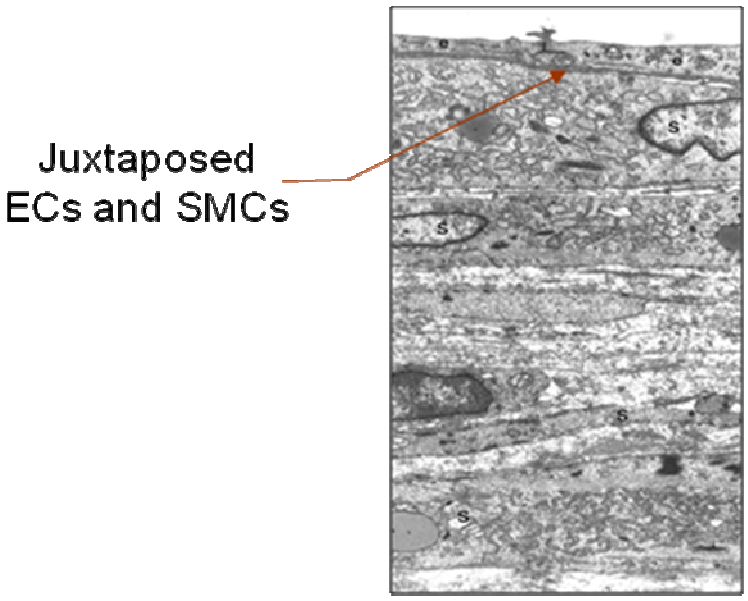

Figure 1.4. Electron micrograph of a fibrous cap formation developing in an atheromatous plaque in the blood vessel intima showing adjacent layers of smooth muscle cells (s) just below the endothelial cell surface (e). Smooth muscle cells form direct contact with the endothelium[24].

Low density lipoprotein accumulation in subendothelial regions of arterial vessels is a salient feature of atherosclerosis. In addition, leukocyte extravasations and intimal hyperplasia lead to further intimal thickening as the disease matures. Significant vascular wall remodeling may lead to ischemia, thrombosis, vessel occlusion, and myocardial infarction. Remarkably, the endothelium remains intact during the pathogenesis of atherosclerosis while blood-derived transendothelial transport of low density lipoproteins, leukocytes, and cytokines is up regulated. Therefore, endothelial permeability is a key modulator of arterial disease.

Convective luminal mass transport across the aortic endothelium is driven by a transmural pressure gradient. The influence of aortic heterotypic activity and convective luminal mass transport on aortic hydraulic conductivity function is unknown, and is the focus of this dissertation.

Endothelial cell-smooth muscle cell cocultures will be utilized with a variety of manipulations, which include altering the cell inoculation order, proximity, serum content, and culture time. Morphometric analysis will be conducted using immunofluorescent VE-cadherin expression and localization in endothelial cells. A novel pumping apparatus will also be developed to explore continuous transmural media perfusion effects on endothelial transport. Cultured bovine aortic endothelial and smooth muscle cells will then be exposed to hydrostatic pressure-driven transmural flow and aortic hydraulic conductivity will be measured through the use of a bubble tracking apparatus.

1.1 Intercellular Junctions of Endothelial Cells

Lateral protein complexes (Figure 1.5) are located on the outer leaflet of endothelial plasma membranes and limit the diffusion of membrane proteins and lipids from the apical side to the basal side. Selective endothelial permeability results from the adhesion of these lateral protein complexes. From the basal to apical direction, these adhesion complexes include adherens junctions, and tight junctions. The "kissing points" of adherens junctions can be as small as 15-20 nm apart[30].

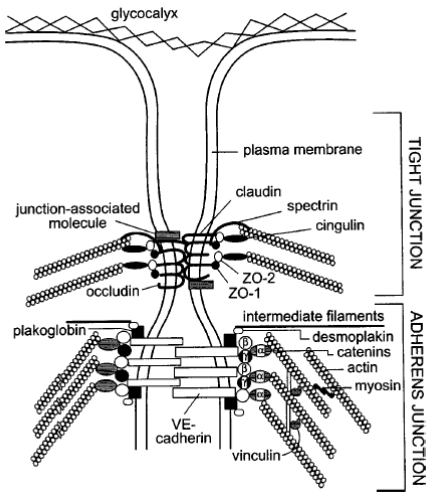

Figure 1.5. Adhesion of lateral protein complexes between endothelial cells. Tight junctions form the most apical adhesion site followed by adherens complexes. Localized membrane proteins provide a means for communication between intercellular junctions and the cytoplasm[28].

However, the circumferential weave of tight junction protein strands (Figure 1.6) actively polymerizes and de-polymerizes to restrict paracellular transport of ions and water-soluble molecules through channels as small as 3 nm wide[32]. The quantity of tight junction strands and their polymerization activity influences the selective permeability of an endothelial monolayer[30]. The efficiency at which the endothelium restricts paracellular transport correlates to the activity of lateral adhesion complexes[2]. Endothelial tissue maintains or restores its permeability even

during periods of endothelial cell turnover, leukocyte and plasma extravasations, and wound healing[11]. Healthy blood vessels utilize routine cell turnover to maintain vessel integrity.

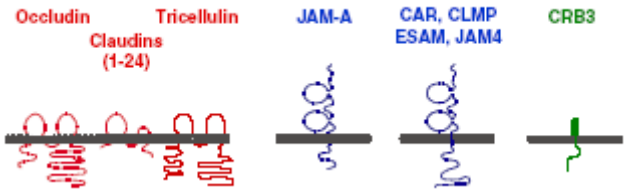

Figure 1.6. Tight junction membrane proteins. Occludin, claudins, and tricellulin have two cytoplasmic tails. The second class of proteins contains two Ig-like domains, and the third class contains a short extracellular domain[11].

During cell turnover, apoptosis and mitosis cause remodeling of lateral adhesion complexes, which modify the selective transport across an endothelium. The widening of intercellular junctions during apoptosis and mitosis create "leaky junctions" that can cause an increase in endothelial permeability to LDL[5, 6] and other large solutes. Additionally, increases in endothelial cell apoptosis and mitosis occur in regions of low wall shear stress. Atherosclerotic prone vascular regions, having a characteristic low wall shear stress, imply that cell turnover generates a leaky pathway for low density lipoprotein transport across an intact endothelium[28].

1.2 Endothelial Permeability Studies

Baetscher and Brune[1] measured transmural flow rates across porcine aortic endothelial cells cultured on a porous substrate. Endothelial hydraulic permeability was observed to decrease within 1-3 hours while being exposed to a flow that was driven by a constant hydrostatic pressure gradient of 20 mmHg. This phenomenon of decreasing endothelial hydraulic permeability in response to constant pressure-driven flow was termed the "sealing effect".

Turner[31] performed simultaneous measurements of hydraulic permeability and transendothelial electrical resistance across bovine arterial endothelial cells using a modified Ussing chamber (Figure 1.7). Bovine arterial endothelial cells were cultured on porous substrates and transmural flow was driven by a constant hydrostatic pressure gradient of 30-35 cmH_2O. Transendothelial electrical resistance was measured by using an Agar bridge that passed electrical current across an endothelial monolayer. Hydraulic permeability results were derived from measuring transmural flow rates and showed a characteristic sealing effect while transendothelial electrical current flow measurements were shown to increase. The author suggested that the contradiction of decreasing hydraulic permeability and increasing electrical current flow may be due to mechanically compressing the endothelial monolayer against its support with fluid pressure, rather than a biological response from endothelial cells. However, prolonged measurement of electrical resistance causes ions to accumulate on one side of the Agar bridge that can give the impression of increasing electrical current flow. In contrast to the accumulation of ions on one side of the endothelial culture, a constant fluid pressure allows for the clearance of effluent transmural flow across endothelial cells.

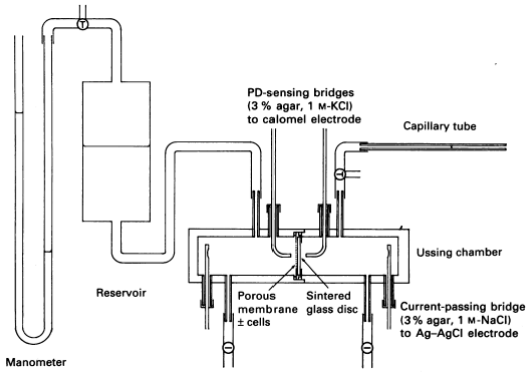

Figure 1.7. Modified Ussing chamber used to measure simultaneous hydraulic permeability and transendothelial electrical resistance across cultured endothelial cells[31].

DeMaio et al.[10] confirmed that during the sealing effect cultured bovine aortic endothelial cells could display a biological response. A constant 10 cmH_2O hydrostatic pressure gradient was used to drive transmural flow across the endothelial cultures. The localization of zonula occludin-1 (ZO-1) to the intercellular junctions was shown to be increased after sealing. Furthermore, hydraulic conductivity as well as albumin and 70 kDa Dextran permeability were measured during the sealing response. In each case, there was a decrease in hydraulic and effective solute permeability. The localization of ZO-1 to the intercellular region following sealing demonstrates that endothelial cells produce a biological response to sustained pressure-driven transmural flow.

Kim et al.[16] used a micro-perfusion technique to measure transvascular filtration and hydraulic conductivity in arterioles and venules. A step change in transvascular pressure from 20 mmHg to 40 mmHg caused an initial jump in hydraulic conductivity in both arterioles and venules with arterioles having a lower increase than venules. However, as the step change in pressure was sustained, a gradual decrease in hydraulic conductivity was observed. An initial increase in hydraulic conductivity suggests that there is a mechanical response to increased pressure but the

gradual decrease in hydraulic conductivity in the presence of a constant pressure supports the presence of a sealing effect in intact vessels.

Muller-Marschhausen and Drenckhahn[21] showed that hydrostatic pressure was necessary to maintain microvascular myocardial endothelial cell and pulmonary artery endothelial cell monolayer integrity. In this application of hydrostatic pressure, convective transport was prevented by culturing endothelial cells on impermeable substrates. Pharmacological agents known to alter endothelial integrity were introduced to endothelial cultures that were exposed to a hydrostatic pressure of 15 cmH_2O or 0 cmH_2O. In cases where hydrostatic pressure was present, the effect of pharmacological agents intended to deplete VE-cadherin were blocked and monolayer integrity was maintained. Without hydrostatic pressure, VE-cadherin was lost at intercellular junctions. This study showed that hydrostatic pressure was an important driving force for endothelial integrity.

Cancel et al.[4] examined the permeability of water, 70 kDa Dextran, and low density lipoprotein under convective conditions. This was the first in vitro study on the effective permeability of an endothelial monolayer to low density lipoprotein in the presence of convective transport. Leaky junctions resulting from cell turnover were suggested to be one avenue of low density lipoprotein transport across an intact endothelial monolayer. A bubble tracking apparatus equipped with fluorescence detection was used to make endothelial permeability measurements. Vesicle and paracellular transport were shown to allow low density lipoproteins to cross endothelial cultures. However, pore models accounting for breaks in tight junctions and leaky junctions revealed that leaky junctions were major pathways for low density lipoproteins to cross an endothelial monolayer exposed to convective transport.

Lee et al.[20] examined the permeability across the aortic walls of mice where low density lipoprotein accumulation progressed to form atherosclerotic lesions. Horseradish peroxidase tracer molecule was injected into the veins of mice and concentration profiles were measured across the wall of atherosclerotic lesions. Permeability was reported to increase as intimal thickness increased and as age increased from five months to twelve months. Both the atherosclerotic region undergoing remodeling and the permeability change suggest that atherosclerotic development is dynamic and intimately linked to changes in transport across the vascular wall.

1.3 Smooth Muscle Cells, Extracellular Matrix, and Interstitial Fluid Flow

Aortic tissue acquires additional complexity due to the presence of subendothelial vascular smooth muscle cells. Vascular smooth muscle cells are normally sequestered in an extracellular matrix of collagen, elastin, and proteoglycans and add stability to the vessel structure. Smooth muscle cells function in response to autocrine and paracrine stimuli, as well as environmental stimuli, such as hemodynamic forces. In addition to their vasoreactive contributions, vascular smooth muscle cells are intimately involved in vascular remodeling during myogenesis, wound healing, intimal hyperplasia, and atherosclerosis development. Smooth muscle cells are capable of migrating, regulating cell turnover, and remodeling extracellular matrix components[3].

Wang and Tarbell[37] showed that pressure-driven interstitial fluid flow elicited biochemical responses from rat aortic smooth muscle cells suspended in collagen gel. Hydrostatic pressure of 90 cmH_2O generated interstitial fluid shear stress of 1 dyn/cm^2 on smooth muscle cells in a 3D gel model. Enzyme-linked immunosorbent assays of effluent media showed that interstitial fluid shear stress increased the production of prostaglandin E_2 and prostaglandin I_2 compared to controls (no flow). Proliferation of smooth muscle in 3D models was lower than that of smooth muscle cells in a 2D model. 3D gel models also supported the quiescent phenotype of smooth muscle cells typically found in native blood vessels.

Interstitial fluid flow also interfaces with the internal elastic lamina and extracellular matrix components, which can indirectly influence vascular smooth muscle cell function. Interstitial fluid flow imposes tensile, compressive, and shearing forces on extracellular matrix components, which can be attached to smooth muscle cells via integrin receptors[25]. Solan et al.[23] showed that a pulsatile interstitial fluid flow altered the composition of extracellular matrix by causing smooth muscle cells to produce matrix metalloproteinase-1. The effects of interstitial fluid flow

and an extracellular matrix on smooth muscle cell function demonstrate the influence of combined tissue-like features on blood vessel function.

The presence of a fenestrated internal elastic lamina (IEL) also channels interstitial fluid flow. For the proposed aortic hydraulic conductivity study, a porous internal elastic lamina will be represented by a porous polyester (PET) membrane having pore diameters (d) and a porous area fraction (f) within range for a normal internal elastic lamina (Table 1.1).

Table 1.1. Comparison of native internal elastic lamina and porous polyester (PET) membrane. The pore diameter and porous area fraction of PET membrane[29] are within the range of pore diameters and porous area fractions of a native internal elastic lamina[27].

Parameter	**IEL**	**PET Membrane**
Pore diameter (d_{IEL})	0.4 – 4 μm	0.4 μm
Porous area fraction (f_{IEL})	0.001-0.036	0.009

1.4 Coculture Constructs

1.4.1 Compartmental Coculture Constructs

Kurzen et al.[18] performed endothelial permeability assays and immunofluorescence staining of lateral adhesion proteins in cocultures of endothelial cells and smooth muscle-like 10T1/2 cells. The goal of this study was to examine how subendothelial 10T1/2 cells contribute to the tightening of EC-EC junctions during the end stage of angiogenesis where solute transport from blood to tissue becomes more selective. Human umbilical vein endothelial cells (HUVECs) were cocultured with smooth muscle-like 10T1/2 cells, with 10T1/2 cells seeded first, for 8 days on opposite sides of Transwell filters (0.4 um pores) at a HUVEC:10T1/2 cell seeding density ratio of 2:1. Biotin-dextran (70 kDa) was added to the top well and aliquots were collected from the bottom well after 3 hours. Controls were monocultures of either HUVECs grown on the top of the filter or 10T1/2 cells grown on the bottom of the filter. Cocultures of HUVECs and 10T1/2 cells were reported to have a higher barrier to biotin-dextran (70 kDa) than both HUVEC and 10T1/2 monoculture controls. Diffusive permeability of biotin-dextran in cocultures was reduced by 32% and 63%, when compared to monocultures of HUVECs and 10T1/2 cells, respectively. Immunofluorescence of occludin was also shown to increase at the EC-EC contacts when endothelial cells were cocultured with 10T1/2 cells. Improved endothelial permeability and increased occludin expression suggests that 10T1/2 cells contribute to the tightening of endothelial cell junctions and maintaining permeability function. This study provides a snapshot of how coculture can influence endothelial permeability. However, the effect of coculture on endothelial permeability with transmural flow was not examined.

Vouyouka et al.[33, 34] cocultured rat aortic endothelial and smooth muscle cells for 5 days in the presence of either high pressure or ambient pressure (Figure 1.8) with control cultures being

smooth muscle cells cultured in ambient pressure. Cocultures in chronic high pressure (130 mmHg) had the effect of reducing smooth muscle cell proliferation, compared to cocultures exposed to ambient pressures. However, the pressurized scenario did not produce transmural flow and smooth muscle cells were grown on the surface of the abluminal well. This study showed that smooth muscle cell function can be modulated by coculturing in shared media and with pressurized conditions.

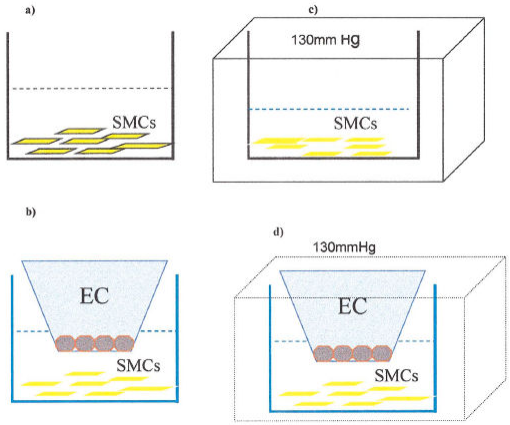

Figure 1.8. Schematic of coculture apparatus designed to create a pressurized environment for cocultures of endothelial cell and smooth muscle cells[34].

Davies et al.[9] conducted a compartmental coculture study which demonstrated that cell-secreted factors influence aortic smooth muscle cell metabolism of low density lipoprotein. A monolayer of aortic endothelial cells was grown on microcarrier beads and separated from smooth muscle cells by a distance of 0.5 to 1 mm (Figure 1.9). Secreted factors were again capable of traveling a short distance through shared culture media. Here again soluble factors stimulated the growth of smooth muscle cells. The number of high affinity low density lipoprotein receptors doubled as a result of coculture and was dependent on the seeding density of cells with the highest number of receptors occurring when the ratio of endothelial cells to smooth muscle cells was 1:1. Coculture has the potential of revealing the influence of heterotypic interactions. This coculture

model showed that a more active environment was created by having endothelial and smooth muscle cells grown in close proximity to one another.

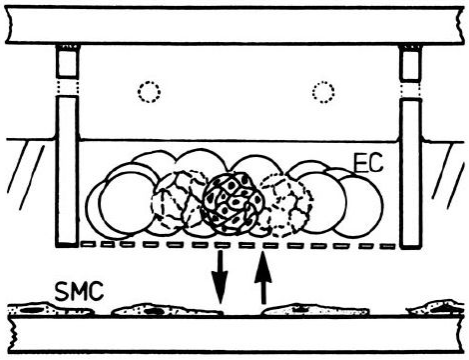

Figure 1.9. Coculture model that prevents direct interaction of endothelial cells and smooth muscle cells. Cell-secreted factors are capable of traveling a distance (0.5 – 1 mm) from the microcarrier to the smooth muscle cell layer[9].

In-vivo, blood flow can impose fluid forces on the vessel wall such as shear stress, pressure, and strain. Hsiai[15] provides a review of the mechanotransducing effects of hemodynamic forces in cocultures of endothelial cells and smooth muscle cells. Chiu et al.[8] incorporated fluid shear stress (12 dyn/cm^2) in a compartmental coculture of human umbilical chord endothelial cells and smooth muscle cells (Figure 1.10). In static cocultures, smooth muscle cells induced endothelial cell gene expression of adhesion molecules and attenuated endothelial gene expression of endothelial nitric oxide synthase (eNOS). In the presence of fluid shear stress, adhesion molecule expression was inhibited. However, this study[8] did not measure or control transmural flow.

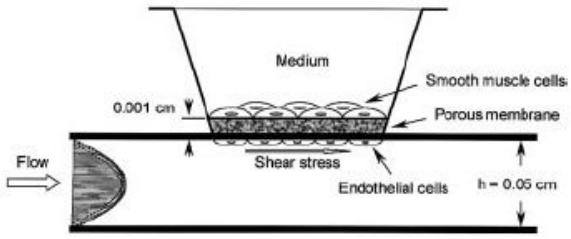

Figure 1.10. Schematic of a compartmental coculture apparatus designed to introduces fluid shear stress to endothelial cells[8].

It was essential to incorporate smooth muscle cells in close proximity to the endothelial cells in order to elicit those biological responses. In healthy arteries, endothelial and smooth muscle cells typically reside within a vessel wall thickness of 1 mm.

Compartmental coculture models allow for the transport of solutes across the coculture construct. It is also possible for smooth muscle cell processes that are closest to the filter to extend through individual pores and make contact with endothelial cells (Figure 1.11). In a normal vessel wall, intact smooth muscle processes are capable of contacting endothelial cells in a similar manner[22]. The possibility of generating direct endothelial-smooth muscle cell contacts is an added advantage of utilizing a bilayer compartmental model. Fillinger et al.[12] cocultured endothelial cells with smooth muscle cells for a maximum of 14 days and reported that the percent of smooth muscle cell projections making contact with endothelial cells increased as coculture time increased from 7 days to 14 days.

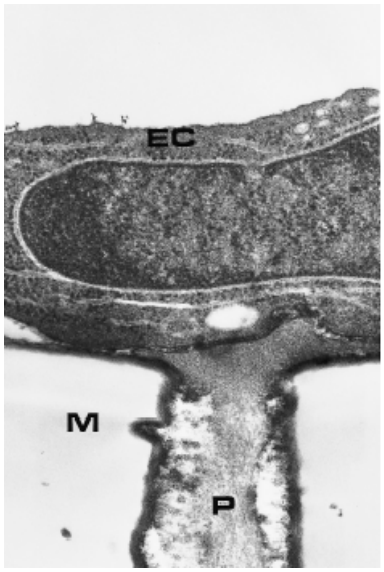

Figure 1.11. An electron micrograph of a bilayer compartmental coculture model showing that smooth muscle cell processes can extend across a 13 um thick membrane and contact endothelial cells[12].

1.4.2 Direct Coculture Constructs

Lavender et al.[19] and Wallace et al.[35, 36] developed direct coculture models (no intervening porous membrane) and examined the adhesion of porcine endothelial cells grown on smooth muscle cells. Smooth muscle cell phenotype was shown to alter endothelial adhesion. Endothelial cells attached better to quiescent smooth muscle cells than proliferative smooth muscle cells with lower passages of endothelial cells (passage 2-5) having better adhesion than higher passages. The adhesion of endothelial cells to smooth muscle cells is useful in engineering blood vessels, and was the motivation for these studies.

Direct contact between endothelial cells and smooth muscle cells has been shown to increase angiogenic factors in endothelial cells. Heydarkhan-Hagvall et al.[14] showed that human saphenous vein endothelial cells cocultured directly on smooth muscle cells for 3 days influenced the gene expression of angiogenic factors. The contact between endothelial cells and

smooth muscle cells caused higher gene expression of vascular endothelial growth factor (VEGF) in both endothelial cells and smooth muscle cells and a higher gene expression of platelet derived growth factor-BB (PDGF-BB), and transforming growth factor-B (TGF-B) in smooth muscle cells compared to monoculture controls.

1.5 Proposed Study of Hydraulic Conductivity for Arterial Cocultures

Pressure-driven transmural flow, heterotypic interactions, and cell phenotype all influence blood vessel function. The proposed coculture models will attempt to mimic these stimuli and assess the roles that they play in modulating arterial hydraulic conductivity. The specific aims of the study are:

Specific Aim 1: To determine the L_p of cocultures that are initiated by endothelial cell culture followed by smooth muscle cell culture. Bovine aortic endothelial cells will be plated on the luminal surface of a porous Transwell filter for 3 days followed by plating of smooth muscle cells on the abluminal surface for 2 days. In other experiments, the smooth muscle cells will be plated remotely on the surface of the companion well. The influence of media serum concentration will also be examined.

Specific Aim 2: To determine the L_p of cocultures that are initiated by smooth muscle cell culture followed endothelial cell culture. Smooth muscle cells will be plated on the luminal or abluminal surface of the filter for 6 days followed by plating of endothelial cells on the luminal surface for 5 days. In other experiments, the smooth muscle cells will be plated on the surface of the companion well. The influence of media serum concentration will also be examined.

Specific Aim 3: To determine the influence on L_p for long term exposure of endothelial cells and coculture to transmural flow. Endothelial cells will be plated on the luminal surface of a porous filter for 3 days followed by 2 days of transmural flow. In other experiments, 3 days of endothelial cell culture will be followed by plating smooth muscle cells on the surface of the companion well and 2 days of transmural flow. The influence of transmural flow rate will also be examined.

1.6 References

1. Baetscher M., and K. Brune. An in vitro system for measuring endothelial permeability under hydrostatic pressure. *Exp. Cell Res.* 148: 541-547, 1983.
2. Bazzoni G., and E. Dejana. Endothelial Cell-to-cell junctions: molecular organization and role in vascular homeostasis. *Physiol. Rev.* 84: 869-901, 2004
3. Berk B.C. Vascular smooth muscle growth: autocrine growth mechanisms. *Physiol. Rev.* 81: 999-1030, 2001.
4. Cancel L., A. Fitting, and J.M. Tarbell. In vitro study of LDL transport under pressurized (convective) conditions. *Am. J. Physiol. Heart Circ. Physiol.* 293: 126-132, 2007.
5. Cancel L.M., and J.M. Tarbell. The role of apoptosis in LDL transport through cultured endothelial cell monolayers. Atherosclerosis 208(2): 335-341, 2010.
6. Cancel L.M., and J.M. Tarbell. The role of mitosis in LDL transport through cultured endothelial cell monolayers. Am. J. Physiol. Heart Circ. Physiol. 300(3): H769-H776, 2011.
7. Caro C.G. Discovery of the role of wall shear in atherosclerosis. *Arterioscler. Thromb. Vasc. Biol.* 29: 158-161, 2009.
8. Chiu J., L. Chen, P. Lee, C. Lee, L. Lo, S. Usami, and S. Chien. Shear stress inhibits adhesion molecule expression in vascular endothelial cells induced by coculture with smooth muscle cells. *Blood* 101: 2667-2674, 2003.
9. Davies P.F., G.A. Truskey, H.B. Warren, S.E. O'Connor, and B.H. Eisenhaure. Metabolic cooperation between vascular endothelial cells and smooth muscle cells in coculture: changes in low density lipoprotein metabolism. *J. Cell Biol.* 101: 871-879, 1985.

10. DeMaio L., J.M. Tarbell, R.C. Scaduto, T.W. Gardner, and D.A. Antonetti. A transmural pressure gradient induces mechanical and biological adaptive responses in endothelial cells. *Am. J. Physiol. Heart Circ. Physiol.* 286: 731-741, 2004.
11. Ebnet K. Organization of multiprotien complexes at cell-cell junctions. *Histochem. Cell Biol.* 130: 1-20, 2008.
12. Fillinger M.F., L.N. Sampson, J.L. Cronenwett, R.J. Powell, and R.J. Wagner. Coculture of endothelial cells and smooth muscle cells in bilayer and conditioned media models. *J. Surg. Res.* 67: 169-178, 1997.
13. Garcia-Cardena G., J. Comander, K.R. Anderson, B.R. Blackman, and M.A. Gimbrone. Biomechanical activation of vascular endothelium as a determinant of its functional phenotype. PNAS 98: 4478-4485, 2001.
14. Heydarkhan-Hagvall S., G. Helenius, B.R. Johansson, J.Y. Li, E. Mattsson, and B. Risberg. Coculture of endothelial cells and smooth muscle cells affects gene expression of angiogenic factors. *J. Cell. Biochem.* 89: 1250-1259, 2003.
15. Hsiai T.K. Mechanosignal transduction coupling between endothelial and smooth muscle cells: role of hemodynamic forces. *Am. J. Physiol. Cell Physiol.* 294: 659-661, 2008.
16. Kim M., N.R. Harris, and J.M. Tarbell. Regulation of hydraulic conductivity in response to sustained changes in pressure. *Am. J. Physiol. Heart Circ. Physiol.* 289: 2551-2558, 2005.
17. Kumar V., A.K. Abbas, and N. Fausto. Unit II: Diseases of organ systems: blood vessels In Robbins & Cotran Pathologic Basis of Disease. 7th Edition. Saunders 2004.

18. Kurzen H., S. Manns, G. Dandekar, T. Schmidt, S. Pratzel, and B.M. Kraling. Tightening of endothelial cell contacts: a physiologic response to cocultures with smooth muscle-like 10T1-2 cells. *J. Invest. Dermatol.* 119: 143-153, 2002.

19. Lavender M.D., Z. Pang, C.S. Wallace, L.E. Niklason, and G.A. Truskey. A system for direct coculture of endothelium on smooth muscle cells. *Biomaterials* 26: 4642-4653, 2005.

20. Lee K., G.M. Saidel, and M.S. Penn. Permeability change of arterial endothelium is an age-dependent function of lesion size in apolipoprotein E-null mice. *Am. J. Physiol. Heart Circ. Physiol.* 295: 2273-2279, 2008.

21. Muller-Marschhausen K., and D. Drenckhahn. Physiological hydrostatic pressure protects endothelial monolayer integrity. *Am. J. Physiol. Cell Physiol.* 294: 324-332, 2008.

22. Ryan U.S., J.W. Ryan, and C. Whitaker. How do kinins affect vascular tone? Adv. Exp. Med. Biol. 120A: 375-391, 1979.

23. Solan A., V. Prabhakar, and L. Niklason. Engineered vessels: importance of the extracellular matrix. *Transplantation Proceedings* 33: 66-68, 2001.

24. Starry H.C., A.B. Chandler, R.E. Dinsmore, V. Fuster, S. Glagov, W. Jr. Insull, M.E. Rosenfeld, C.J. Schwartz, W.D. Wagner, and R.W. Wissler. A definition of advanced types of atherosclerotic lesions and a histological classification of atherosclerosis. Circ. 92(5): 1355-1374, 1995.

25. Stegemann J.P., H. Hong, and R.M. Nerem. Mechanical, biochemical, and extracellular matrix effects on vascular smooth muscle cell phenotype. *J. Appl. Physiol.* 98: 2321-2327, 2005.

26. Stevens T., R. Rosenberg, W. Arid, T. Quertermous, F.L. Johnson, J. Garcia, R.P. Hebbel, R.M. Tuder, and S. Garfinkel. NHLBI workshop report endothelial cell phenotypes in heart, lung and blood diseases. *Am. J. Physiol.* 281: 1422-1433, 2001.

27. Tada S., and J.M. Tarbell. Interstitial flow through the internal elastic lamina affects shear stress on arterial smooth muscle cells. *Am. J. Physiol. Heart Circ. Physiol.* 278: 1589-1597, 2000.

28. Tarbell J.M. Mass transport in arteries and the localization of atherosclerosis. *Ann. Rev. Biomed. Eng.* 5: 79-118, 2003.

29. Corning Life Sciences, Transwell permeable supports selection and use guide. CLS-CC-007W REV5.

30. Tsukita S., M. Furuse, and M. Itoh. Multifunctional strands in tight junctions. *Nature Reviews: Mol. Cell Biol.* 2: 285-293, 2001.

31. Turner M.R. Flows of liquid and electrical current through monolayers of cultured bovine arterial endothelium. *J. Physiol.* 449: 1-20, 1992.

32. Vandenbroucke E., D. Mehta, R. Minshall, and M.B. Malik. Regulation of endothelial junctional permeability. *Ann. NY Acad. Sci.* 1123: 134-145, 2008.

33. Vouyouka A.G, S.S. Salib, S. Cala, J.D. Marsh, and M.D. Basson. Chronic high pressure potentiates the antiproliferative effect and abolishes contractile phenotype changes caused by endothelial cells in cocultured smooth muscle cells. *J. Surg. Res.* 110: 344-351, 2003.

34. Vouyouka A.G., Y. Jiang, and M.D. Basson. Pressure alters endothelial effects upon vascular smooth muscle cells by decreasing smooth muscle cell proliferation and increasing smooth cell apoptosis. *Surgery* 136: 282-290, 2004.

35. Wallace C.S., J.C. Champion, and G.A. Truskey. Adhesion and function of human endothelial cells cocultured on smooth muscle cells. *Ann. Biomed. Eng.* 35: 375-386, 2007.

36. Wallace C.S., S.A. Strike, and G.A. Truskey. Smooth muscle cell rigidity and extracellular matrix organization influence endothelial cell spreading and adhesion formation in coculture. *Am. J. Physiol. Heart Circ. Physiol.* 293: 1978-1986, 2007.

37. Wang S., and J.M. Tarbell. Effect of fluid flow on smooth muscle cells in a 3-dimensional collagen gel model. *Arterioscler. Thromb. Vasc. Biol.* 20: 2220-2225, 2000.

CHAPTER 2

HYDRAULIC CONDUCTIVITY OF ENDOTHELIAL CELL-INITIATED ARTERIAL COCULTURES

2.1 Abstract

Vascular smooth muscle contributes to complex arterial wall functions. This study uses arterial smooth muscle cell (SMC) and endothelial cell (EC) cultures to measure arterial coculture hydraulic conductivity (L_p). We hypothesized that arterial coculture configurations would alter arterial L_p, compared to the L_p of SMC and EC monoculture controls. This research presents the first *in-vitro* observations of arterial coculture L_p, which includes EC-initiated coculture configurations. Bovine aortic smooth muscle cells (BASMCs) and bovine aortic endothelial cells (BAECs) were cocultured on Transwell Permeable Supports, with BAECs seeded first, and then exposed to a pressure-driven transmural flow. Hydraulic conductivity across each culture was measured by using a bubble tracking apparatus that determined water flux (J_v). Our results indicate that arterial L_p is significantly modulated by the proximity of BASMCs to BAECs on the porous membrane, and serum content in culture. The L_p of actual cocultures was also compared to the L_p results for series summations of hydraulic resistances of individual culture components to distinguish the contributions of real heterotypic culture compositions. Conditions that lead to significantly reduced coculture L_p, compared to BAEC monoculture controls, have been uncovered. Also, VE-cadherin immunostaining of intact BAEC monolayers in coculture and monoculture configurations identifies that EC-SMC proximity on a porous membrane has a dynamic influence on BAEC morphology patterns.

2.2 Introduction

Tissues consist of both homotypic and heterotypic cell configurations and, depending on the proximity of cells, communication may occur through soluble and contact-mediated pathways (Figure 2.1). Local mechanical and chemical signaling mechanisms are both essential for maintaining a tissue's structure and function. Intimal endothelial cells (ECs) and medial smooth muscle cells (SMCs) are neighboring cells in the arterial wall. Typical homotypic cell functions include contact-inhibited endothelial growth, and smooth muscle contraction, and the closer proximity of ECs and SMCs within the arterial wall yields heterotypic cell functions. This study examines, for the first time, whether heterotypic cultures of arterial ECs and SMCs influence arterial wall transport, specifically, hydraulic conductivity (L_p). In this article we report the L_p responses of EC-initiated arterial cocultures.

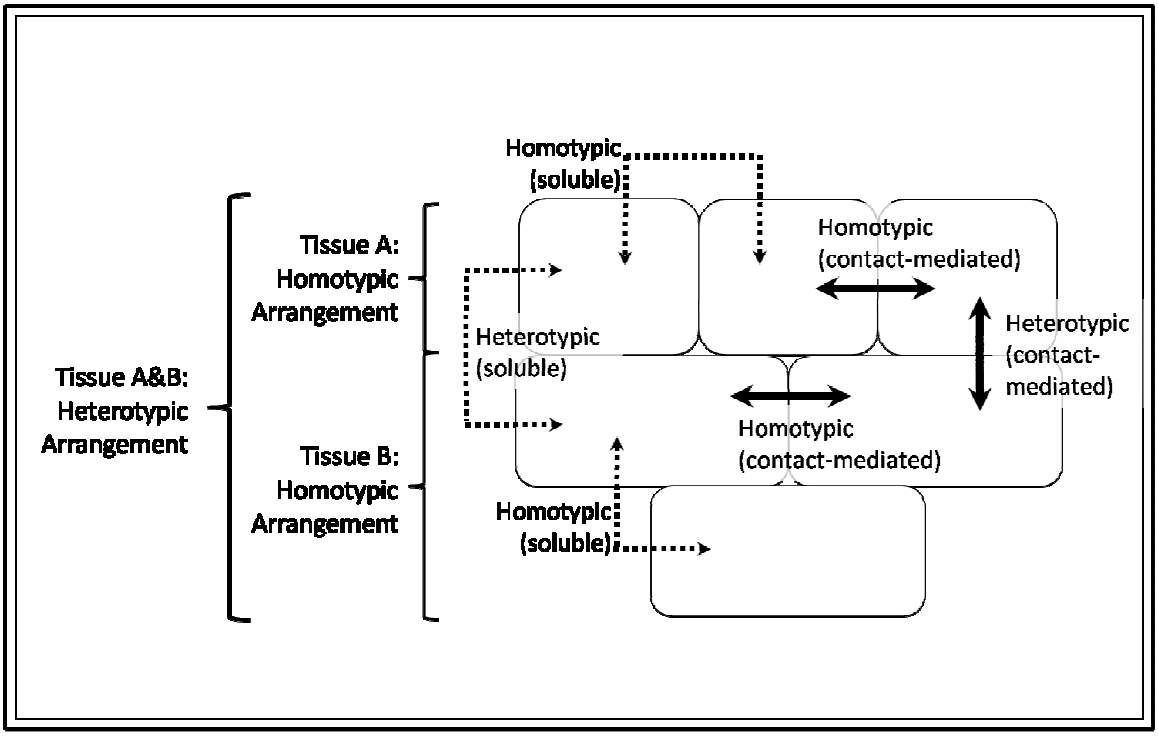

Figure 2.1. Homotypic and heterotypic arrangements of tissues A and B showing combinations of soluble (dashed arrows) and contact-mediated (continuous arrows) signal pathways for cell interactions. Double-sided arrows indicate that cell signaling is also bidirectional and reciprocal.

In-vivo, the order in which ECs and SMCs are established in the vessel wall, and the proximity between ECs and SMCs, varies with the event(s) that are taking place in the localized region of the vasculature. For example, during arteriogenesis, a heterotypic tissue structure develops as SMCs are recruited to form a dense sub-endothelial medial region near a preexisting intact endothelium [3, 8, 27, 32]. In healthy arterial walls, the porous internal elastic lamina is sandwiched between the intimal endothelium and a relatively dense medial region of SMCs[16]. Endothelial cells and SMCs can then establish direct heterotypic contacts by extending their cell processes through the pores of the internal elastic lamina[11, 17, 26].

Previous work with coculture systems[9, 14] has clearly demonstrated that ECs can influence SMC function. Coculturing bovine aortic endothelial cells (BAECs) and bovine aortic smooth muscle cells (BASMCs) on opposing sides of a sandwiched porous membrane (bilayer coculture), as well as through shared media alone (conditioned-media coculture), was shown[14] to cause significant changes in SMC proliferation rates, density, transmembrane projections, and protein synthesis compared to SMC monocultures.

Bilayer coculturing of ECs and SMCs, with a laminar fluid shear stress apparatus, also elicited changes in EC gene expressions[7]. Endothelial cell gene expression for adhesion molecules was inhibited when the coculture flow apparatus was used to expose ECs to laminar fluid shear stress. In static (no-flow) conditions, however, SMCs induced EC gene expression for adhesion molecules and lowered EC gene expression for nitric oxide synthase. Incorporating a porous membrane interface between ECs and SMCs in both static and laminar fluid shear stressed conditions was essential to induce those changes in ECs.

Varying both serum content and culture time in bilayer cocultures and monocultures were also shown to cause changes in human aortic SMC cytokine secretions[25]. Cytokine secretions from

cocultured SMCs were found to be significantly different from monocultured SMCs when supplied with higher fetal bovine serum concentrations and cultured for longer periods of time. Those findings illustrated that serum supplemented and time-dependent arterial coculturing methods stimulate heterotypic activities. Also, in directly cocultured porcine arterial ECs and SMCs (without an intervening porous membrane), proximity, serum content, and culture time were all demonstrated to be precursors in the chain of events regulating indicators of thrombogenicity[22].

There has been only one previous study of transport in arterial-like coculture models. In porous bilayer cocultures of human umbilical vein ECs and murine smooth muscle-like 10T ½ cells, the diffusive permeability of 70 kDa biotin-dextran was shown to be lower when compared to monoculture controls of ECs and 10T ½ cells[20]. Similar coculture constructs pairing brain ECs and astrocytes have been exploited in blood-brain barrier transport measurements[21]. To date, however, it is unclear how arterial EC-SMC coculture configurations may influence arterial transport.

Hydraulic conductivity of BAECs grown on Transwell Permeable Supports and supplied with 10% fetal bovine serum in culture media has been measured in previous studies[4, 6, 10, 12, 19, 30] conducted in our laboratory, and there has been a quantitative consistency in these measurements over the last 20 years[29]. The present study determines L_p for various monoculture and coculture configurations of BAECs and BASMCs. Our results identify that the cocultured proximity of BASMCs to BAECs on the porous membrane, along with serum content in monocultures and cocultures, modulates arterial L_p. Arterial cocultures that mimic the arrangement of ECs and SMCs in a healthy arterial wall feature an intact monolayer of ECs with an elongated

morphology pattern, and lead to one of the lowest L_p values reported for an *in-vitro* arterial model.

2.3 Materials and Methods

2.3.1 Materials

Transwell 0.4 μm pore diameter polyester permeable supports were purchased from Corning, Inc., NY. T-75 Tissue Culture Flasks were purchased from Becton Dickinson, NJ. A T-25 Flask of primary BAECs was purchased form VEC Technologies, Inc, NY. A cryopreserved ampule of primary BASMCs was purchased from Cell Applications, Inc., CA. Fibronectin (FN) 0.1% from bovine plasma; Triton X-100; Trypsin-EDTA; Penicillin Streptomycin (PS); 200mM L-Glutamine (LG); 30% Albumin solution from Bovine Serum (BSA); and Phenol Red Minimum Essential Medium (MEM) were purchased from Sigma-Aldrich, Inc., MO. Fetal Bovine Serum (FBS) Defined and Paraformaldehyde (PFA) were purchased from Thermo Fischer Scientific, Inc. Phenol Red Free Minimum Essential Medium (PRF-MEM) and Calcium and Magnesium Free Phosphate Buffered Saline (CMF-PBS) were purchased from Mediatech, Inc., VA. VE-Cadherin Primary Antibody (PAb), and Anti-rabbit IgG (H+L), F(ab')$_2$ Fragment (Alexa Fluor 488 Conjugate) Secondary Antibody (SAb) were purchased from Cell Signaling Technology Inc. MA.

2.3.2 Defined Cell Culture Media

Serum-free MEM (SF-MEM) consisted of MEM with 1% LG, and 1% PS. 10% FBS MEM (10FB-MEM) consisted of MEM with 10% FBS, 1% LG, and 1% PS. 10FB-MEM was used for culturing cells in tissue culture flasks and on Transwell Permeable Supports. 2.5% FBS MEM (2.5FB-MEM) was made by combining 1 part 10FB-MEM with 3 parts SF-MEM. 2.5FB-MEM was also used for culturing cells on Transwell Permeable Supports. Experimental MEM (E-MEM) consisted of PRF-MEM with 1 % BSA, 1% LG, and 1% PS, and was used when calculating L_p.

The cell culture incubator was maintained at a constant temperature of 36.7^{o}C with 5% medical grade CO_2. Aseptic techniques were performed in a laminar flow hood. Cell culture media was pre-warmed to 37^{o}C in a waterbath and then buffered with 5% CO_2 for 20 minutes in an incubator prior to being introduced into the cell culture environment.

2.3.3 Cell Culture in Tissue Culture Flasks

A primary BAEC culture was expanded up to passage 2 subcultures in T-75 tissue culture flasks and then cryopreserved in 1 mL cryovials at a concentration of 1.0e6 cells/mL. A primary BASMC culture was expanded to passage 3 subcultures in T-75 tissue culture flasks and then cryopreserved in 1 mL cryovials at a concentration of 7.5e5 cells/mL.

Cryogencially frozen vials of either passage 2 primary BAEC cultures or passage 3 primary BASMC cultures were thawed for 2 minutes in a 37^{o}C waterbath and the cell suspensions were transferred to separate sterile T-75 tissue culture flasks. 10FB-MEM was added to the flask according to the manufacturer's volume recommendations (15 mL/T-75 flask) and the cultures were incubated until grown to be 80% confluent. Each culture was then passed into three new sterile tissue culture flasks by trypsinizing, pelleting, resuspending in 10FB-MEM, and splitting the cell suspension equally. These subcultures were grown until 80% confluent. BAEC and BASMC cultures were each passed a total of three times and then inoculated on Transwell inserts or companion wells. Passage 5 BAEC and passage 6 BASMC subcultures were inoculated on Transwell inserts or companion wells in specific monoculture and coculture arrangements and supplied with 10FB-MEM or 2.5FB-MEM.

2.3.4 Cell Culture with Transwell Permeable Supports

2.3.4.1 Transwell insert membranes. Transwell inserts containing a 10 μm thick polyester (PET) membrane with a total growth area of 1.12 cm^2 were used. While the PET membrane is

almost one order thicker than a normal internal elastic lamina[1], the 0.4 μm diameter membrane pores and membrane pore density of 4.0e6 pores/cm^2 were chosen to fall within the normal ranges found in internal elastic lamina[28].

2.3.4.2 Coating PET membranes cultures with Fibronectin. BAEC and BASMC cultures were inoculated on membranes that were pre-coated with FN diluted to 30 μg/mL with MEM. 224 μL of diluted FN was pipetted on either the apical or basal side of the Transwell insert membrane. FN coated Transwell inserts in companion plates were incubated for 2 hours and then excess FN was removed.

2.3.4.3 Cell culture media for Transwell Permeable Supports. The recommended Transwell insert to companion well volume ratio was 1:3, respectively, with 0.5mL of culture media contained in the Transwell insert and 1.5mL of culture media contained in the companion well. To culture cells with 10FB-MEM, the defined media was placed in both compartments. To create 2.5FB-MEM culture media, SF-MEM was placed in the companion well and 10FB-MEM was placed in the Transwell insert.

2.3.4.4 BAEC and BASMC plating densities, locations, and culture times. BAEC and BASMC cultures were inoculated with a 1:1 plating density ratio of 1.25e5 cells/cm^2. BAECs in monoculture and coculture formats were always the most apical culture on the Transwell membrane. BASMCs in monoculture or coculture formats were either inoculated on the basal side of the Transwell membrane or on the bottom surface of the companion well. The total BASMC culture time in all monocultures and cocultures was 2 days. The total BAEC culture time in all monoculture and coculture arrangements was 5 days.

2.3.4.5 BAEC and BASMC monocultures and cocultures.

2.3.4.5.1 BAEC monocultures

A BAEC culture was inoculated on an apical FN coated Transwell membrane. The culture was supplied with either 10FB-MEM or 2.5FB-MEM and incubated for 5 days.

2.3.4.5.2 BASMC monocultures

A BASMC culture was inoculated on an inverted basal FN coated Transwell membrane. The inverted Transwell membrane was placed in an incubator for 30 minutes while BASMCs settled and attached to the basal side of the membrane. The upright Transwell membrane with basal BASMC culture was then supplied with either 10FB-MEM or 2.5FB-MEM and incubated for 2 days.

2.3.4.5.3 BAEC and BASMC cocultures

i) Basal Transwell membrane BASMCs cocultured with a BAEC culture:

A BAEC culture was inoculated on an apical FN coated Transwell membrane. The BAEC culture was supplied with either 10FB-MEM or 2.5FB-MEM and incubated for 3 days. The Transwell membrane was then inverted and a BASMC culture was inoculated on the basal side of the FN coated membrane. The inverted Transwell membrane was placed in an incubator for 30 minutes while BASMCs settled and attached to the basal side of the membrane. The upright Transwell membrane coculture was then supplied with either 10FB-MEM or 2.5FB-MEM, respectively, and incubated for 2 days.

ii) Companion well BASMCs cocultured with a BAEC culture:

A BAEC culture was inoculated on an apical FN coated Transwell membrane. The BAEC culture was supplied with either 10FB-MEM or 2.5FB-MEM and incubated for 3 days. A BASMC culture was then inoculated in a separate companion well and allowed to settle and

attach to this surface during a 30 minute incubation period. The Transwell insert containing the BAEC culture was then paired with the companion well containing the BASMC culture. The coculture was then supplied with either 10FB-MEM or 2.5FB-MEM, respectively, and incubated for 2 days. These cocultures were dissociated on day 5 in order to measure endothelial L_p.

2.3.4.6 Monoculture and coculture notations and formats on Transwell Permeable Supports. The apical and basal locations of the Transwell membrane will be denoted as (a) and (b), respectively. The bottom surface of the companion well is denoted as (c). BAEC culture inoculums are abbreviated as (EC), and BASMC culture inoculums are abbreviated as (SMC). Monoculture formats are described by [Location (Inoculum)]. Coculture formats are described by [Location (First Inoculum); Location (Second Inoculum)]. Monoculture and coculture notations and formats are presented in Figure 2.2.

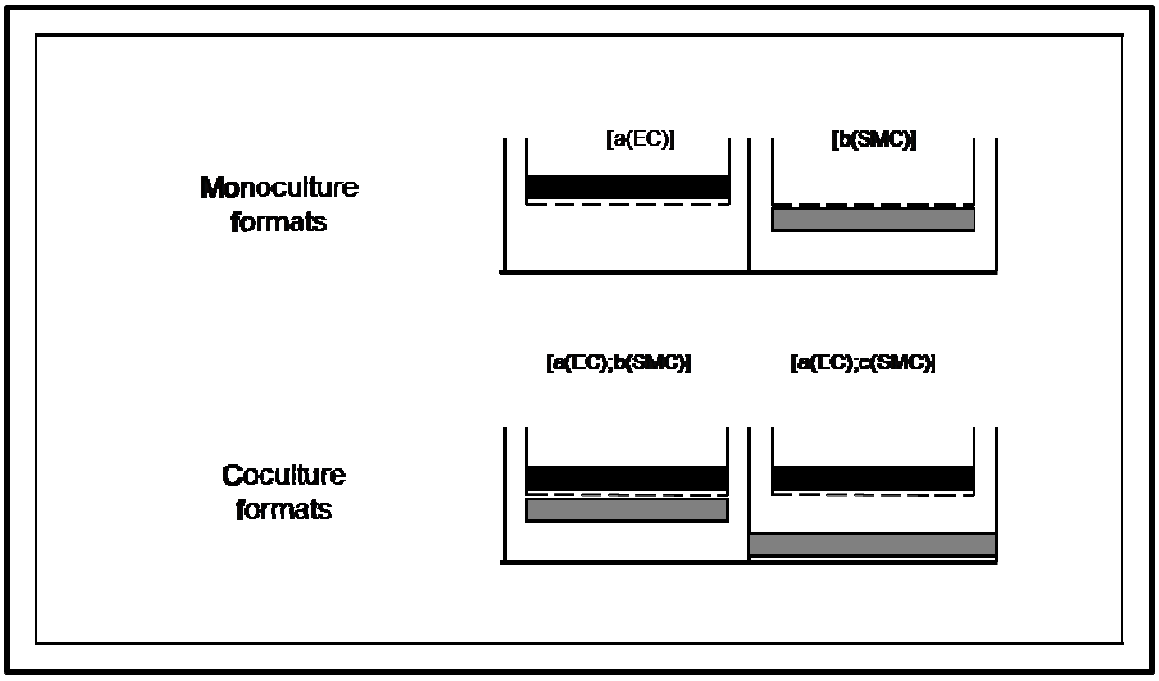

Figure 2.2. Schematic of BAEC and BASMC monoculture and coculture formats on Transwell membranes and companion wells. The horizontal dashed line indicates the location of the porous Transwell membrane. The black band indicates the location of BAEC cultures. The grey band indicates the location of BASMC cultures. Monoculture formats include [a(EC)], and [b(SMC)]. Coculture formats include [a(EC);b(SMC)], and [a(EC);c(SMC)].

2.3.4.7 Calculating L_p of Transwell cultures. Fluid flux (J_v) across Transwell insert cultures was measured in pairs with a bubble tracking apparatus and those measurements were then used to calculate L_p. Both the bubble tracking apparatus and the equations for calculating L_p have been previously described[10] and are briefly explained here. Following the prescribed monoculture and coculture times with Transwell Permeable Supports, the Transwell insert was transferred to a bubble tracking apparatus. E-MEM was added above and below the Transwell insert culture to eliminate the development of an osmotic pressure gradient. The L_p calculation for each culture was reduced to the ratio of the E-MEM fluid flux, J_v, across the Transwell insert culture and the hydrostatic pressure gradient, $\Delta P = 10$ cmH_2O, driving the transmembrane fluid flow (Equation 1). The units for J_v were cm/s, and the units of L_p were $cm/s/cmH_2O$. Each measurement was repeated 6 times.

$$L_p = J_v / \Delta P \qquad \text{(Eqn. 1)}$$

2.3.4.8 Monoculture resistances-in-series models of coculture L_p. Hydraulic conductivity measurements for BAEC monocultures were combined with L_p measurements for BASMC monocultures to distinguish their deviations from actual coculture L_p given the absence of real heterotypic compositions. Monoculture L_p values were first inverted to represent hydraulic resistances (Equations 2 and 3), which were then summed up in series. However, a PET membrane is included as a substrate in each monoculture and the hydraulic resistance of this membrane region ($R_{[PET]}$) was duplicated during series summations of monoculture hydraulic resistances. Therefore, a constant value for the hydraulic resistance of one porous membrane, $R_{[PET]}$ = 1.196e4 $cmH_2O/cm/s$ ($L_{p[PET]}$ = 8.361e-5 $cm/s/cmH_2O$), was subtracted from combinations of monoculture hydraulic resistances in order to account for the hydraulic resistance of a single PET membrane that is present in the actual coculture formats. The

combination of monoculture hydraulic resistances was then inverted to represent a resistances-in-series model of coculture L_p (Equation 4).

$$R_{[a(EC)]} = 1/L_{p\ [a(EC)]} \quad \text{(Eqn. 2)}$$

$$R_{[b(SMC)]} = 1/L_{p\ [b(SMC)]} \quad \text{(Eqn. 3)}$$

$$L_{p\ [a(EC)]+[b(SMC)]-[PET]} = 1/(R_{[a(EC)]} + R_{[b(SMC)]} - 1R_{[PET]}) \quad \text{(Eqn. 4)}$$

2.3.4.9 Statistical analysis of L_p. Hydraulic conductivity measurements for each culture format are presented as the mean L_p +/- the standard error of the mean (SEM). A Student's *t*-test with a two-tailed distribution was used to determine the significance level, p, between paired L_p measurements. Hydraulic conductivity measurements for paired BAEC monocultures, paired BASMC monocultures, and cocultures paired with BAEC monocultures were considered statistically significant if $p < 0.05$.

A Bonferroni procedure was used to test for statistical significance between L_p of different coculture formats that were paired to BAEC monoculture L_p. Hydraulic conductivity measurements for cocultures were normalized to paired BAEC monoculture L_p. The critical significance level was corrected to $\beta_b = \alpha/k$. Where $k = 3$ pairwise comparisons between normalized L_p measurements for each coculture format and BAEC monoculture, and $\beta_b = 0.0167$. Normalized L_p were considered statistically significant when $p < 0.0167$.

A Bonferroni procedure was also used to test for statistical significance between L_p of monoculture resistances-in-series models, and related membrane cocultures that were normalized to paired BAEC monoculture L_p. The critical significance level was corrected to $\beta_b = \alpha/k$. Where $k = 3$ to account for the relationship among the modeled group and relevant coculture group and the endothelial monoculture group, and $\beta_b = 0.0167$. Modeled L_p were considered statistically significant compared to related coculture L_p measurements when $p < 0.0167$.

2.3.5 Immunofluorescence

2.3.5.1 Immunofluorescence solutions. Paraformaldehyde fixative was diluted with CMF-PBS to 1% PFA and filtered through a 0.45 μm syringe filter. Fixative was freshly made on the day of use. Triton X-100 was diluted with CMF-PBS to a 0.2% Triton X-100 permeabilizing solution. Blocking buffer consisted of BSA and Triton X-100 diluted in CMF-PBS to 10% BSA and 0.1% Triton X-100. Primary antibody (PAb) was diluted 15:1000 in blocking buffer. Secondary antibody (SAb) was diluted 2:1000 in blocking buffer.

2.3.5.2 Immunofluorescence of VE-cadherin in Transwell cultures. All rinses with CMF-PBS were immediately removed after being added. All Transwell filters remained in the same companion well throughout the immunofluorescence procedure. All solutions were added to the insert first and then, when required, to the companion well second. All solutions were carefully vacuum aspirated from the companion well first and then from the insert without touching the membrane. Rinses with CMF-PBS followed a ratio of 0.5 mL/insert and 1 mL/companion well. All steps were carried out in room temperature (RT) conditions and in a laminar flow hood.

Remaining cell culture media was aspirated. The culture was quickly rinsed once and, immediately, 0.5 mL of fixative was added to the apical side of the insert. The culture was fixed for 10 minutes. Fixative was then removed. The culture was then rinsed once and 0.5 mL of permeabilizing solution was added to the apical side of the insert. The culture was permeabilized for 10 minutes. Permeabilizing solution was then removed. The culture was rinsed once and 0.5 mL of blocking buffer was added to the apical side of the insert. The culture was blocked for 60 minutes. Meanwhile, the PAb dilution was prepared. Blocking buffer was then removed. The culture was rinsed once and 200 μL of diluted PAb was added the apical side of the insert. The culture was incubated at RT with PAb for 3 hours. Meanwhile, in a dark room, the SAb dilution

was prepared. PAb was then removed and the culture was rinsed five times. The remaining steps were all carried out in a dark environment.

200 µL of diluted SAb was added to the apical side of the insert. The culture was incubated at RT with SAb for 60 minutes. SAb was then removed and the culture was rinsed four times. 0.5 mL of rinse solution was added to the apical side of the insert and the insert was transferred to a clean glass slide set on a Nikon TE 2000 microscope stage equipped with epi-fluorescence microscopy and MetaVue Imaging Software (Universal Imaging Corp. PA). The culture was imaged in the center field and then in four peripheral fields with a 10x objective. Five more similar fields were imaged with a 20x objective.

2.3.6 Morphometric Analysis

2.3.6.1 BAEC shape factors. The shape factors of BAECs in VE-cadherin immunostained monocultures and cocultures were calculated using the instructions that were provided in the MetaVue software. Briefly, a trace region tool was used to outline individual BAECs. MetaVue's Region Statistics of the outline generated calibrated pixel areas and perimeters for each cell. The shape factors for BAECs were then calculated with the formula $(4\pi * area)/(perimeter)^2$, where values ranged between zero and one; a value of one is a perfect circle and a value near zero is a flattened or elongated object.

2.3.6.2 Statistical analysis of shape factors. A Student's *t*-test with a two-tailed distribution was used to test for the statistical significance level, p, between BAEC shape factors from paired culture formats. BAEC shape factors for each culture format were considered statistically significant compared to BAECs in monoculture [a(EC)] 10FB-MEM if $p < 0.05$.

2.4 Results

2.4.1 BAEC monoculture L_p. The L_p measurements of BAEC monocultures supplied with 10FB-MEM were paired with L_p measurements of BAEC monocultures supplied with 2.5FB-MEM and are presented in Figure 2.3. BAEC monocultures supplied with 2.5FB-MEM had a significantly lower L_p than monocultures supplied with 10FB-MEM.

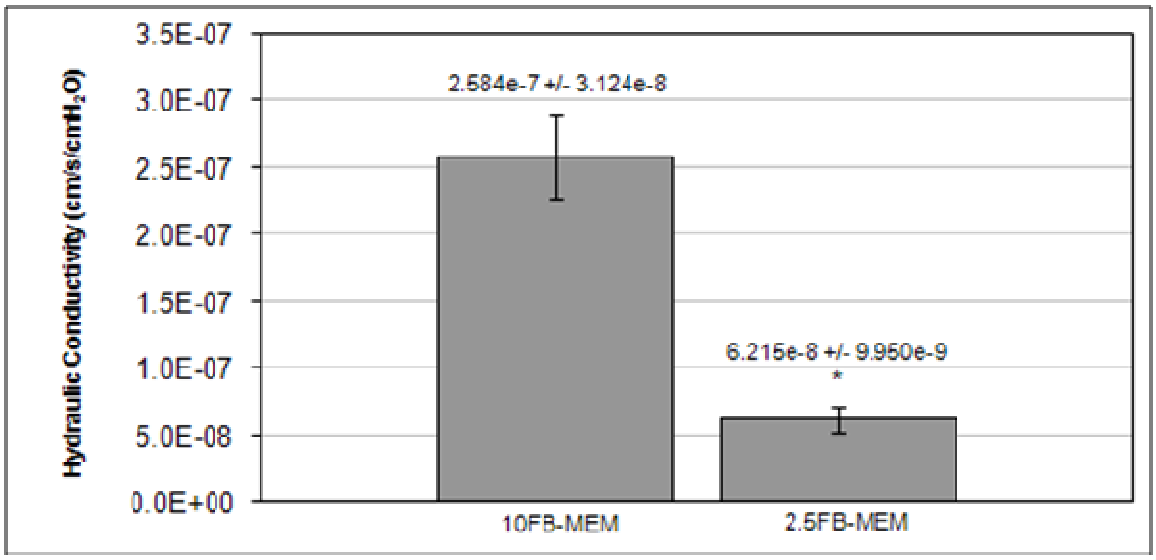

Figure 2.3. Hydraulic conductivity of 5 day apical EC ([a(EC)]) monocultures supplied with 10FB-MEM and 2.5FB-MEM. Data are presented as mean +/- SEM. * - $p < 0.05$ compared to 10FB-MEM; n = 6.

2.4.2 BASMC monoculture L_p. The L_p measurements of BASMC monocultures supplied with 10FB-MEM were paired with the L_p measurements of BASMC monocultures supplied with 2.5FB-MEM and are presented in Figure 2.4. These measurements show that BASMC monoculture L_p was significantly lower when supplied with 2.5FB-MEM. Note that BASMC L_p was more than 10 fold higher than BAEC L_p.

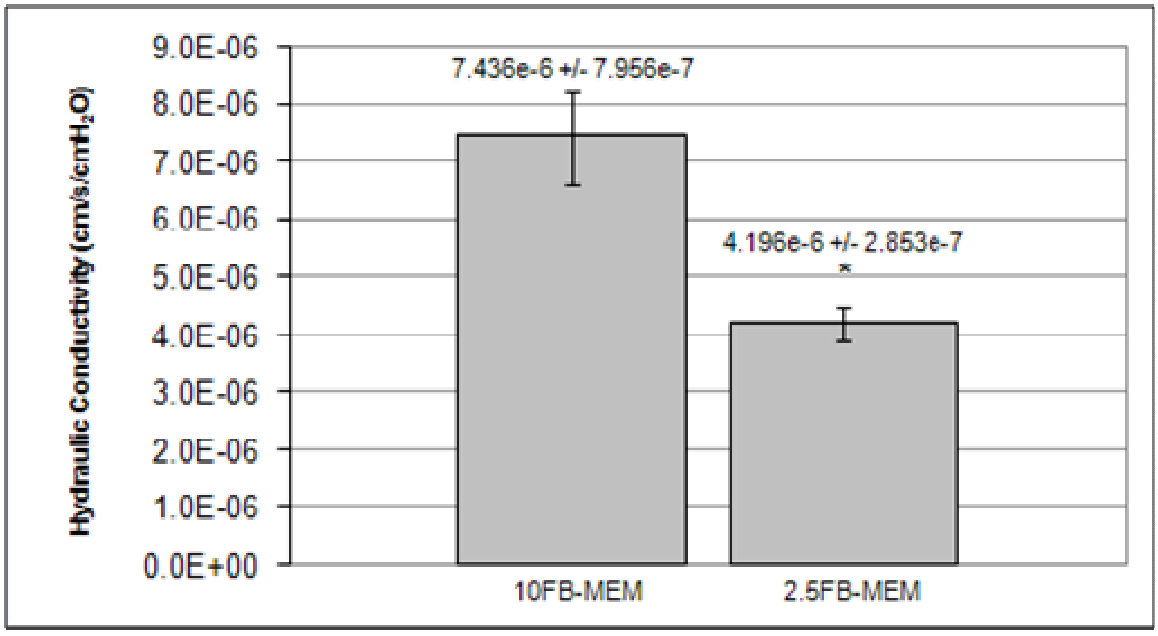

Figure 2.4. Hydraulic conductivity of 2 day basal SMC ([b(SMC)]) monocultures supplied with 10FB-MEM and 2.5FB-MEM. Data are presented as mean +/- SEM. * - $p < 0.05$ compared to 10FB-MEM; n = 6.

2.4.3 BAEC-BASMC coculture L_p. The L_p measurements of each coculture format supplied with either 10FB-MEM or 2.5FB-MEM were paired with the L_p measurements of BAEC monocultures supplied with either 10FB-MEM or 2.5FB-MEM, respectively. The L_p of each coculture was normalized to the paired L_p of each BAEC monoculture. The normalized mean L_p values of each coculture format for either 10FB-MEM or 2.5FB-MEM are presented in Figures 2.5 and 2.6, respectively. In Figure 2.5, [a(EC);b(SMC)] L_p was significantly lower than both [a(EC)] L_p and [a(EC);c(SMC)] L_p measurements. In Figure 2.6, both coculture formats had L_p values that were significantly lower than [a(EC)] L_p.

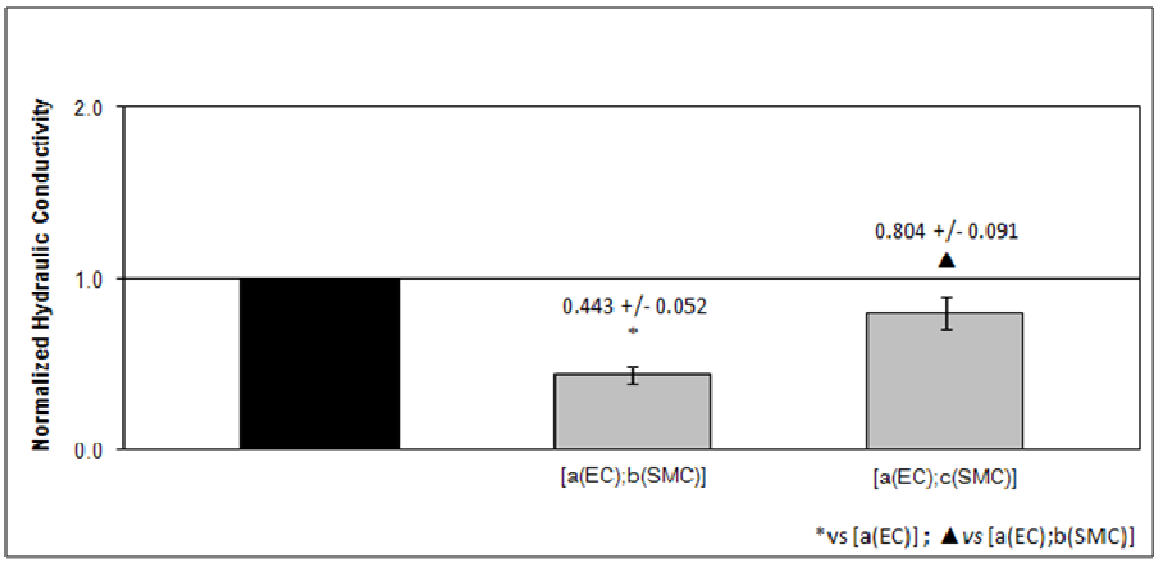

Figure 2.5. Hydraulic conductivity of each coculture [a(EC);b(SMC)] and [a(EC);c(SMC)] normalized to the mean L_p of paired endothelial monocultures [a(EC)]. Each culture format was supplied with 10FB-MEM. Statistical significance ($p < 0.05$) of coculture L_p normalized to paired endothelial L_p were denoted by a * symbol (* *vs* [a(EC)]). ▲ symbol denotes statistically significant differences of multiple ($\beta_b = \alpha/3 = 0.0167$) pairwise comparisons using a Bonferroni correction. ▲ indicates the normalized L_p values of each culture that were statistically significant compared to the normalized L_p of [a(EC);b(SMC)] coculture (▲ *vs* [a(EC);b(SMC)]). n = 6.

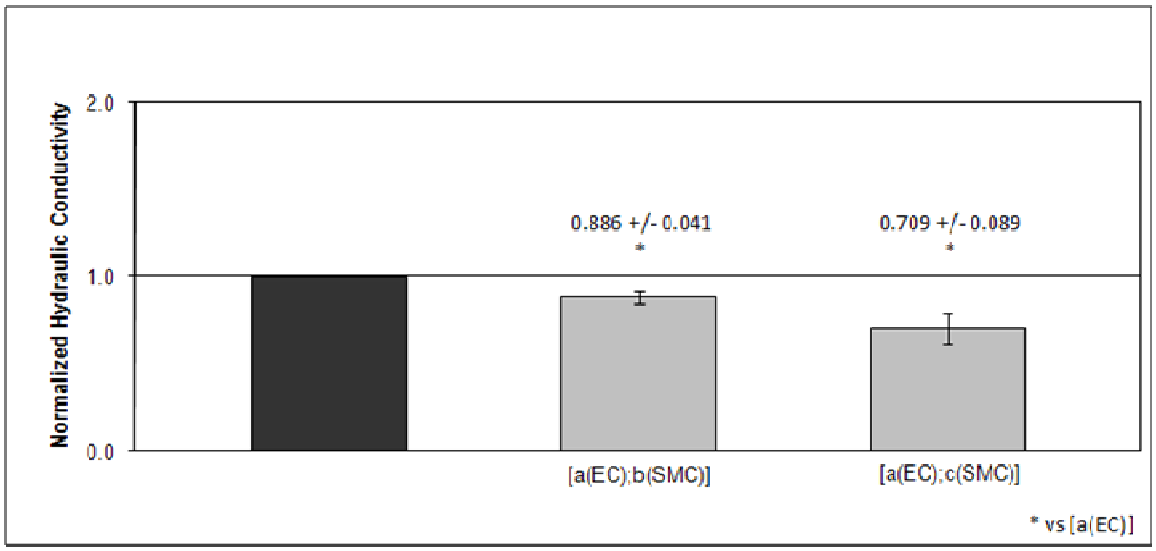

Figure 2.6. Hydraulic conductivity of each coculture [a(EC);b(SMC)] and [a(EC);c(SMC)] normalized to the mean L_p of paired endothelial monocultures [a(EC)]. Each culture format was supplied with 2.5FB-MEM. Statistical significance ($p < 0.05$) of coculture L_p normalized to paired endothelial L_p were denoted by a * symbol (* *vs* [a(EC)]). n = 6.

2.4.4 Monoculture resistances-in-series models of coculture L_p. Monoculture resistances-in-series models of coculture L_p (Eqn. 4) representative of each membrane coculture configuration were normalized to paired endothelial monoculture L_p. Resistances-in-series L_p values were plotted along with L_p measurements of the real membrane cocultures that were supplied with either 10FB-MEM (Figure 2.7) or 2.5 FB-MEM (Figure 2.8) in order to distinguish the influence of actual heterotypic arrangements. Monoculture resistances-in-series L_p was significantly higher than the real [a(EC);b(SMC)] coculture L_p when cultures were supplied with 10FB-MEM (Figure 2.7), and resistances-in-series L_p was similar to the actual coculture L_p measurements when cultures were supplied with 2.5FB-MEM (Figure 2.8).

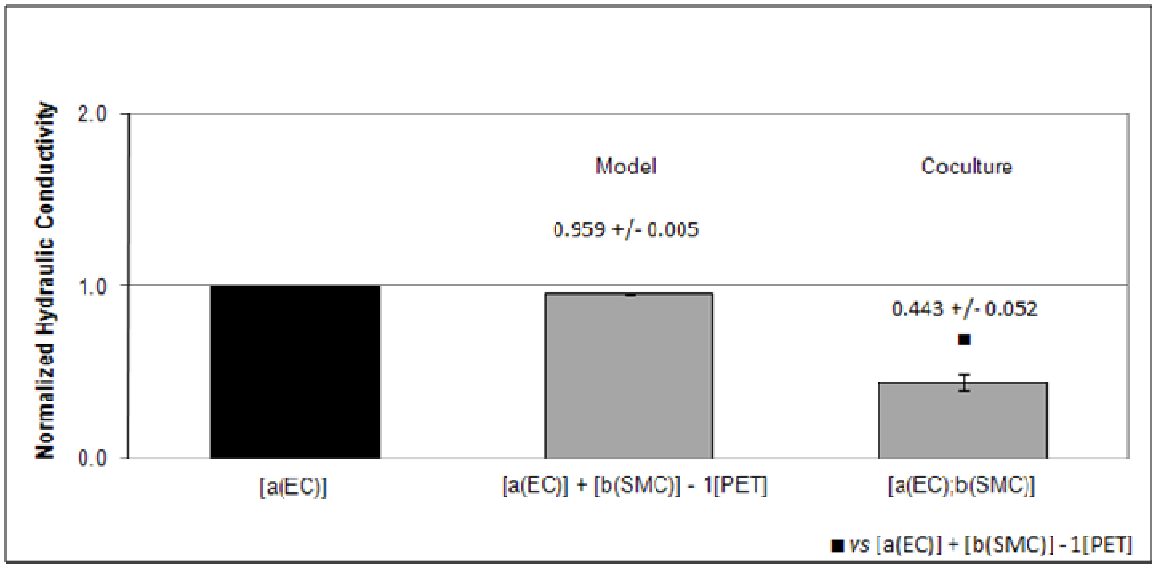

Figure 2.7. Hydraulic conductivity of membrane coculture [a(EC);b(SMC)], and resistances-in-series model predictions of membrane coculture format [a(EC)] + [b(SMC)] normalized to the mean L_p of paired endothelial monocultures [a(EC)]. Each culture was supplied with 10FB-MEM. The critical significance level was corrected to $\beta_b = \alpha/3 = 0.0167$ to account for the specific membrane coculture group, the resistances-in-series model, and the paired endothelial monoculture group. Statistical significance ($p < \beta_b$) of membrane coculture L_p compared to resistances-in-series L_p was denoted by a ■ symbol (■ *vs* [a(EC)] + [b(SMC)]). n = 6.

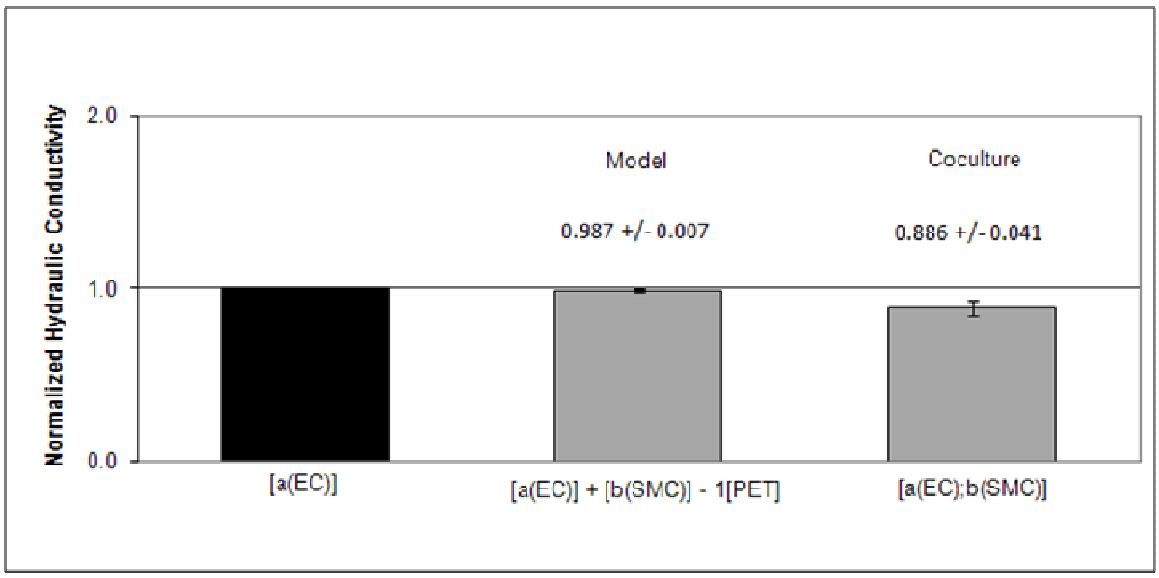

Figure 2.8. Hydraulic conductivity of membrane coculture [a(EC);b(SMC)], and resistances-in-series model predictions of membrane coculture format [a(EC)] + [b(SMC)] normalized to the mean L_p of paired endothelial monocultures [a(EC)]. Each culture was supplied with 2.5FB-MEM. The critical significance level was corrected to $\beta_b = \alpha/3 = 0.0167$ to account for the specific membrane coculture group, the resistances-in-series model, and the paired endothelial monoculture group. n = 6.

2.4.5 Immunostaining of VE-cadherin. BAEC VE-cadherin was immunostained for each coculture and BAEC monoculture. Center field 10x objective images for each coculture and BAEC monoculture supplied with either 10FB-MEM or 2.5FB-MEM are presented in Figure 2.9. VE-cadherin was expressed in each culture format and was localized at the cell border as expected. Endothelial cells imaged in coculture [a(EC);b(SMC)] appeared more elongated when compared to any of the other cultures.

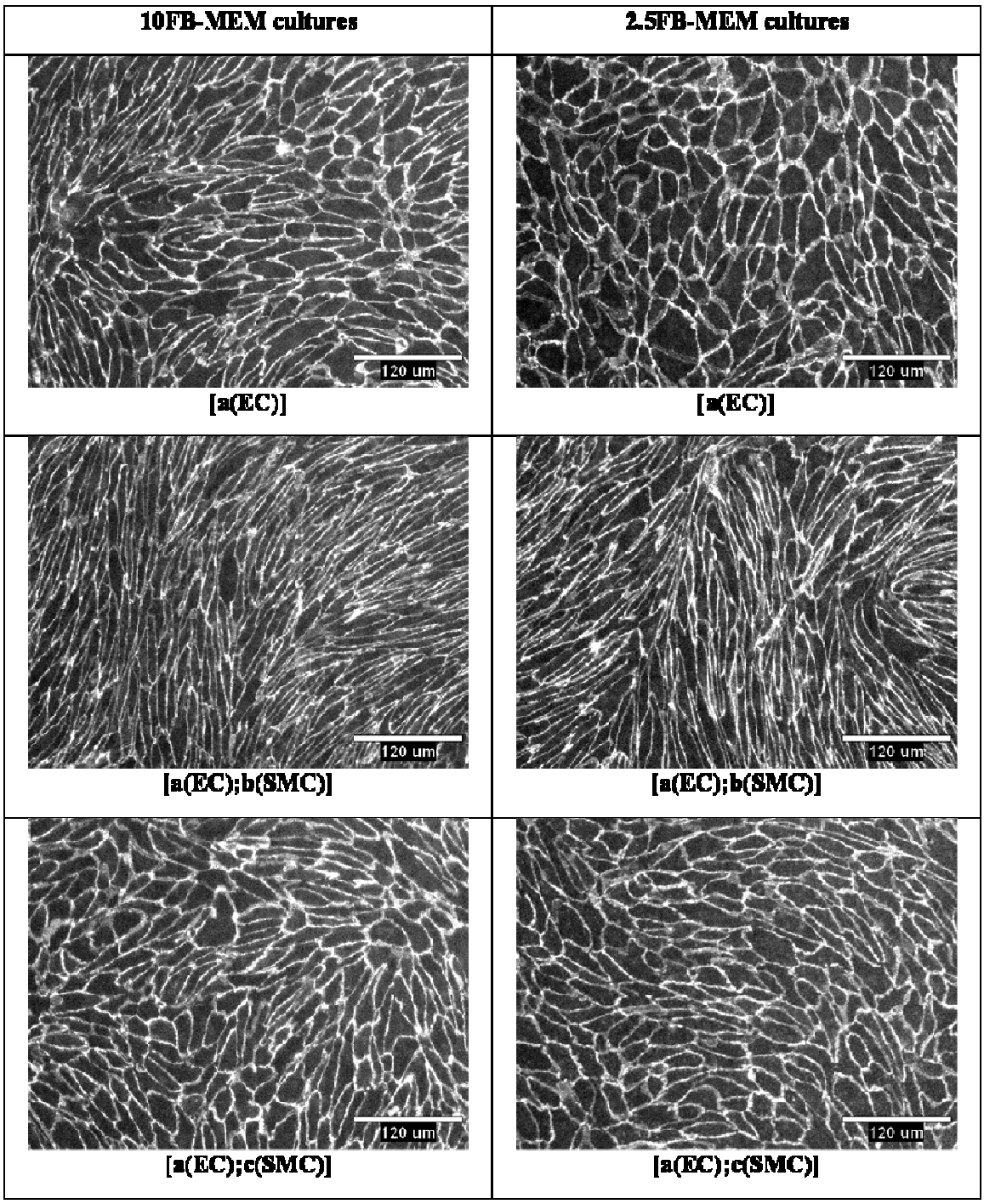

Figure 2.9. Representative images of VE-cadherin immunostaining in BAEC monocultures and cocultures supplied with either 10FB-MEM or 2.5FB-MEM. 10x objective. Scale bar 120 um.

2.4.6 BAEC morphometry. The sample mean, standard deviation (SD), and SEM for random samples of 10 BAEC shape factors from each culture format are presented in Table 2.1. The mean shape factor for BAECs in the [a(EC);b(SMC)] coculture was much closer to zero, compared to any other culture, which indicated that these BAECs were the most elongated. In addition, the BAEC shape factors in that coculture were significantly lower in comparison to shape factors for BAECs in the 10FB-MEM [a(EC)] monoculture.

Table 2.1. Sample means, SDs, and SEMs for BAEC shape factors (n = 10) for each culture format. * $p < 0.05$ compared to [a(EC)] 10FB-MEM; n = 10.

	Culture Format					
	[a(EC)]		[a(EC);b(SMC)]		[a(EC);c(SMC)]	
Media[MEM]	10FB	2.5FB	10FB	2.5FB	10FB	2.5FB
Sample mean (n=10)	0.5291	0.5865	0.2378*	0.2497*	0.5574	0.5450
Sample SD (+/-)	0.0847	0.1179	0.0547	0.0472	0.1333	0.1399
Sample SEM (+/-)	0.0268	0.0373	0.0173	0.0149	0.0422	0.0442

2.5 Discussion

2.5.1 Serum concentration modulates BAEC L_p. The influence of serum concentration on BAEC L_p response was determined by first growing BAEC monocultures in either 2.5FB-MEM or 10FB-MEM for 5 days and then measuring L_p. Hydraulic conductivity of [a(EC)] supplied with 2.5FB-MEM was found to be significantly lower than the L_p of [a(EC)] supplied with 10FB-MEM (Figure 2.3) by a factor of 4. This is likely a result of decreased EC motility and turnover in lower serum[5, 13]. This indicates that, *in-vitro,* endothelial L_p function is directly related to the percentage of serum that is present in culture media. Hydraulic conductivity of [b(SMC)] supplied with 2.5FB-MEM was found to be significantly lower than [b(SMC)] supplied with 10FB-MEM (Figure 2.4), but still 1-2 orders of magnitude higher than L_p of [a(EC)]. To our knowledge, there is no other research which describes the serum effect on L_p.

2.5.2 Arterial cocultures exhibit a range of L_p. In healthy arteries, the intimal and medial regions, which consist of an endothelial monolayer and dense multilayered SMCs, respectively, share the same porous internal elastic lamina[16]. Our coculture [a(EC);b(SMC)] best mimics this organization. The total culture time of BAECs in monocultures and cocultures was 5 days, and the total culture time of BASMCs in monocultures and cocultures was 2 days. The L_p measurements of each coculture supplied with either 10FB-MEM or 2.5FB-MEM were paired with L_p measurements for [a(EC)] monocultures that were also supplied with either 10FB-MEM (Figure 2.5) or 2.5FB-MEM (Figure 2.6).

Sandwiching the 10 μm thick porous membrane between ECs and SMCs in the [a(EC);b(SMC)] coculture (Figure 2.2) brings both cell types into close proximity to each other, compared to the [a(EC);c(SMC)] coculture, which distances ECs from SMCs by a 1 mm space of media (Figure 2.2). As we noted earlier, in our materials and methods section, this porous membrane is almost

one order thicker than a normal internal elastic lamina[1]. Pairwise comparisons of coculture L_p normalized to paired [a(EC)] L_p (Figures 2.5 and 2.6) reveal that the [a(EC);b(SMC)] L_p was significantly lower than [a(EC)] L_p for both the 10FB-MEM and 2.5FB-MEM cases. The L_p value of 5.507e-8 +/- 4.080e-10 cm/s/cmH_2O for the 2.5FB-MEM [a(EC);b(SMC)] coculture (Figure 2.6), which housed a sandwiched porous membrane, is one of the lowest values reported in the literature for an *in-vitro* model. This value is also within the same order for L_p in intact arteries[15, 24, 31].

A lower [a(EC);b(SMC)] L_p, compared to [a(EC)] L_p, suggests that directing vascular SMCs to form a medial region in the presence of an existing endothelial monolayer, as in arteriogenesis, is one of the localized approaches to improving arterial wall barrier function. The significant differences in arterial coculture L_p, compared to EC monocultures, also suggests their potential application in generating unique tissue-engineered blood vessels that have physiological transport barrier properties.

2.5.3 Coculturing in shared media influences BAEC L_p. Coculture configuration [a(EC);c(SMC)] distances ECs from SMCs by approximately 1 mm, and permits coculturing that is restricted to the sharing of media (Figure 2.2). That *in-vitro* coculture arrangement differs from *in-vivo* vascular wall anatomies where the porous elastic lamina forms an interface between ECs and SMCs. In 2.5FB-MEM, ECs that were cultured in shared media had a significantly reduced L_p compared to EC monocultures (Figure 2.6). That trend was not preserved in 10FB-MEM shared media cultures (Figure 2.5). Also, the L_p of ECs derived from shared media cocultures was significantly higher in comparison to the porous membrane interface coculture, [a(EC);b(SMC)], in 10FB-MEM conditions (Figure 2.5). However, this trend was not preserved in low serum concentrations (Figure 2.6) where there was no significant difference. The

significant changes in endothelial L_p resulting from shared media coculturing methods indicate that heterotypic interactions and serum concentrations regulate L_p.

2.5.4 Comparison of coculture to monoculture resistances-in-series modeled L_p. Resistances-in-series modeled L_p values were derived from series combinations of monoculture hydraulic resistances, and were nearly identical to the values of [a(EC)] L_p for ECs alone for both serum levels (Figures 2.7 and 2.8). These series combinations emphasize that in the absence of a true heterotypic interaction, the EC component provides the majority of hydraulic resistance to water flux, compared to the membrane and SMC components. In 10FB-MEM conditions, the significant reduction in L_p for coculture [a(EC);b(SMC)], compared to a modeled resistances-in-series prediction of L_p, distinguishes the effect of an actual heterotypic interaction (Figure 2.7). In 2.5FB-MEM, the actual coculture L_p was also lower than resistances-in-series modeled L_p but not quite significant ($p = 0.0553$) (Figure 2.8). Comparisons of actual coculture to monoculture resistances-in-series modeled L_p values presented in Figures 2.7 and 2.8 demonstrate that heterotypic regulation of L_p is also dependent on serum concentrations in culture media.

Since the [a(EC);b(SMC)] coculture configuration most closely represents the arrangement between ECs and SMCs in an intact arterial wall, it is tempting to conclude that this heterotypic configuration enhances the transport barrier for normal blood vessels. Reversing the order of EC and SMC inoculation on the porous substrate actually elevates arterial L_p, compared to EC monocultures as shown in the next chapter. Inoculating SMCs first will also produce an additional arterial coculture arrangement, [a(SMC);a(EC)], in which both cell types are on the apical side of the membrane. That configuration will support direct contact between ECs and SMCs, and is relevant to intimal arrangements of ECs and SMCs that arise when SMCs invade

the intima in disease states. Additional research will be required to elaborate upon local mechanical and chemical signaling mechanisms that mediate barrier enhancement in arterial cocultures.

Potential mediators of L_p include the activity of interendothelial adhesion junctions, subendothelial hydraulic resistance, and chemical signaling. VE-cadherin is one of the adherens junction proteins of adhesion junction complexes localized at the lateral border of endothelial cells. VE-cadherin expression in those parcellular pathways in each arterial coculture condition indicates that the activity of adherens junctions is engaged. The activity of tight junctions within this pathway should also be explored. Subendothelial hydraulic resistance may also participate in modulating arterial L_p. For example, EC and SMC process invasions of pores in an intervening membrane may restrict the pathway for J_v and, therefore, those contributions should be assessed. Chemical signaling could also influence arterial transport. Growth factors secreted from both cell types, for example, may alter EC and SMC growth rates and turnover, which could modify arterial wall barrier properties. Thus, chemical signaling pathways that mediate arterial L_p should also be examined.

2.5.5 Coculture arrangements regulate patterns in BAEC morphology. Contact-inhibited formation of BAEC monolayers is a characteristic homotypic function. A 10x microscope objective was used to image wide fields of view and we observed intact BAEC monolayers in every culture configuration (Figure 2.9). Figure 2.9, and Table 2.1 shows that the shape of ECs in the shared media coculture, [a(EC);c(SMC)], is similar to those in the [a(EC)] monoculture. However, the BAECs in the porous membrane interface coculture, [a(EC);b(SMC)], in 10FB-MEM and 2.5FB-MEM conditions, were unique because they displayed a more elongated morphology in comparison to all other cell culture arrangements (Figure 2.9). Endothelial cell

shape factor comparisons to BAECs in [a(EC)] 10FB-MEM cultures, shown in Table 2.1, confirmed that the BAECs in [a(EC);b(SMC)] conditions were in fact significantly elongated. An increase in the intercellular junction perimeter per unit of surface area that is apparent in Figure 2.9 for the elongated pattern of BAECs in [a(EC);b(SMC)] arterial cocultures suggests a greater junctional area for water transport and increased J_v. And yet the [a(EC);b(SMC)] coculture displayed a significantly lower L_p than the [a(EC)] monoculture (Figures 2.5 and 2.6). Therefore, within the [a(EC);b(SMC)] coculture, both the porous membrane region and the SMC region must provide additional resistances to J_v that are necessary for significantly reducing arterial L_p or additional modes of communication with the ECs enhance their barrier properties.

Various coculturing methods have been developed to capture more *in-vivo*-like tissue features, in comparison to monoculture cases. For example, elongated EC shapes were noticed when they were cultured directly above a matrix of collagen type I gel that was embedded with SMCs[33]. Previous studies[18] have also shown that coculturing techniques modulate a variety of protein secretions from both ECs and SMCs. It was demonstrated that directly coculturing ECs on top of preexisting SMCs led to different VEGF, PDGF-BB, TGF-β and bFGF secretions from both ECs and SMCs[18]. The proximity and inoculation order of SMCs and ECs in that study[18] differed from our [a(EC);b(SMC)] coculture (Figure 2.2) and did not include basal culture media and a porous membrane necessary for J_v measurements.

Coculturing methods in another study[25], which incorporated an intervening porous membrane between ECs and SMCs, induced changes in endothelial secretions of IL-1 and MCP-1. Smooth muscle cells were also characterized as being either 'more' or 'less secretory' as a result of changes in serum content in culture media[25]. The distance between ECs and SMCs in that coculture was most similar to what is found in coculture format [a(EC);b(SMC)] (Figure 2.2),

however, both the coculture inoculation order and the culture time varied from our present study, and a transmural J_v was not present.

2.5.6 Concluding remarks. In the present study, all preexisting osmotic pressure effects were removed from each culture condition prior to introducing J_v and measuring L_p. However, including osmotic pressure effects in culture while simultaneously exposing constructs to J_v may influence L_p. Serum level in cultures had a significant influence on regulating L_p responses. Lowering the serum concentration in culture by four fold resulted in a proportionate reduction in [a(EC)] L_p, which was the largest serum-dependent shift in L_p that we observed. Also, [a(EC);b(SMC)] coculture, which mimics the EC-SMC arrangement in a healthy arterial wall, led to a significantly lower L_p than ECs alone. Since soluble factors produced in [a(EC);c(SMC)] did not reduce L_p to the same level as [a(EC);b(SMC)], it is plausible that additional resistances to J_v in the porous membrane region and the SMC region of the [a(EC);b(SMC)] coculture compensate for the pattern of an increased paracellular pathway (junction perimeter per unit of surface area) (Figure 2.9 and Table 2.1).

Membrane pores sandwiched within the [a(EC);b(SMC)] coculture provide the pathways for J_v, as well as for invasions of EC and SMC processes, including EC-SMC contacts. Electron micrographs of small arteries have identified EC and SMC process invasions in pores of the intervening internal elastic lamina, which also extended to form intact endo-myothelial and myo-endothelial junctions[26]. In a previous bilayer coculture study[14], electron micrographs also revealed intact myo-endothelial junctions, formed by SMCs extending their cell processes through 0.4 μm diameter pores and across a 13 μm thick membrane to make intimate contact with ECs. That coculture closely resembled the heterotypic cell arrangement in our [a(EC);b(SMC)] coculture and our membrane parameters of pore diameter (0.4 μm), membrane

thickness (10 μm), and pore density (4.0e6 pores/cm^2) provide ample opportunities for the invasion of both EC and SMC processes. Endothelial cell and SMC process invasions and EC-SMC contacts in the membrane pores of a sandwiched PET membrane region could effectively diminish the necessary interstitial pathway area and increase the pore resistance for J_v (Figure 2.10). A process having a radius of 15% of the pore radius could reduce J_v by 50%, assuming that all pores contain a process. Therefore it is plausible that the sandwiched PET membrane region that is included in the [a(EC);b(SMC)] coculture configuration is a contributing factor in significantly reducing L_p (Figures 2.5 and 2.6).

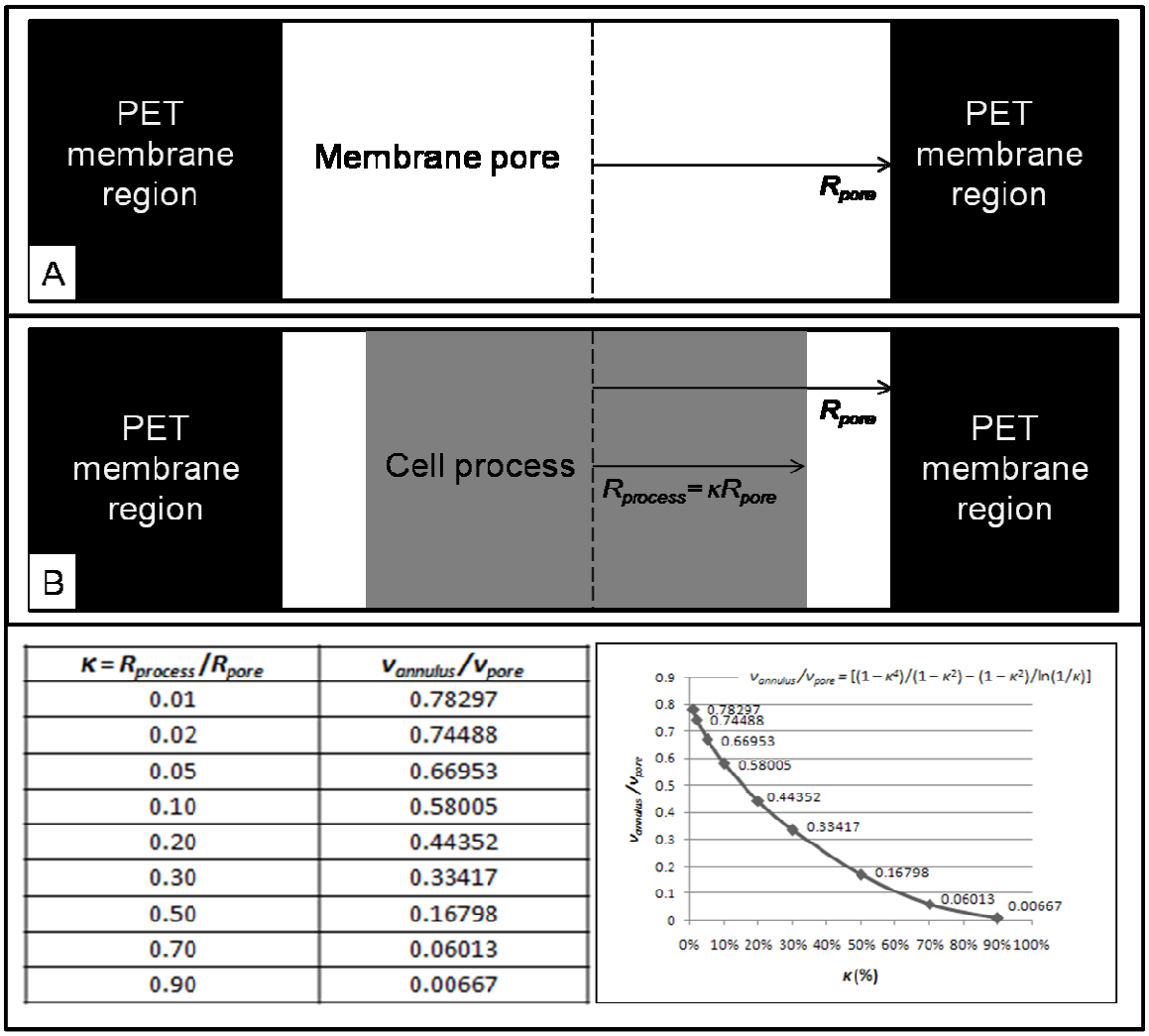

$\kappa = R_{process}/R_{pore}$	$v_{annulus}/v_{pore}$
0.01	0.78297
0.02	0.74488
0.05	0.66953
0.10	0.58005
0.20	0.44352
0.30	0.33417
0.50	0.16798
0.70	0.06013
0.90	0.00667

Figure 2.10. (continued on page 55).

Figure 2.10. (continued from page 54) Cross-section diagrams of a membrane pore and an idealized cell process invasion, depicted as a central cylinder, within the pore of a PET membrane with uniform parameters. Panel A shows a nude membrane pore of radius $r = R_{pore}$. Panel B shows an axisymmetric annulus that is formed by a cylindrical cell process invasion of radius $r = R_{process} = \kappa R_{pore}$ in the pore where $0 < \kappa \leq 1$. Taking the Poiseuille equation into consideration and using no-slip boundary conditions at each boundary for a fluid having a viscosity μ and driven by an axial pressure drop ΔP over the pore length L, the average fluid velocity v in the nude pore in Panel A is

$$v_{pore} = -(\Delta P R^2_{pore})/(8\mu L), \quad \text{(Eqn. 5)}$$

and, assuming the same pressure drop, the average fluid velocity in the axisymmetric annulus[2] in Panel B is

$$v_{annulus} = v_{pore}[(1-\kappa^4)/(1-\kappa^2) - (1-\kappa^2)/\ln(1/\kappa)]. \quad \text{(Eqn. 6)}$$

The ratio of average velocities $v_{annulus}/v_{pore} = [(1-\kappa^4)/(1-\kappa^2) - (1-\kappa^2)/\ln(1/\kappa)]$ from Equations 5 and 6 is used to assess the modification to fluid flow[23] that is caused by the presence of the cell process in the membrane pore. Numerical values in the table and the plot for the average velocity for fluid flow in the annulus, $v_{annulus}$, in comparison to flow in the nude pore, v_{pore}, for several ratios of $\kappa = R_{process}/R_{pore}$ show that flow is considerably modified by the presence of a central cell process in the membrane pore.

Overall, we have demonstrated that L_p is an inextricable result of EC and SMC coculture arrangements. In particular, we have produced an arterial coculture system, [a(EC);b(SMC)], that includes a sandwiched porous membrane and mimics the arrangement of ECs and SMCs in a healthy arterial wall. This coculture produced a pattern of significantly elongated ECs, and one of the lowest *in-vitro* L_p values that is reported in the literature.

2.6 References

1. Aiello V.D., P.S. Gutierrez, M.J.F. Chaves, A.A.B. Lopes, M.L. Higuchi, and J.A.F. Ramires. Morphology of the internal elastic lamina in arteries from pulmonary hypertensive patients: a confocal laser microscopy study. Mod. Pathol. 16(5): 411-416, 2003.

2. Bird B.R., W.E. Stewart, and E.N. Lightfoot. "Shell momentum balances and velocity distributions in laminar flow." In: Transport Phenomena, edited by New York: John Wiley & Sons Inc., 2007, pp. 53-55.

3. Buschmann I., and W. Schaper. Arteriogenesis versus angiogenesis: two mechanisms of vessel growth. Am. J. Physiol. Physiol. 14: 121-125, 1999.

4. Cancel L.M., A. Fitting, and J.M. Tarbell. In-vitro study of LDL transport under pressurized (convective) conditions. Am. J. Physiol. Heart Circ. Physiol. 293: H126-H132, 2007.

5. Castellot, Jr. J.E., M.J. Karnovsky, and B.M. Spiegelman. Potent stimulation of vascular endothelial cell growth by differentiated 3t3 adipocytes. Cell Biol. 77(10): 6007-6011, 1980.

6. Chang Y.S., J.A. Yaccino, S. Lakshminarayanan, J.A. Frangos, and J.M. Tarbell. Shear-induced increases in hydraulic conductivity in endothelial cells is mediated by a nitric oxide-dependent mechanism. Arterioscler. Thromb. Vasc. Biol. 20: 35-42, 2000.

7. Chiu J., L. Chen, P. Lee, C. Lee, L. Lo, S. Usami, and S. Chien. Shear stress inhibits adhesion molecule expression in vascular endothelial cells induced by coculture with smooth muscle cells. Blood 101: 2667-2674, 2003.

8. Conway E.M., D. Collen, and P. Carmeliet. Molecular mechanisms of blood vessel growth. Cardiovasc. Res. 49: 507-521, 2001.
9. Davies P.F., G.A. Truskey, H.B. Warren, S.E. O'Connor, and B.H. Eisenhaure. Metabolic cooperation between vascular endothelial cells and smooth muscle cells in co-culture: changes in low density lipoprotein metabolism. J. Cell Biol. 101: 871-879, 1985.
10. DeMaio L., J.M. Tarbell, R.C. Scaduto, T.W. Gardner, and D.A. Antonetti. A transmural pressure gradient induces mechanical and biological adaptive responses in endothelial cells. Am. J. Physiol. Heart Circ. Physiol. 286: 731-741, 2004.
11. De Wit C., M. Boettcher, and V.J. Schmidt. Signaling across myoendothelial gap junctions – fact or fiction? Cell Commun. Adhes. Sep 15(3): 231-245, 2008.
12. Dull R.O., H. Jo, H. Sill, T.M. Hollis, and J.M. Tarbell. The effect of varying albumin concentration and hydrostatic pressure on hydraulic conductivity and albumin permeability of cultured endothelial monolayers. Microvasc. Res. 41(3): 390-407, 1991.
13. Duthu G.S. and J.R. Smith. In vitro proliferation and lifespan of bovine aorta endothelial cells: effect of culture conditions and fibroblast growth factor. J. Cell Physiol. 103(3): 385-392, 1980.
14. Fillinger M.F., L.N. Sampson, J.L. Cronenwett, R.J. Powell, and R.J. Wagner. Coculture of endothelial cells and smooth muscle cells in bilayer and conditioned media models. J. Surg. Res. 67: 169-178, 1997.
15. Gaballa M.A., T.E. Raya, B.R. Simon, and S. Goldman. Arterial mechanics in spontaneously hypertensive rats. Mechanical properties, hydraulic conductivity, and two-phase (solid/fluid) finite element models. Circ. Res. 71: 145-158, 1992.

16. Gartner L.P., and J.L. Hiatt. “Circulatory System.” In: Color Textbook of Histology, edited by Philadelphia: Saunders Co., 2001, pp. 251-256.

17. Heberlein K., A. Straub, and B.E. Isakson. The myoendothelial junction: breaking through the matrix? Microcirculation 16(4): 307-322, 2009.

18. Heydarkhan-Hagvall S., G. Helenius, B.R. Johansson, J.Y. Li, E. Mattsson, and B. Risberg. Co-culture of endothelial cells and smooth muscle cells affects gene expression of angiogenic factors. J. Cell Biochem. 89: 1250-1259, 2003.

19. Hillsley M.V., and J.M. Tarbell. Oscillatory shear alters endothelial hydraulic conductivity and nitric oxide levels. Biochem. Biophys. Res. Commun. 293: 1466-1471, 2002.

20. Kurzen H., S. Manns, G. Dandekar, T. Schmidt, S. Pratzel, and B.M. Kräling. Tightening of endothelial cell contacts: a physiologic response to cocultures with smooth muscle-like 10 T1/2 cells. J. Invest. Dermatol. 119: 143-153, 2002.

21. Li G., M.J. Simon, L.M. Cancel, Z.D. Shi, X. Ji, J.M. Tarbell, B. Morrison 3rd, and B.M. Fu. Permeability of endothelial and astrocyte cocultures: in vitro blood brain barrier models for drug delivery studies. Ann. Biomed. Eng. 38(8): 2499-2511, 2010.

22. Pang Z., L.E. Niklason, and G.A. Truskey. Porcine endothelial cells cocultured with smooth muscle cells became procoagulant in vitro. Tissue Eng. Part A. 16(6): 1835-1844, 2010.

23. Pnueli D., and C. Gutfinger. “Exact solutions of the Navier-Stokes equations.” In: Fluid Mechanics, edited by New York: Cambridge University Press, 1992, pp. 193-196.

24. Renkin E.M., and F.E. Curry. Endothelial permeability: Pathways and modulations. Ann. NY Acad. Sci. 401: 248-259, 1982.

25. Rose S.L., and J.E. Babensee. Complimentary endothelial cell/smooth muscle cell co-culture systems with alternate smooth muscle cell phenotypes. Ann. Biomed. Eng. 35: 1382-1390, 2007.

26. Ryan U.S., J.W. Ryan, and C. Whitaker. How do kinins affect vascular tone? Adv. Exp. Med. Biol. 120A: 375-391, 1979.

27. Schaper W., and I. Buschmann. Arteriogenesis, the good and bad of it. Cardiovasc. Res. 43: 835-837, 1999.

28. Tada S., and J.M. Tarbell. Interstitial flow through the internal elastic lamina affects shear stress on arterial smooth muscle cells. Am. J. Physiol. Heart Circ. Physiol. 278: H1589-H1597, 2000.

29. Tarbell J.M.. Shear stress and the endothelial transport barrier. Cardiovasc. Res. 87: 320-330, 2010.

30. Tarbell J.M., L. DeMaio, and M.M. Zaw. Effect of pressure on hydraulic conductivity of endothelial monolayers: role of endothelial cleft shear stress. J. Appl. Physiol. 87: 261-268, 1999.

31. Tarbell J.M., M.J. Lever, and C.G. Caro. The effect of varying albumin concentration of the hydraulic conductivity of the rabbit common carotid artery. Microvasc. Res. 35: 204-220, 1988.

32. van Oostrom M.C., O. van Oostrom, P.H.A. Quax, M.C. Verhaar, and I.E. Hoefer. Insights into the mechanisms behind arteriogenesis: what does the future hold? J. Leukocyte Biol. 84: 1379-1391, 2008.

33. Ziegler T., R.W. Alexander, and R.M. Nerem. An endothelial cell-smooth muscle cell co-culture model for use in the investigation of flow effects in vascular biology. Ann. Biomed. Eng. 23: 216-225, 1995.

CHAPTER 3

HYDRAULIC CONDUCTIVITY OF SMOOTH MUSCLE CELL-INITIATED ARTERIAL COCULTURES

3.1 Abstract

Vascular smooth muscle contributes to complex arterial wall functions. This study uses arterial smooth muscle cell (SMC) and endothelial cell (EC) cultures to measure arterial coculture hydraulic conductivity (L_p). We hypothesized that arterial coculture configurations would alter arterial L_p, compared to the L_p of SMC and EC monoculture controls. This research presents the first *in-vitro* observations of arterial coculture L_p, which includes SMC-initiated coculture configurations. Bovine aortic smooth muscle cells (BASMCs) and bovine aortic endothelial cells (BAECs) were cocultured on Transwell Permeable Supports, with BASMCs seeded first, and then exposed to a pressure-driven transmural flow. Hydraulic conductivity across each culture was measured by using a bubble tracking apparatus that determined water flux (J_v). Our results indicate that arterial L_p is significantly modulated by the proximity of BASMCs to BAECs on the porous membrane, and serum content in culture. The L_p of cocultures was also compared to the L_p predictions of a resistances-in-series model based on summations of hydraulic resistances of individual culture components, to distinguish the contributions of real heterotypic cellular interactions. Conditions that lead to significantly elevated coculture L_p, compared to BAEC monoculture controls, have been uncovered. Also, VE-cadherin immunostaining of intact BAEC monolayers in coculture and monoculture configurations identifies that EC-SMC proximity on a porous membrane has a dynamic influence on BAEC morphology patterns.

3.2 Introduction

Tissues consist of either homotypic or heterotypic cellular interactions and, depending on the proximity of cells, communication may occur through soluble and contact-mediated pathways (Figure 3.1). Local mechanical and chemical signaling mechanisms are both essential for maintaining a tissue's structure and function. Intimal endothelial cells (ECs) and medial smooth muscle cells (SMCs) are neighboring cells in the arterial wall. Typical homotypic cell functions include contact-inhibited endothelial growth, and smooth muscle contraction, and the close proximity of ECs and SMCs within the arterial wall yield heterotypic interactions. This study examines, for the first time, whether heterotypic cultures of arterial ECs and SMCs with SMCs plated first, influence arterial wall transport, specifically, hydraulic conductivity (L_p).

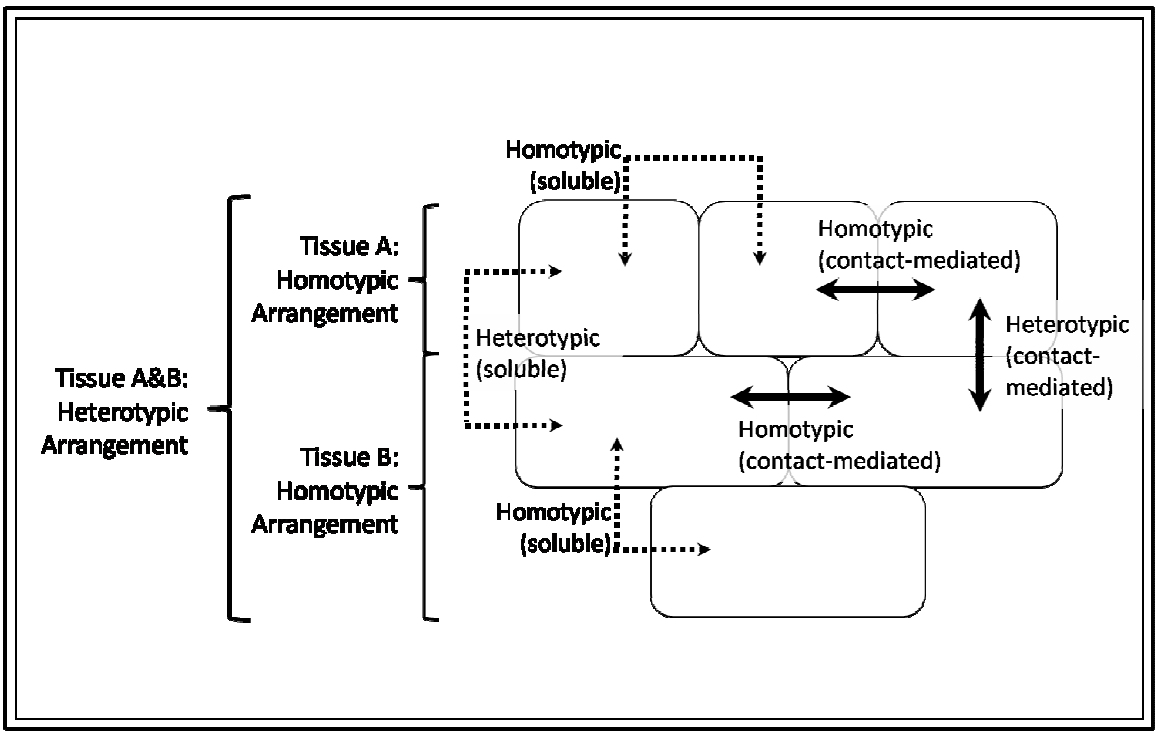

Figure 3.1. Homotypic and heterotypic arrangements of tissues A and B showing combinations of soluble (dashed arrows) and contact-mediated (continuous arrows) signal pathways for cell interactions. Double-sided arrows indicate that cell signaling is also bidirectional and reciprocal.

In-vivo, the order in which ECs and SMCs are established in the vessel wall, and the proximity between ECs and SMCs, varies with the event(s) that are taking place in the localized region of the vasculature. In healthy arterial walls, the porous internal elastic lamina (IEL) is sandwiched between the intimal endothelium and a relatively dense medial region of SMCs[14]. Endothelial cells and SMCs can then establish direct heterotypic contact through soluble factors and by extending cell processes through the pores of the internal elastic lamina[10, 15, 24]. In the event of intimal denudation, a close proximity between ECs and SMCs can be reestablished by reendothelialization in the presence of preexisting medial SMCs without the intervening IEL[3]. In cases where both cell types are intact in the arterial wall, an increasing number of medial SMCs come into direct contact with ECs during intimal hyperplasia or fibroatheroma formation during the progression of atherosclerosis[25]. The normal location of the porous internal elastic lamina is not preserved by those intimal arrangements of ECs and SMCs.

Earlier work with coculture systems[13] has clearly demonstrated how ECs can influence SMC function. Coculturing bovine aortic endothelial cells (BAECs) and bovine aortic smooth muscle cells (BASMCs) on opposing sides of a sandwiched porous membrane (bilayer coculture), as well as through shared media alone (conditioned-media coculture), was shown[13] to cause significant changes in SMC proliferation rates, density, transmembrane projections, and protein synthesis compared to SMC monocultures.

In another coculture study[16], human saphenous vein ECs and SMCs that were in direct contact, without an intervening porous membrane, were shown to cause significant changes in gene expressions in both ECs and SMCs when compared to similar gene expressions in EC and SMC monocultures. The changes in gene expressions for those direct cocultures were also proposed to be key angiogenic factors[16].

Bilayer coculturing of ECs and SMCs, with a laminar fluid shear stress apparatus, also elicited changes in EC gene expressions[7]. Endothelial cell gene expression for adhesion molecules was inhibited when the flow apparatus was used to expose ECs to laminar fluid shear stress. In static (no-flow) conditions, however, SMCs induced EC gene expression for adhesion molecules and lowered EC gene expression for nitric oxide synthase. Incorporating a porous membrane interface between ECs and SMCs in both static and laminar fluid shear stressed conditions was essential to induce those changes in ECs.

Smooth muscle cell proliferation can be reduced by omitting serum supplements from culture media and a temporary serum-free culture period of 2-5 days may induce SMCs to adopt a contractile (quiescent) phenotype[2, 8]. Serum-dependent SMC proliferation can also be restored by reintroducing serum into culture media. The serum-dependent modulation of porcine arterial SMC phenotypes was shown to dramatically affect EC monolayer formation when ECs were cultured directly above existing SMCs[19]. That study[19] demonstrated how ECs could not develop into a monolayer when paired with proliferative SMCs. In contrast, EC monolayer formation was only achieved after switching the proliferative SMC phenotype to a quiescent SMC phenotype through a short period of serum starvation.

Varying both serum content and culture time in bilayer cocultures and monocultures were also shown to cause changes in human aortic SMC cytokine secretions[23]. Cytokine secretions from cocultured SMCs were found to be significantly different from monocultured SMCs when supplied with higher fetal bovine serum concentrations and cultured for longer periods of time. Those findings illustrated that serum supplemented and time-dependent arterial coculturing methods stimulate heterotypic activities. Also, in directly cocultured porcine arterial ECs and SMCs (without an intervening porous membrane), proximity, serum content, and culture time

were also demonstrated to be precursors in the chain of events regulating indicators of thrombogenicity[21].

There has been only one previous study of transport in arterial-like coculture models. In porous bilayer cocultures of human umbilical vein ECs and murine smooth muscle-like 10T ½ cells, the diffusive permeability of 70 kDa biotin-dextran was shown to be lower when compared to monoculture controls of ECs and 10T ½ cells[18]. Similar coculture constructs pairing brain ECs and astrocytes have been exploited in blood-brain barrier transport measurements[20]. To date, however, it is unclear how arterial EC-SMC coculture configurations may influence arterial L_p.

Hydraulic conductivity of BAECs grown on Transwell Permeable Supports and supplied with 10% fetal bovine serum in culture media has been measured extensively in previous studies[4, 6, 9, 11, 17, 28] conducted in our laboratory, and there has been a quantitative consistency in these measurements over the last 20 years[27]. The present study determines L_p for several monoculture and coculture configurations of BAECs and BASMCs with the BASMCs plated first. Our results reveal that the proximity of cocultured BASMCs to BAECs on the porous membrane, along with serum content, modulate arterial L_p. Arterial cocultures that mimic the intimal arrangement of ECs and SMCs after intimal damage (direct contact) feature an intact monolayer of ECs with a circular morphology pattern, and lead to elevated L_p values compared to EC monoculture controls. This suggests that although ECs appear to be intact after recovery from intimal damage, their transport properties are impaired.

3.3 Materials and Methods

3.3.1 Materials

Transwell 0.4 μm pore diameter polyester permeable supports were purchased from Corning, Inc., NY. T-75 Tissue Culture Flasks were purchased from Becton Dickinson, NJ. A T-25 Flask of primary BAECs was purchased form VEC Technologies, Inc, NY. A cryopreserved ampule of primary BASMCs was purchased from Cell Applications, Inc., CA. Fibronectin (FN) 0.1% From Bovine Plasma; Triton X-100; Trypsin-EDTA; Penicillin Streptomycin (PS); 200mM L-Glutamine (LG); 30% Albumin solution from Bovine Serum (BSA); and Phenol Red Minimum Essential Medium (MEM) were purchased from Sigma-Aldrich, Inc., MO. Fetal Bovine Serum (FBS) Defined and Paraformaldehyde (PFA) were purchased from Thermo Fischer Scientific, Inc. Phenol Red Free Minimum Essential Medium (PRF-MEM) and Calcium and Magnesium Free Phosphate Buffered Saline (CMF-PBS) were purchased from Mediatech, Inc., VA. VE-Cadherin Primary Antibody (PAb), and Anti-rabbit IgG (H+L), F(ab')$_2$ Fragment (Alexa Fluor 488 Conjugate) Secondary Antibody (SAb) were purchased from Cell Signaling Technology Inc. MA.

3.3.2 Defined Cell Culture Media

Serum-free MEM (SF-MEM) consisted of MEM with 1% LG, and 1% PS. Direct adaptation to SF-MEM was used for temporarily suspending the proliferation of BASMC cultures. 10% FBS MEM (10FB-MEM) consisted of MEM with 10% FBS, 1% LG, and 1% PS. 10FB-MEM was used for culturing cells in tissue culture flasks and on Transwell Permeable Supports. 2.5% FBS MEM (2.5FB-MEM) was made by combining 1 part 10FB-MEM with 3 parts SF-MEM. 2.5FB-MEM was also used for culturing cells on Transwell Permeable Supports. Experimental MEM

(E-MEM) consisted of PRF-MEM with 1 % BSA, 1% LG, and 1% PS, and was used when calculating L_p.

The cell culture incubator was maintained at a constant temperature of 36.7^{o}C with 5% medical grade CO_2. Aseptic techniques were performed in a laminar flow hood. Cell culture media was pre-warmed to 37^{o}C in a waterbath and then buffered with 5% CO_2 for 20 minutes in an incubator prior to being introduced into the cell culture environment.

3.3.3 Cell Culture in Tissue Culture Flasks

A primary BAEC culture was expanded up to passage 2 subcultures in T-75 tissue culture flasks and then cryopreserved in 1 mL cryovials at a concentration of 1.0e6 cells/mL. A primary BASMC culture was expanded to passage 3 subcultures in T-75 tissue culture flasks and then cryopreserved in 1 mL cryovials at a concentration of 7.5e5 cells/mL.

Cryogencially frozen vials of either passage 2 primary BAEC cultures or passage 3 primary BASMC cultures were thawed for 2 minutes in a 37^{o}C waterbath and the cell suspensions were transferred to separate sterile T-75 tissue culture flasks. 10FB-MEM was added to the flask according to the manufacturer's volume recommendations (15 mL/T-75 flask) and the cultures were incubated until grown to be 80% confluent. Each culture was then passed into three new sterile tissue culture flasks by trypsinizing, pelleting, resuspending in 10FB-MEM, and splitting the cell suspension equally. These subcultures were grown until 80% confluent. BAEC and BASMC cultures were each passed a total of three times and then inoculated on Transwell inserts or companion wells. Passage 5 BAEC and passage 6 BASMC subcultures were inoculated on Transwell inserts or companion wells in specific monoculture and coculture arrangements and supplied with 10FB-MEM, 2.5FB-MEM, or SF-MEM.

3.3.4 Cell Culture with Transwell Permeable Supports

3.3.4.1 Transwell insert membranes. Transwell inserts containing a 10 μm thick polyester (PET) membrane with a total growth area of 1.12cm^2 were used. While the PET membrane is almost one order thicker than a normal IEL[1], the 0.4 μm diameter membrane pores and a membrane pore density of 4.0e6 pores/cm^2 fall within the normal ranges found in IEL[26].

3.3.4.2 Coating PET membranes and preexisting BASMC membrane cultures with Fibronectin. BAEC and BASMC cultures were inoculated on membranes that were pre-coated with FN diluted to 30 μg/mL with MEM. 224 μL of diluted FN was pipetted on either the apical or basal side of the Transwell insert membrane. Diluted FN was also placed on top of existing BASMC cultures, which were on the apical side of the membrane, prior to inoculating BAEC cultures directly above BASMC cultures. FN coated Transwell inserts in companion plates were incubated for 2 hours and then excess FN was removed.

3.3.4.3 Cell culture media for Transwell Permeable Supports. The recommended Transwell insert to companion well volume ratio was 1:3, respectively, with 0.5mL of culture media contained in the Transwell insert and 1.5mL of culture media contained in the companion well. To culture cells with either SF-MEM or 10FB-MEM, the defined media was placed in both compartments. To create 2.5FB-MEM culture media, SF-MEM was placed in the companion well and 10FB-MEM was placed in the Transwell insert.

3.3.4.4 BAEC and BASMC plating densities, locations, and culture times. BAEC and BASMC cultures were inoculated with a 1:1 plating density ratio of 1.25e5 cells/cm^2. BAECs in monoculture and coculture formats were always the most apical culture on the Transwell membrane. BASMCs in monoculture or coculture formats were either inoculated on the apical or basal side of the Transwell membrane or on the bottom surface of the companion well. The

total BASMC culture time in all monocultures and cocultures was 11 days. The total BAEC culture time in all monoculture and coculture arrangements was 5 days.

3.3.4.5 Monoculture and coculture notations and formats on Transwell Permeable Supports. The apical and basal locations of the Transwell membrane will be denoted as (a) and (b), respectively. The bottom surface of the companion well is denoted as (c). BAEC culture inoculums are abbreviated as (EC), and BASMC culture inoculums are abbreviated as (SMC). Monoculture formats are described by [Location (Inoculum)]. Coculture formats are described by [Location (First Inoculum); Location (Second Inoculum)]. Monoculture and coculture notations and formats are presented in Figure 3.2.

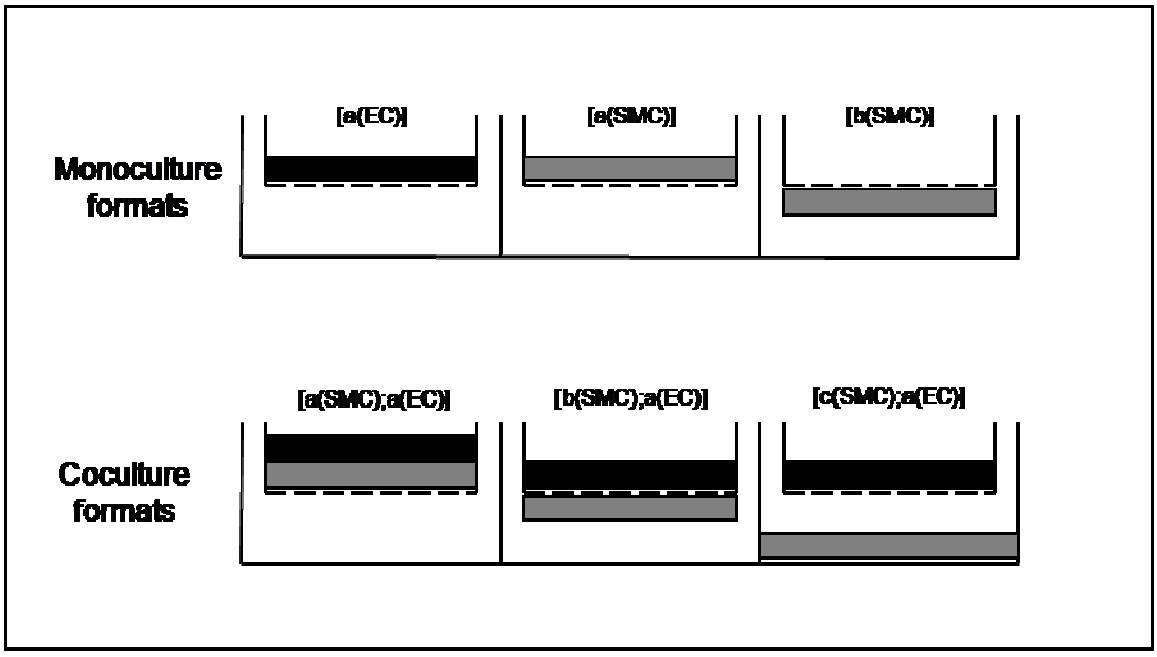

Figure 3.2. Schematic of BAEC and BASMC monoculture and coculture formats on Transwell membranes and companion wells. The horizontal dashed line indicates the location of the porous Transwell membrane. The black band indicates the location of BAEC cultures. The grey band indicates the location of BASMC cultures. Monoculture formats include [a(EC)], [a(SMC)], and [b(SMC)]. Coculture formats include [a(SMC);a(EC)], [b(SMC);a(EC)], and [c(SMC);a(EC)].

3.3.4.6 BAEC and BASMC monocultures and cocultures.

3.3.4.6.1 BAEC and BASMC monocultures

i) [a(EC)] monocultures:

A BAEC culture was inoculated on an apical FN coated Transwell membrane. The culture was supplied with either 10FB-MEM or 2.5FB-MEM and incubated for 5 days.

ii) [a(SMC)] and [b(SMC)] monocultures:

A BASMC culture was inoculated on either an apical or inverted basal FN coated Transwell membrane. Inverted Transwell membranes were incubated for 30 minutes while BASMCs settled and attached to the basal side of the membrane. Upright Transwell membranes with either apical or basal BASMC cultures were supplied with 10FB-MEM for 3 days. That culture media was then replaced with SF-MEM and the culture was incubated for 3 days. SF-MEM was then replaced with either 10FB-MEM or 2.5FB-MEM and the culture was incubated for 5 days.

3.3.4.6.2 BAEC and BASMC cocultures

i) [a(SMC);a(EC)] cocultures:

A BASMC culture was inoculated on an apical FN coated Transwell membrane and supplied with 10FB-MEM for 3 days. BASMC culture media was replaced with SF-MEM and the culture was returned to the incubator for 3 days. SF-MEM was then removed and the apical BASMC culture was coated with FN. A BAEC culture was then inoculated above the apical FN coat. The coculture was supplied with either 10FB-MEM or 2.5FB-MEM and incubated for 5 days.

ii) [b(SMC);a(EC)] cocultures:

A BASMC culture was inoculated on an inverted basal FN coated Transwell membrane. The inverted Transwell membrane was placed in an incubator for 30 minutes while BASMCs settled and attached to the basal side of the membrane. The upright Transwell membrane with basal

BASMC culture was then supplied with 10FB-MEM for 3 days. BASMC culture media was then replaced with SF-MEM and the culture was incubated for 3 days. SF-MEM was then removed and the apical side of the Transwell membrane was coated with FN. A BAEC culture was then inoculated on the apical side of the Transwell membrane. The coculture was then supplied with either 10FB-MEM or 2.5FB-MEM and cultured for 5 days.

iii) [c(SMC);a(EC)] cocultures:

A BASMC culture was inoculated on the bottom surface of a companion well and supplied with 10FB-MEM for 3 days. BASMC culture media was then replaced with SF-MEM and the culture was incubated for 3 days. A BAEC culture was then inoculated on the apical side of an FN coated Transwell membrane. BASMC culture media was then removed and the BAEC Transwell culture was paired with the BASMC culture in the companion well. The coculture was supplied with either 10FB-MEM or 2.5FB-MEM, respectively, and incubated for 5 days. These cocultures were dissociated on day 5 in order to measure endothelial L_p.

3.3.4.7 Calculating L_p of Transwell cultures. Fluid flux (J_v) across Transwell insert cultures was measured in pairs with a bubble tracking apparatus and those measurements were then used to calculate L_p. Both the bubble tracking apparatus and the equations for calculating L_p have been previously described[9] and are briefly explained here. Following the prescribed monoculture and coculture times with Transwell Permeable Supports, the Transwell insert was transferred to a bubble tracking apparatus. E-MEM was added above and below the Transwell insert culture to eliminate the development of an osmotic pressure gradient. The L_p calculation for each culture was reduced to the ratio of the E-MEM fluid flux, J_v, across the Transwell insert culture and the hydrostatic pressure gradient, $\Delta P = 10$ cmH_2O, driving the transmembrane fluid

flow (Equation 1). The units for J_v were cm/s and the units of L_p were cm/s/cmH_2O. Each measurement was repeated 6 times.

$$L_p = J_v / \Delta P \qquad \text{(Eqn. 1)}$$

3.3.4.8 Monoculture resistances-in-series models of coculture L_p. Hydraulic conductivity measurements for BAEC monocultures were combined with L_p measurements for BASMC monocultures to distinguish their deviations from actual coculture L_p given the absence of real heterotypic compositions. Monoculture L_p values were first inverted to represent hydraulic resistances (Equations 2, 3, and 4), which were then summed up in series. However, a PET membrane is included as a substrate in each monoculture and the hydraulic resistance of this membrane region ($R_{[PET]}$) was duplicated during series summations of monoculture hydraulic resistances. Therefore, a constant value for the hydraulic resistance of one porous membrane, $R_{[PET]}$ = 1.196e4 cmH_2O/cm/s ($L_{p[PET]}$ = 8.361e-5 cm/s/cmH_2O), was subtracted from combinations of monoculture hydraulic resistances in order to account for the hydraulic resistance of a single PET membrane that is present in the coculture formats. Each combination of monoculture hydraulic resistances was then inverted to represent a resistances-in-series model of coculture L_p (Equations 5 and 6).

$$R_{[a(EC)]} = 1/L_{p\,[a(EC)]} \qquad \text{(Eqn. 2)}$$

$$R_{[a(SMC)]} = 1/L_{p\,[a(SMC)]} \qquad \text{(Eqn. 3)}$$

$$R_{[b(SMC)]} = 1/L_{p\,[b(SMC)]} \qquad \text{(Eqn. 4)}$$

$$L_{p\,[a(EC)]+[a(SMC)]-[PET]} = 1/(R_{[a(EC)]} + R_{[a(SMC)]} - 1R_{[PET]}) \qquad \text{(Eqn. 5)}$$

$$L_{p\,[a(EC)]+[b(SMC)]-[PET]} = 1/(R_{[a(EC)]} + R_{[b(SMC)]} - 1R_{[PET]}) \qquad \text{(Eqn. 6)}$$

3.3.4.9 Statistical analysis of L_p. Hydraulic conductivity measurements for each culture format are presented as the mean L_p +/- the standard error of the mean (SEM). A Student's *t*-test with a

two-tailed distribution was used to determine the significance level, p, between paired L_p measurements. Hydraulic conductivity measurements for paired BAEC monocultures, paired BASMC monocultures, and cocultures paired with BAEC monocultures were considered statistically significant if $p < 0.05$.

A Bonferroni procedure was used to test for statistical significance between L_p of different coculture formats that were paired to BAEC monoculture L_p. Hydraulic conductivity measurements for cocultures were normalized to paired BAEC monoculture L_p. The critical significance level was corrected to $\beta_b = \alpha/k$. Where $k = 6$ pairwise comparisons between normalized L_p measurements for each coculture format and BAEC monoculture, and $\beta_b = 0.0083$. Normalized L_p were considered statistically significant when $p < 0.0083$.

A Bonferroni procedure was also used to test for statistical significance between L_p of monoculture resistances-in-series models, and related membrane cocultures that were normalized to paired BAEC monoculture L_p. The critical significance level was corrected to $\beta_b = \alpha/k$. Where $k = 3$ to account for the relationship among the modeled group and relevant coculture group and the endothelial monoculture group, and $\beta_b = 0.0167$. Modeled L_p were considered statistically significant compared to related coculture L_p measurements when $p < 0.0167$.

3.3.5 Immunofluorescence

3.3.5.1 Immunofluorescence solutions. Paraformaldehyde fixative was diluted with CMF-PBS to 1% PFA and filtered through a 0.45 μm syringe filter. Fixative was freshly made on the day of use. Triton X-100 was diluted with CMF-PBS to a 0.2% Triton X-100 permeabilizing solution. Blocking buffer consisted of BSA and Triton X-100 diluted in CMF-PBS to 10% BSA and 0.1% Triton X-100. Primary antibody (PAb) was diluted 15:1000 in blocking buffer. Secondary antibody (SAb) was diluted 2:1000 in blocking buffer.

3.3.5.2 Immunofluorescence of VE-cadherin in Transwell cultures. All rinses with CMF-PBS were immediately removed after being added. All Transwell filters remained in the same companion well throughout the immunofluorescence procedure. All solutions were added to the insert first and then, when required, to the companion well second. All solutions were carefully vacuum aspirated from the companion well first and then from the insert without touching the membrane. Rinses with CMF-PBS followed a ratio of 0.5 mL/insert and 1 mL/companion well. All steps were carried out in room temperature (RT) conditions and in a laminar flow hood.

Remaining cell culture media was aspirated. The culture was quickly rinsed once and, immediately, 0.5 mL of fixative was added to the apical side of the insert. The culture was fixed for 10 minutes. Fixative was then removed. The culture was then rinsed once and 0.5 mL of permeabilizing solution was added to the apical side of the insert. The culture was permeabilized for 10 minutes. Permeabilizing solution was then removed. The culture was rinsed once and 0.5 mL of blocking buffer was added to the apical side of the insert. The culture was blocked for 60 minutes. Meanwhile, the PAb dilution was prepared. Blocking buffer was then removed. The culture was rinsed once and 200 µL of diluted PAb was added the apical side of the insert. The culture was incubated at RT with PAb for 3 hours. Meanwhile, in a dark room, SAb dilution was prepared. PAb was then removed and the culture was rinsed five times. The remaining steps were all carried out in a dark environment.

200 µL of diluted SAb was added to the apical side of the insert. The culture was incubated at RT with SAb for 60 minutes. SAb was then removed and the culture was rinsed four times. 0.5 mL of rinse solution was added to the apical side of the insert and the insert was transferred to a clean glass slide set on a Nikon TE 2000 microscope stage equipped with epi-fluorescence microscopy and MetaVue Imaging Software (Universal Imaging Corp. PA). The culture was

imaged in the center field and then in four peripheral fields with a 10x objective. Five more similar fields were imaged with a 20x objective.

3.3.6 Morphometric Analysis

3.3.6.1 BAEC shape factors. The shape factors of BAECs in VE-cadherin immunostained monocultures and cocultures were calculated using the instructions that were provided in the MetaVue software. Briefly, a trace region tool was used to outline individual BAECs. MetaVue's Region Statistics of the outline generated calibrated pixel areas and perimeters for each cell. The shape factors for BAECs were then calculated with the formula $(4\pi * area)/(perimeter)^2$, where values ranged between zero and one; a value of one is a perfect circle and a value near zero is a flattened or elongated object.

3.3.6.2 Statistical analysis of shape factors. A Student's *t*-test with a two-tailed distribution was used to test for the statistical significance level, p, between BAEC shape factors from paired culture formats. BAEC shape factors for each culture format were considered statistically significant compared to BAECs in monoculture [a(EC)] 10FB-MEM if $p < 0.05$.

3.4 Results

3.4.1 BAEC monoculture L_p. The L_p measurements of BAEC monocultures supplied with 10FB-MEM were paired with L_p measurements of BAEC monocultures supplied with 2.5FB-MEM and are presented in Figure 3.3. BAEC monocultures supplied with 2.5FB-MEM had a significantly lower L_p than monocultures supplied with 10FB-MEM.

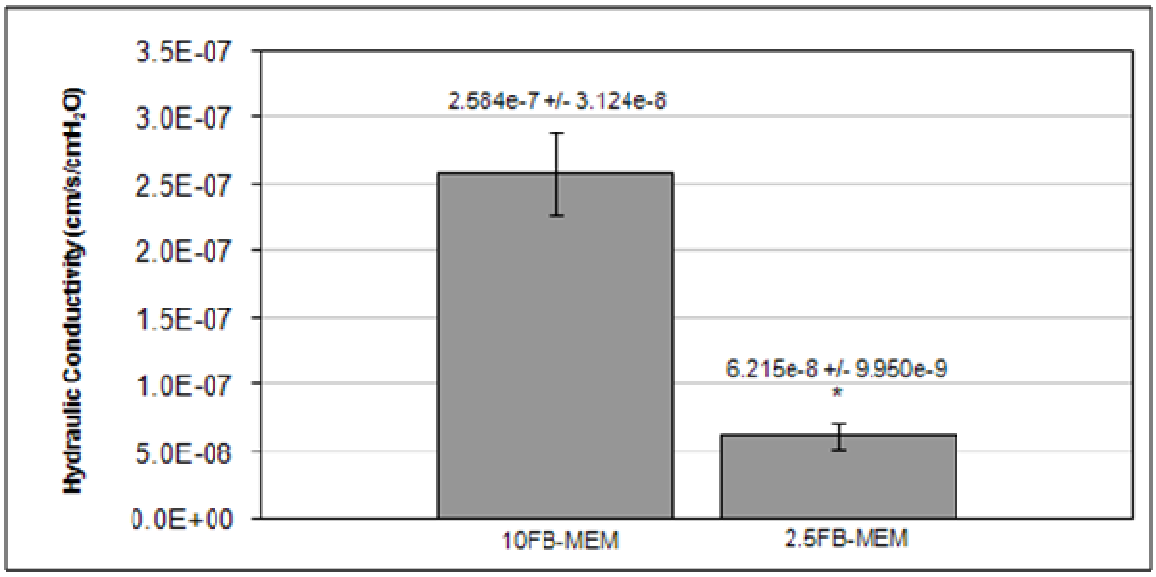

Figure 3.3. Hydraulic conductivity of 5 day apical EC ([a(EC)]) monocultures supplied with 10FB-MEM and 2.5FB-MEM. Data are presented as mean +/- SEM. * - $p < 0.05$ compared to 10FB-MEM; n = 6.

3.4.2 BASMC monoculture L_p. The L_p measurements of BASMC monocultures supplied with 10FB-MEM were paired with the L_p measurements of BASMC monocultures supplied with 2.5FB-MEM and are presented in Figures 3.4 and 3.5. Figure 3.4 shows that apical cultures of BASMCs in the format [a(SMC)] that were supplied with 2.5FB-MEM had a significantly higher L_p than when supplied with 10FB-MEM. Figure 3.5 identifies that similar changes made to serum content did not significantly alter L_p when BASMCs were cultured on the basal side of the insert in the format [b(SMC)]. The L_p values in the [a(SMC)] configuration were lower than the [b(SMC)] configuration.

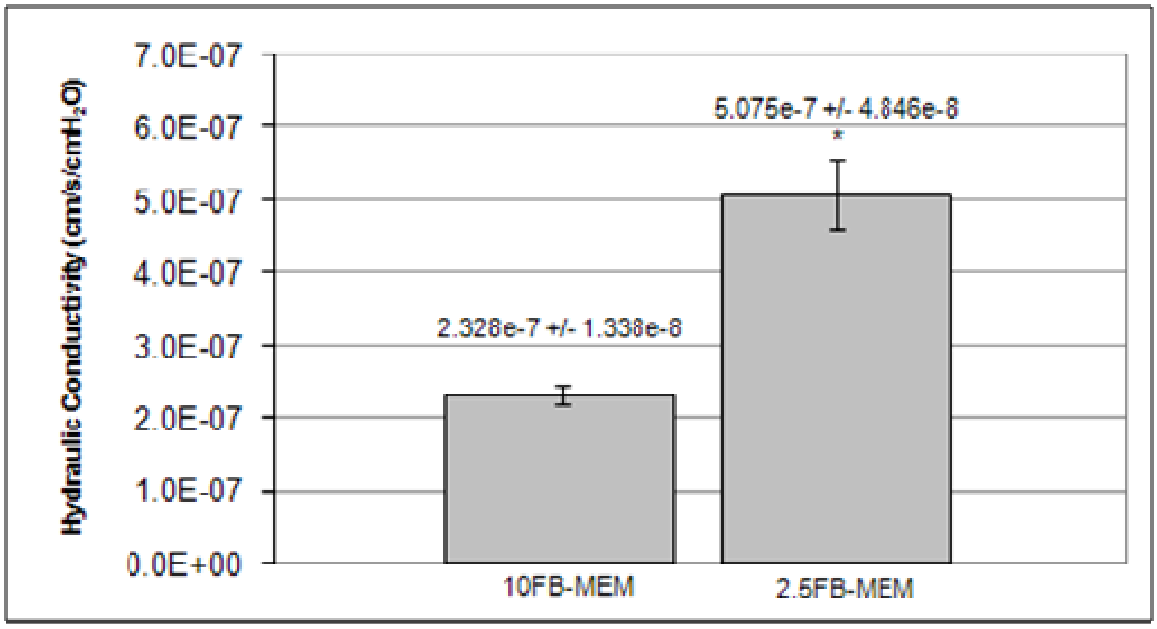

Figure 3.4. Hydraulic conductivity of 11 day apical SMC ([a(SMC)]) monocultures supplied with 10FB-MEM and 2.5FB-MEM. Data are presented as mean +/- SEM. * - $p < 0.05$ compared to 10FB-MEM; n = 6.

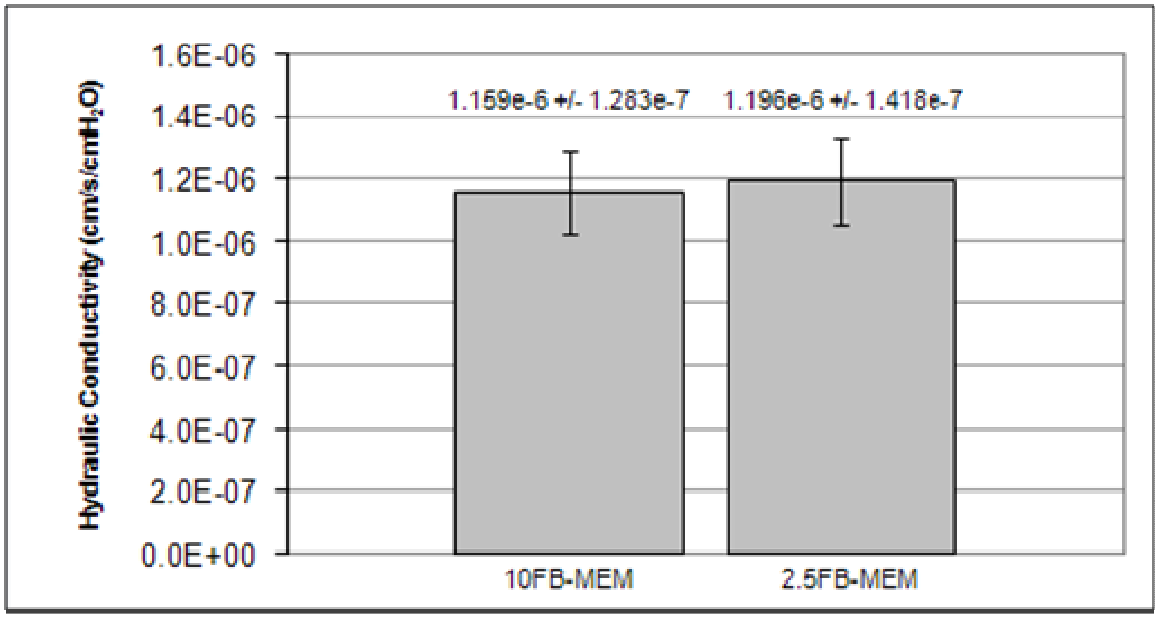

Figure 3.5. Hydraulic conductivity of 11 day basal SMC ([b(SMC)]) monocultures supplied with 10FB-MEM and 2.5FB-MEM. Data are presented as mean +/- SEM. n = 6.

3.4.3 BAEC-BASMC coculture L_p. The L_p measurements of each coculture format supplied with either 10FB-MEM or 2.5FB-MEM were paired with the L_p measurements of BAEC monocultures supplied with either 10FB-MEM or 2.5FB-MEM, respectively. The L_p of each coculture was normalized to the paired L_p of each BAEC monoculture. The normalized mean L_p values of each coculture format for either 10FB-MEM or 2.5FB-MEM are presented in Figures 3.6 and 3.7, respectively. In both Figures 3.6 and 3.7, [a(SMC);a(EC)] L_p and [c(SMC);a(EC)] L_p values were significantly higher than [a(EC)] L_p. Figure 3.7 also shows that [c(SMC);a(EC)] L_p was significantly lower than [a(SMC);a(EC)] L_p.

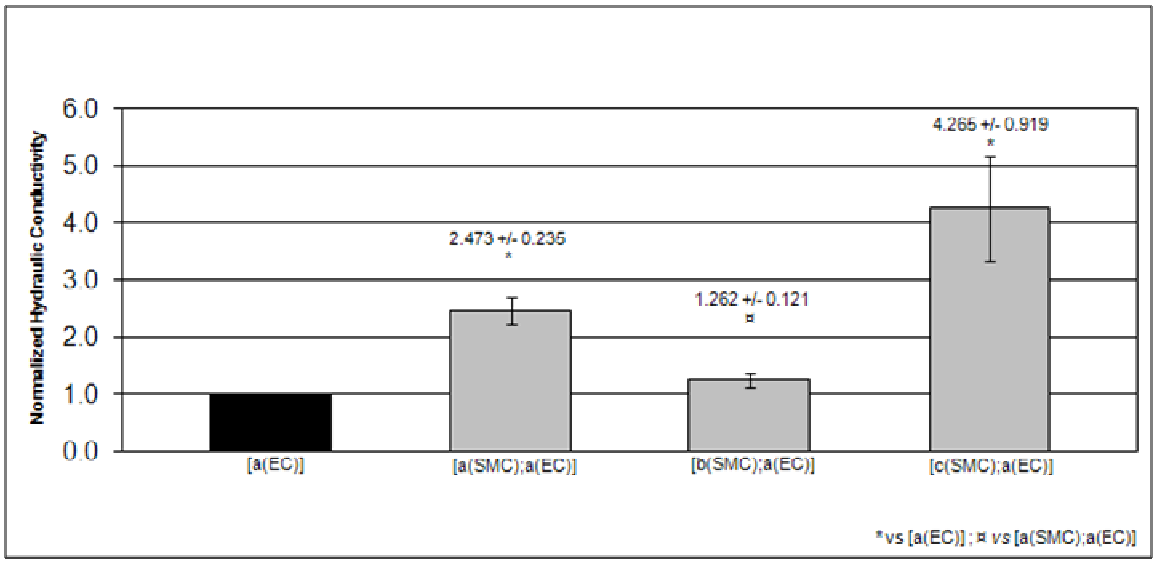

Figure 3.6. Hydraulic conductivity of each coculture [a(SMC);a(EC)], [b(SMC);a(EC)], and [c(SMC);a(EC)] normalized to the mean L_p of paired endothelial monocultures [a(EC)]. Each culture format was supplied with 10FB-MEM. Statistical significance ($p < 0.05$) of coculture L_p normalized to paired endothelial L_p were denoted by a * symbol (* *vs* [a(EC)]). A ¤ symbol denotes statistically significant differences of multiple ($\beta_b = \alpha/6 = 0.0083$) pairwise comparisons using a Bonferroni correction. ¤ indicates normalized L_p values of each culture that were statistically significant compared to the normalized L_p of [a(SMC);a(EC)] coculture (¤ *vs* [a(SMC);a(EC)]). n = 6.

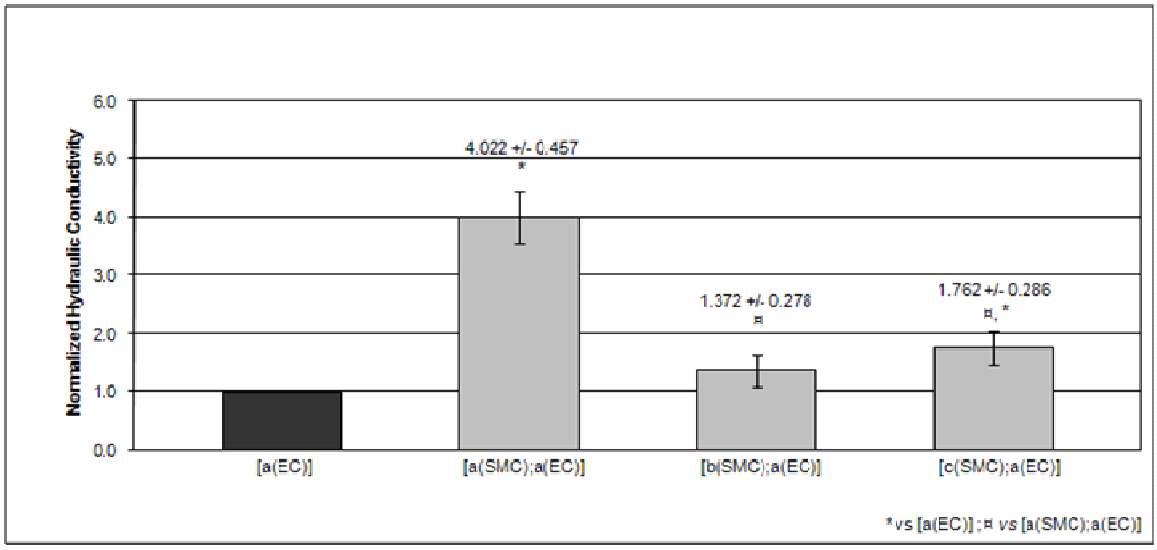

Figure 3.7. Hydraulic conductivity of each coculture [a(SMC);a(EC)], [b(SMC);a(EC)], and [c(SMC);a(EC)] normalized to the mean L_p of paired endothelial monocultures [a(EC)]. Each culture format was supplied with 2.5FB-MEM. Statistical significance ($p < 0.05$) of coculture L_p normalized to paired endothelial L_p were denoted by a * symbol (* *vs* [a(EC)]). A ¤ symbol denotes statistically significant differences of multiple ($\beta_b = \alpha/6 = 0.0083$) pairwise comparisons using a Bonferroni correction. ¤ indicates normalized L_p values of each culture that were statistically significant compared to the normalized L_p of [a(SMC);a(EC)] coculture (¤ *vs* [a(SMC);a(EC)]). n = 6.

3.4.4 Monoculture resistances-in-series models of coculture L_p. Resistances-in-series models of coculture L_p (Eqn. 5 and 6) representative of each membrane coculture configuration were normalized to paired endothelial monoculture L_p. Mean resistances-in-series L_p values were plotted along with L_p measurements of the real membrane cocultures that were supplied with either 10FB-MEM (Figure 3.8) or 2.5 FB-MEM (Figure 3.9) in order to distinguish the influence of actual heterotypic arrangements. In Figure 3.8, [a(EC)] + [b(SMC)] – 1[PET], and [a(EC)] + [c(SMC)] – 1[PET] resistances-in-series L_p values were significantly lower than the actual [b(SMC);a(EC)], and [c(SMC);a(EC)] L_p measurements, respectively. In Figure 3.9, the [a(EC)] + [a(SMC)] -1[PET] resistances-in-series L_p values were significantly lower than the actual [a(SMC);a(EC)] L_p .

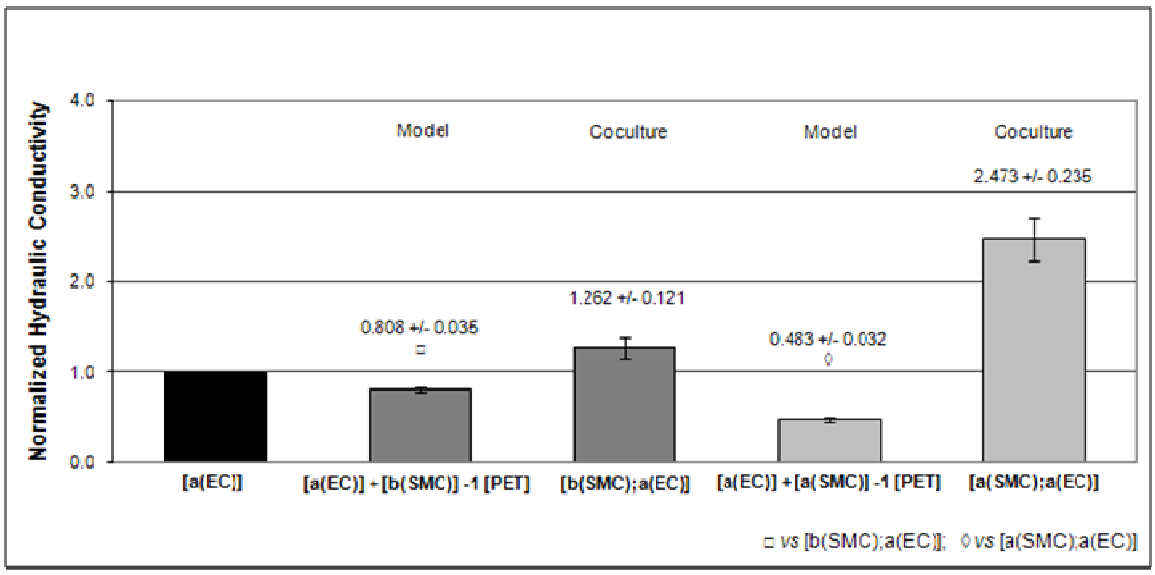

Figure 3.8. Hydraulic conductivities of membrane cocultures [a(SMC);a(EC)], [b(SMC);a(EC)], and resistances-in-series model predictions of membrane coculture formats [a(EC)] + [a(SMC)], [a(EC)] + [b(SMC)] normalized to the mean L_p of paired endothelial monocultures [a(EC)]. Each culture was supplied with 10FB-MEM. The critical significance level was corrected to $\beta_b = \alpha/3 = 0.0167$ to account for a specific membrane coculture group, a resistances-in-series model, and the paired endothelial monoculture group. Statistical significance ($p < \beta_b$) of resistances-in-series L_p compared to related membrane coculture L_p was denoted by □ and ◊ symbols (□ *vs* [b(SMC);a(EC)]; and ◊ *vs* [a(SMC);a(EC)]). n = 6.

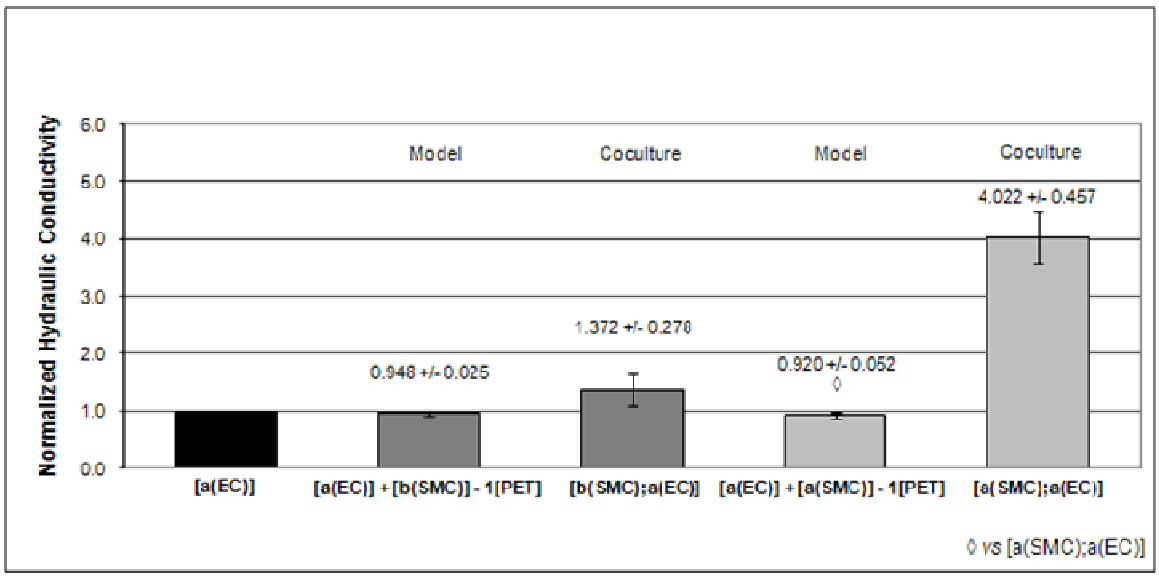

Figure 3.9. Hydraulic conductivities of membrane cocultures [a(SMC);a(EC)], [b(SMC);a(EC)], and resistances-in-series model predictions of membrane coculture formats [a(EC)] + [a(SMC)], [a(EC)] + [b(SMC)] normalized to the mean L_p of paired endothelial monocultures [a(EC)]. Each culture was supplied with 2.5FB-MEM. The critical significance level was corrected to $\beta_b = \alpha/3 = 0.0167$ to account for a specific membrane coculture group, a resistances-in-series model, and the paired endothelial monoculture group. Statistical significance ($p < \beta_b$) of resistances-in-series L_p compared to related membrane coculture L_p was denoted by a ◊ symbol (◊ *vs* [a(SMC);a(EC)]). n = 6.

3.4.5 Immunostaining of VE-cadherin. BAEC VE-cadherin was immunostained for each coculture and BAEC monoculture. Center field 10x objective images for each coculture and BAEC monoculture supplied with either 10FB-MEM or 2.5FB-MEM are presented in Figure 3.10. VE-cadherin was expressed in each culture format and was localized at the cell border as expected. Endothelial cells imaged in coculture [a(SMC);a(EC)] with 10FB-MEM appeared more circular, and BAECs imaged in [c(SMC);a(EC)] with 2.5FB-MEM appeared more elongated when compared to any of the other cultures.

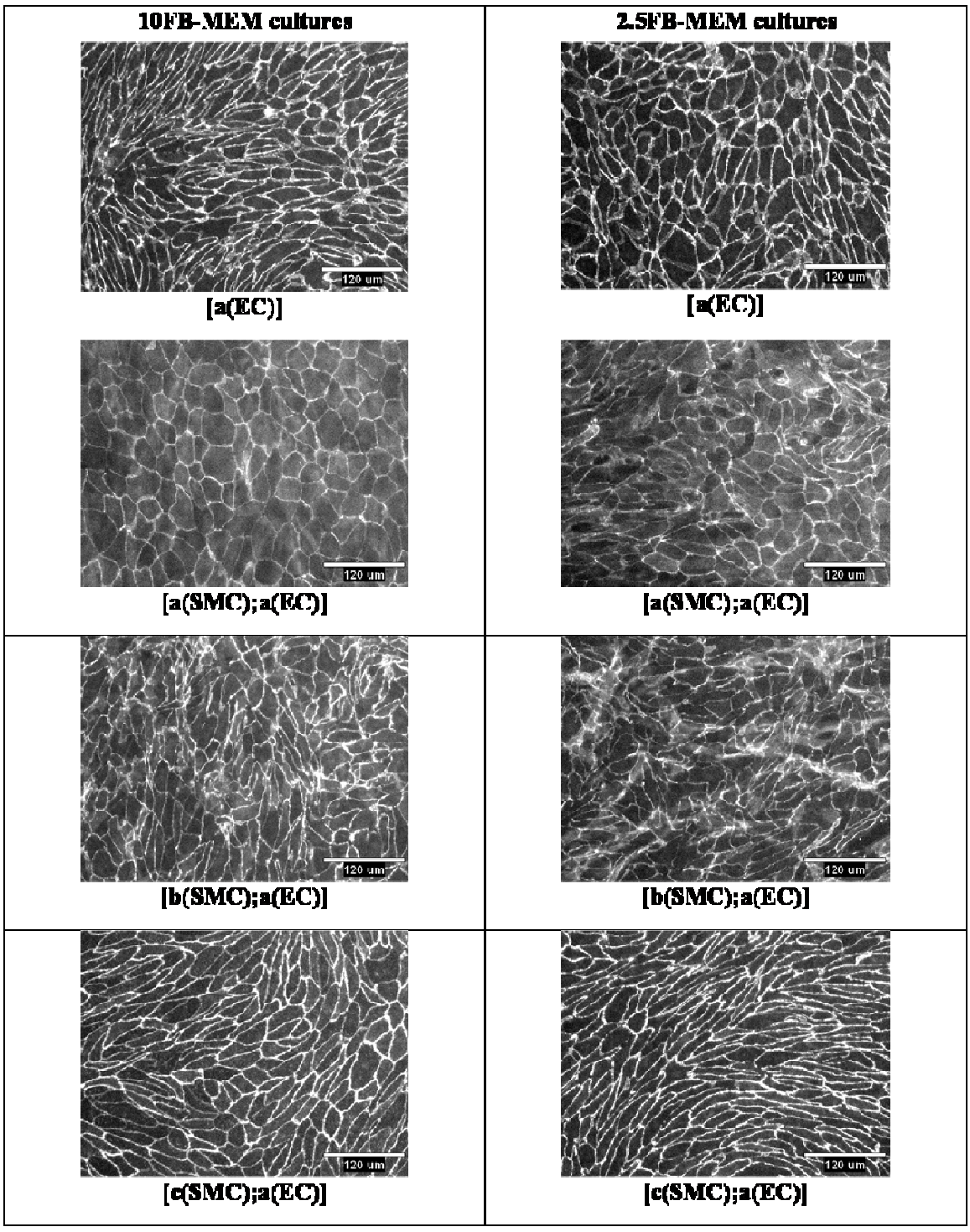

Figure 3.10. Representative images of VE-cadherin immunostaining in BAEC monocultures and cocultures supplied with either 10FB-MEM or 2.5FB-MEM. 10x objective. Scale bar 120 um.

3.4.6 BAEC morphometry. The sample mean, standard deviation (SD), and SEM for random samples of 10 BAEC shape factors from each culture format are presented in Table 3.1. The mean shape factor for BAECs in the [a(SMC);a(EC)] coculture supplied with 10FB-MEM was much closer to one, and the mean shape factor for BAECs in the [c(SMC);a(EC)] coculture supplied with 2.5FB-MEM was much closer to zero, when compared to any other culture, which indicated that these BAECs were the most circular and the most elongated, respectively. In addition, the BAEC shape factors for both of those cocultures were significantly different in comparison to the shape factors for BAECs in the 10FB-MEM [a(EC)] monoculture.

Table 3.1. Sample means, SDs, and SEMs for BAEC shape factors (n = 10) for each culture format. *p < 0.05 compared to [a(EC)] 10FB-MEM; n = 10.

	Culture Format							
	[a(EC)]		[a(SMC);a(EC)]		[b(SMC);a(EC)]		[c(SMC);a(EC)]	
Media(MEM)	10FB	2.5FB	10FB	2.5FB	10FB	2.5FB	10FB	2.5FB
Sample mean (n=10)	0.5291	0.5865	0.7764*	0.6357	0.5063	0.4584	0.5478	0.3563*
SD (+/-)	0.0847	0.1179	0.0673	0.1729	0.1184	0.1302	0.1441	0.1421
SEM (+/-)	0.0268	0.0373	0.0213	0.0547	0.0374	0.0412	0.0456	0.0449

3.5 Discussion

3.5.1 Serum concentration modulates BAEC L_p. The influence of serum concentration on BAEC L_p response was determined by first growing BAEC monocultures in either 2.5FB-MEM or 10FB-MEM for 5 days and then measuring L_p. Hydraulic conductivity of [a(EC)] supplied with 2.5FB-MEM was found to be significantly lower than the L_p of [a(EC)] supplied with 10FB-MEM (Figure 3.3) by a factor of 4. This is possibly due to a decrease in EC motility and turnover in lower serum[5, 12]. This indicates that, *in-vitro*, endothelial L_p function is directly related to the percentage of serum that is present in culture media.

3.5.2 Membrane location and serum concentration alters BASMC L_p. BASMC monocultures were inoculated on either the apical or basal side of porous membranes to identify the influence that the membrane location may have on isolated BASMC L_p. During apical and basal BASMC culture periods, proliferation was temporarily suspended through direct adaptation to SF-MEM and then supplied with either 10FB-MEM or 2.5FB-MEM to regulate SMC proliferation rates. The L_p of [a(SMC)] supplied with 2.5FB-MEM was significantly higher than [a(SMC)] supplied with 10FB-MEM (Figure 3.4) suggesting that the proliferation rate of apical membrane BASMC cultures affects their L_p response. Proliferation rates would be expected to be higher in high serum[22], contributing to more cell mass to reduce L_p. However, L_p of [b(SMC)] cultures supplied with either 10FB-MEM or 2.5FB-MEM were not different from each other (Figure 3.5), and were higher in magnitude than the L_p of [a(SMC)] cultures (Figure 3.4). The transition to much higher L_p values for the [b(SMC)] configuration (Figure 3.5) compared to the [a(SMC)] configuration (Figure 3.4) may be explained by several possible mechanisms. A previous mathematical model[26] of fluid flowing through the pores of an internal elastic lamina (like the supporting filter) demonstrated that the laminar profile of fluid flow in the pore

becomes complex at the exit site of individual pores draining into a layer of SMCs. This may contribute to loosen cell connections to the membrane and lowering resistance. It is also very likely that gravitational settling prevents SMC from accumulating in the [b(SMC)] case.

3.5.3 Arterial cocultures exhibit a range of L_p. In healthy arteries, the intimal and medial regions, which consist of an endothelial monolayer and dense multilayered SMCs, respectively, share the same porous internal elastic lamina[14]. Our coculture [b(SMC);a(EC)] best mimics this organization. During events such as intimal hyperplasia and fibroatheroma formation, medial vascular SMCs breach the porous lamina and take up residence in the intima, which subsequently leads to a closer proximity between an intact endothelium and intimal SMCs[25]. Coculture [a(SMC);a(EC)] represents that intimal arrangement of ECs and SMCs.

Measurements of L_p for each coculture supplied with either 10FB-MEM or 2.5FB-MEM were paired with measurements of [a(EC)] monoculture L_p that were supplied with either 10FB-MEM (Figure 3.6) or 2.5FB-MEM (Figure 3.7). While the L_p of [b(SMC);a(EC)] cocultures were similar to that of [a(EC)] monocultures in both 10FB-MEM and 2.5FB-MEM (Figures 3.6 and 3.7), the L_p of [a(SMC);a(EC)] cocultures were significantly higher than [b(SMC);a(EC)] cocultures for both serum conditions (Figures 3.6 and 3.7). Those variations in coculture L_p demonstrate how EC-SMC arrangements on the porous membrane can regulate arterial L_p. In particular, coculture L_p is significantly elevated when ECs and SMCs are placed in the closest possible proximity to each other, and above a porous membrane.

3.5.4 Coculturing in shared media influences BAEC L_p. Coculture configuration [c(SMC);a(EC)] separates ECs from SMCs by approximately 1 mm, and permits interactions that are restricted to soluble factors in the shared media (Figure 3.2). That *in-vitro* coculture arrangement differs from *in-vivo* vascular wall anatomies where the porous elastic lamina forms

an interface between ECs and SMCs. However, ECs, which were cultured in shared media had a significantly higher L_p compared to [a(EC)] monocultures (Figures 3.6 and 3.7). Also, the L_p of ECs derived from shared media cocultures [c(SMC);a(EC)] were higher than related cocultures [b(SMC);a(EC)] where cell could interact through membrane processes potentially plugging pores and increasing resistance (Figures 3.6 and 3.7). These significant changes in L_p reinforce that L_p is regulated by soluble and physical heterotypic interactions and serum concentration.

3.5.5 Comparison of coculture to monoculture resistances-in-series modeled L_p. Resistances-in-series modeled L_p values were derived from series combinations of monoculture hydraulic resistances (Figures 3.8 and 3.9). Those resistances-in-series modeled L_p were lower than the L_p values for ECs alone in [a(EC)] monocultures when supplied with 10FB-MEM (Figure 3.8), and nearly identical to the values of [a(EC)] L_p in 2.5FB-MEM (Figure 3.9). This serum-dependent change in resistances-in-series L_p indicates that the SMC component can provide additional resistance to J_v (recall Figures 3.4 and 3.5).

Actual [a(SMC);a(EC)] coculture L_p was significantly higher than the related monoculture resistances-in-series modeled L_p in both 10FB-MEM (Figure 3.8) and 2.5FB-MEM (Figure 3.9) conditions. A similar, but much smaller, effect on L_p was observed between modeled and actual [b(SMC);a(EC)] coculture L_p (Figures 3.8 and 3.9). These significant deviations between modeled and actual coculture L_p values shown in Figures 3.8 and 3.9 distinguish the effects of true heterotypic interactions.

Since the [a(SMC);a(EC)] coculture configuration most closely represents the intimal organization of ECs and SMCs in intimal hyperplasia and fibroatheroma, it is tempting to conclude that this heterotypic configuration diminishes the transport barrier for blood vessels, tending to sustain disease states. Reversing the inoculation order of ECs and SMCs may work to

lower arterial L_p, compared to EC monocultures. Additional research will also be required to elaborate upon local mechanical and chemical signaling mechanisms that mediate transport in arterial cocultures.

3.5.6 Coculture arrangements regulate patterns in BAEC morphology. Contact-inhibited formation of BAEC monolayers is a characteristic homotypic function. Figure 3.10 shows that the ECs in apical coculture, [a(SMC);a(EC)] with 10FB-MEM, displayed a more circular morphology than ECs in any other culture configuration. Also, ECs in shared media coculture, [c(SMC);a(EC)] with 2.5FB-MEM, displayed a more elongated morphology in comparison to any other cell culture arrangement. Endothelial cell shape factor comparisons to BAECs in the [a(EC)] 10FB-MEM culture condition, shown in Table 3.1, confirmed that the BAECs in [a(SMC);a(EC)] 10FB-MEM conditions, and those in [c(SMC);a(EC)] 2.5FB-MEM conditions were in fact significantly more circular, and elongated, respectively. A decrease in the area of intercellular junctions (that provide the pathway for J_v) per unit of surface area is a consequence of the circular pattern of BAECs in [a(SMC);a(EC)] arterial cocultures (Figure 3.10 and Table 3.1). And yet the [a(SMC);a(EC)] coculture displayed a significantly higher L_p than [a(EC)] monocultures (Figures 3.6 and 3.7). Therefore, along with limited contributions from the EC region, the SMC region in [a(SMC);a(EC)] cocultures collectively work to diminish the overall resistance to J_v that is necessary for significantly elevating L_p. In summary, the circular BAEC morphology pattern (Figure 3.10 and Table 3.1) and the significant elevation in L_p (Figures 3.6 and 3.7) for [a(SMC);a(EC)] cocultures are the products of coculturing ECs and SMCs on the apical side of a porous membrane to achieve the closest possible heterotypic configuration.

Various coculturing methods have been exploited to capture more *in-vivo*-like tissue features, in comparison to endothelial monocultures. For example, elongated EC shapes were noticed when

cultured directly above a matrix of collagen type I gel that was embedded with SMCs[29]. Previous studies[16] have also shown that coculturing techniques modulate a variety of protein secretions from both ECs and SMCs. It was demonstrated that directly coculturing ECs on top of preexisting SMCs led to different VEGF, PDGF-BB, TGF-β and bFGF secretions from both ECs and SMCs[16]. The EC-SMC coculture construct in that study[16] differed from our [a(SMC);a(EC)] coculture (Figure 3.2) by excluding basal culture media and a porous membrane necessary for J_v.

Coculturing methods in another study[23], which incorporated an intervening porous membrane between ECs and SMCs, induced changes in endothelial secretions of IL-1 and MCP-1. Smooth muscle cells were also classified as being either 'more' or 'less secretory' as a result of changes in serum content in culture media[23]. While the proximity and inoculation order of ECs and SMCs in that coculture were most similar to coculture format [b(SMC);a(EC)] (Figure 3.2), the culture time differed and a transmural J_v was not present.

3.5.7 Concluding remarks. In the present study, all preexisting osmotic pressure effects were removed from each culture condition prior to introducing J_v, and measuring L_p. Serum level in cultures had a significant influence in regulating L_p of arterial cocultures. Increasing the serum concentration in culture by four fold resulted in a proportionate increase in [a(EC)] L_p. This was likely a result of increased EC motility and turnover in higher serum. Also, L_p of arterial coculture [a(SMC);a(EC)] was significantly higher than the L_p of ECs alone or cocultures with an intervening porous membrane [b(SMC);a(EC)]. This coculture L_p result was associated with a characteristic rounding of the ECs and emphasized the difference between direct EC-SMC contact, as in intimal hyperplasia and atherogenesis, and close proximity of ECs and SMCs, as in

normal arterial development with an intact IEL. Overall, we have demonstrated that arterial L_p is an inextricable result of EC and SMC coculture arrangements.

3.6 References

1. Aiello V.D., P.S. Gutierrez, M.J.F. Chaves, A.A.B. Lopes, M.L. Higuchi, and J.A.F. Ramires. Morphology of the internal elastic lamina in arteries from pulmonary hypertensive patients: a confocal laser microscopy study. Mod. Pathol. 16(5): 411-416, 2003.

2. Ainslie K.M., J.S. Garanich, R.O. Dull, and J.M. Tarbell. Vascular smooth muscle cell glycocalyx influences shear stress-mediated contractile response. J. Appl. Physiol. 98: 242-249, 2005.

3. Borg-Capra C., M. Fournet-Bourguignon, P. Janiak, N. Villeneuve, J. Bidouard, J. Vilaine, and P.M. Vanhoutte. Morphological heterogeneity with normal expression but altered function of G proteins in porcine cultured regenerated coronary endothelial cells. Br. J. Pharmacol. 122: 999-1008, 1997.

4. Cancel L.M., A. Fitting, and J.M. Tarbell. In-vitro study of LDL transport under pressurized (convective) conditions. Am. J. Physiol. Heart Circ. Physiol. 293: H126-H132, 2007.

5. Castellot, Jr. J.E., M.J. Karnovsky, and B.M. Spiegelman. Potent stimulation of vascular endothelial cell growth by differentiated 3t3 adipocytes. Cell Biol. 77(10): 6007-6011, 1980.

6. Chang Y.S., J.A. Yaccino, S. Lakshminarayanan, J.A. Frangos, and J.M. Tarbell. Shear-induced increases in hydraulic conductivity in endothelial cells is mediated by a nitric oxide-dependent mechanism. Arterioscler. Thromb. Vasc. Biol. 20: 35-42, 2000.

7. Chiu J., L. Chen, P. Lee, C. Lee, L. Lo, S. Usami, and S. Chien. Shear stress inhibits adhesion molecule expression in vascular endothelial cells induced by coculture with smooth muscle cells. Blood 101: 2667-2674, 2003.
8. Civelek M., K. Ainslie, J.S. Garanich, and J.M. Tarbell. Smooth muscle cells contract in response to fluid flow via a Ca+-independent signaling mechanism. J. Appl. Physiol. 93: 1907-1917, 2002.
9. DeMaio L., J.M. Tarbell, R.C. Scaduto, T.W. Gardner, and D.A. Antonetti. A transmural pressure gradient induces mechanical and biological adaptive responses in endothelial cells. Am. J. Physiol. Heart Circ. Physiol. 286: 731-741, 2004.
10. De Wit C., M. Boettcher, and V.J. Schmidt. Signaling across myoendothelial gap junctions – fact or fiction? Cell Commun. Adhes. Sep 15(3):231-245, 2008.
11. Dull R.O., H. Jo, H. Sill, T.M. Hollis, and J.M. Tarbell. The effect of varying albumin concentration and hydrostatic pressure on hydraulic conductivity and albumin permeability of cultured endothelial monolayers. Microvasc Res 41(3): 390-407, 1991.
12. Duthu G.S. and J.R. Smith. In vitro proliferation and lifespan of bovine aorta endothelial cells: effect of culture conditions and fibroblast growth factor. J. Cell Physiol. 103(3): 385-392, 1980.
13. Fillinger M.F., L.N. Sampson, J.L. Cronenwett, R.J. Powell, and R.J. Wagner. Coculture of endothelial cells and smooth muscle cells in bilayer and conditioned media models. J. Surg. Res. 67: 169-178, 1997.
14. Gartner L.P., and J.L. Hiatt. “Circulatory System.” In: Color Textbook of Histology, edited by Philadelphia: Saunders Co., 2001, pp. 251-256.

15. Heberlein K., A. Straub, and B.E. Isakson. The myoendothelial junction: breaking through the matrix? Microcirculation 16(4): 307-322, 2009.

16. Heydarkhan-Hagvall S., G. Helenius, B.R. Johansson, J.Y. Li, E. Mattsson, and B. Risberg. Co-culture of endothelial cells and smooth muscle cells affects gene expression of angiogenic factors. J. Cell Biochem. 89: 1250-1259, 2003.

17. Hillsley M.V., and J.M. Tarbell. Oscillatory shear alters endothelial hydraulic conductivity and nitric oxide levels. Biochem. Biophys. Res. Commun. 293: 1466-1471, 2002.

18. Kurzen H., S. Manns, G. Dandekar, T. Schmidt, S. Pratzel, and B.M. Kräling. Tightening of endothelial cell contacts: a physiologic response to cocultures with smooth muscle-like 10 T1/2 cells. J. Invest. Dermatol. 119: 143-153, 2002.

19. Lavender M.D., Z. Pang, C.S. Wallace, L.E. Niklason, and G.A. Truskey. A system for direct co-culture of endothelium on smooth muscle cells. Biomaterials 26: 4642-4653, 2005.

20. Li G., Simon M.J., Cancel L.M., Shi Z.D., Ji X., Tarbell J.M., Morrison B. 3rd, and Fu B.M. Permeability of endothelial and astrocyte cocultures: in vitro blood brain barrier models for drug delivery studies. Ann. Biomed. Eng. 38(8): 2499-2511, 2010.

21. Pang Z., Niklason L.E., and Truskey G.A. Porcine endothelial cells cocultured with smooth muscle cells became procoagulant in vitro. Tissue Eng. Part A. 16(6): 1835-1844, 2010.

22. Patel N.A., C.E. Chalfant, M. Yamamoto, J.E. Watson, D.C. Eichler, and D.R. Cooper. Acute hyperglycemia regulates transcription and posttranscriptional stability of PKCbetaII mRNA in vascular smooth muscle cells. FASEB J. 13: 103–113, 1999.

23. Rose S.L., and J.E. Babensee. Complimentary endothelial cell/smooth muscle cell co-culture systems with alternate smooth muscle cell phenotypes. Ann. Biomed. Eng. 35: 1382-1390, 2007.

24. Ryan U.S., J.W. Ryan, and C. Whitaker. How do kinins affect vascular tone? Adv. Exp. Med. Biol. 120A:375-391, 1979.

25. Stary H.C., B. Chandler, R.E. Dinsmore, V. Fuster, S. Glagov, W. Insull Jr., M.E. Rosenfeld, C.J. Schwartz, W.D. Wagner, and R.W. Wissler. A definition of advanced types of atherosclerotic lesions and a histological classification of atherosclerosis: a report from the committee on vascular lesions of the council on atherosclerosis, American Heart Association. Circulation 92: 1355-1374, 1995.

26. Tada S., and J.M. Tarbell. Interstitial flow through the internal elastic lamina affects shear stress on arterial smooth muscle cells. Am. J. Physiol. Heart Circ. Physiol. 278: 1589-1597, 2000.

27. Tarbell J.M. Shear stress and the endothelial transport barrier. Cardiovasc. Res. 87: 320-330, 2010.

28. Tarbell J.M., L. DeMaio, and M.M. Zaw. Effect of pressure on hydraulic conductivity of endothelial monolayers: role of endothelial cleft shear stress. J. Appl. Physiol. 87: 261-268, 1999.

29. Ziegler T., R.W. Alexander, and R.M. Nerem. An endothelial cell-smooth muscle cell co-culture model for use in the investigation of flow effects in vascular biology. Ann. Biomed. Eng. 23:216-225, 1995.

CHAPTER 4

HYDRAULIC CONDUCTIVITY OF BOVINE AORTIC ENDOTHELIAL CELLS EXPOSED TO CONTINUOUS TRANSMURAL MEDIA PERFUSION

4.1 Abstract

Endothelial cells (ECs), *in-vivo,* are continuously exposed to tran**s**mural flow driven by a pressure gradient across the blood vessel wall. Here, we describe an *in-vitro* system that cultures bovine aortic endothelial cells (BAECs) with physiological levels of continuous transmural media perfusion. We then use hydraulic conductivity (L_p) measurements to characterize the effect of transmural flow on the endothelial transport barrier. Previous *in-vitro* studies[20] have shown that EC exposure to transmural flow for up to 6 hours led to a significant increase in EC L_p. Our results show that EC L_p, after exposure to 48 hours of transmural flow, is not significantly different from L_p obtained after 1 hour of transmural flow. This implies that, after an initial transient increase in L_p, EC monolayers adapt to transmural flow and L_p values return to their original baseline levels.

4.2 Introduction

While perfusion culture devices gained early successes in extending the *in-vitro* life of whole organ cultures[14], a more practical approach to sustaining smaller scale *in-vitro* cell cultures, such as arterial endothelial cells (ECs), is to replace the complexities of continuous media perfusion systems with the periodic replacement of culture media. However, arterial wall viability is supported by a continuous supply of nutrients that is delivered by perfusion from the lumen and diffusion from the vasa vasorum[1, 9, 10, 25]. In particular, intimal arterial regions are nourished primarily from luminal blood and may also receive supplemental nutrients diffusing from the vasa vasorum of medial and adventitial regions[9, 25].

Luminal blood perfusion across the arterial wall is driven by a transmural pressure gradient. Theoretical modeling of flow through the intima[17, 18] describes how pressure driven interstitial fluid flow enters through the clefts between ECs and exits through internal elastic lamina pores. Acute (1 hour) hydraulic conductivity (L_p) across EC cultures has been determined extensively[2, 4, 5, 11, 19, 20] using measurements of transmural water flux driven by a hydrostatic pressure gradient. Bovine aortic endothelial cell (BAEC) L_p measurements, over a period of 6 hours**,** demonstrated that stepwise increases in transmural pressure (10, 20, and 30 cmH_2O) resulted in transient step increases in $L_{p,}$ which did not return baseline values[20]. Similar hydrostatic pressure-mediated step increases in L_p, for up to 3 hours, have been observed in bovine lung ECs[6]. Similar observations were made in isolated whole lungs perfused at increasing pressures over 4 hours[7].

In the present study we determined the L_p responses of BAECs that were cultured with continuous transmural media perfusion for 48 hours. Bovine aortic smooth muscle cells (BASMCs) were also used for developing cocultures with BAECs. Endothelial L_p of media

perfused monocultures and cocultures was measured with paired controls (cultures without media perfusion). Our results identify that endothelial L_p, following 48 hours of continuous transmural media perfusion, was not significantly different from the L_p of endothelial cultures in static media. A similar L_p trend was observed for BAECs that were cocultured with BASMCs.

4.3 Materials and Methods

4.3.1 Materials

Transwell 0.4 μm pore diameter polyester permeable supports were purchased from Corning, Inc., NY. T-75 Tissue Culture Flasks were purchased from Becton Dickinson, NJ. A T-25 Flask of primary BAECs was purchased form VEC Technologies, Inc, NY. A cryopreserved ampule of primary BASMCs was purchased from Cell Applications, Inc., CA. Fibronectin (FN) 0.1% From Bovine Plasma; Trypsin-EDTA; Penicillin Streptomycin (PS); 200mM L-Glutamine (LG); 30% Albumin solution from Bovine Serum (BSA); and Phenol Red Minimum Essential Medium (MEM) were purchased from Sigma-Aldrich, Inc., MO. Fetal Bovine Serum (FBS) Defined was purchased from Thermo Fischer Scientific, Inc. Phenol Red Free Minimum Essential Medium (PRF-MEM) was purchased from Mediatech, Inc., VA. PharMed BPT tubing (Cat. No. EW-95692-12), Pump Drive (Cat. No. RX-07551-00), Cartridges (Cat. No. RX-07519-85), and Pump Head (Cat. No. RX-07519-25) were purchased from Cole-Parmer. PEEK tubing (Cat. No. 1532) and luer connectors were purchased from IDEX-HS, WA.

4.3.2 Defined Cell Culture Media

10% FBS MEM (10FB-MEM) consisted of MEM with 10% FBS, 1% LG, and 1% PS and was used for culturing cells in tissue culture flasks and on Transwell Permeable Supports in both static and interstitial fluid flow (IFF) environments. Experimental MEM (E-MEM) consisted of PRF-MEM with 1 % BSA, 1% LG, and 1% PS and was used to determine L_p.

The cell culture incubator was maintained at a constant temperature of 36.7^{o}C with 5% medical grade CO_2. Aseptic techniques were performed in a laminar flow hood. Cell culture media was pre-warmed to 37^{o}C in a waterbath and then buffered with 5% CO_2 for 20 minutes in an incubator prior to being introduced into the cell culture environment.

4.3.3 Cell Culture in Tissue Culture Flasks

A primary BAEC culture was expanded up to passage 2 subcultures in T-75 tissue culture flasks and then cryopreserved in 1 mL cryovials at a concentration of 1.0e6 cells/mL. A primary BASMC culture was expanded to passage 3 subcultures in T-75 tissue culture flasks and then cryopreserved in 1 mL cryovials at a concentration of 7.5e5 cells/mL.

Cryogencially frozen vials of either passage 2 primary BAEC cultures or passage 3 primary BASMC cultures were thawed for 2 minutes in a 37^{o}C waterbath and the cell suspensions were transferred to separate sterile T-75 tissue culture flasks. 10FB-MEM was added to the flask according to the manufacturer's volume recommendations (15 mL/T-75 flask) and the cultures were incubated until grown to be 80% confluent. Each culture was then passed into three new sterile tissue culture flasks by trypsinizing, pelleting, resuspending in 10FB-MEM, and splitting the cell suspension equally. These subcultures were grown until 80% confluent. BAEC and BASMC cultures were each passed a total of three times and then inoculated on Transwell inserts or companion wells. Passage 5 BAEC and passage 6 BASMC subcultures were inoculated on Transwell inserts or companion wells in specific monoculture and coculture arrangements and supplied with 10FB-MEM.

4.3.3.1 BAEC growth curve. Replicate subcultures of Passage 5 BAECs in culture flasks, supplied with 10FB-MEM, were sampled and counted during a 5 day culture period. BAECs were seeded at a density of 1.25e5 cells/cm^2 and a heamocytometer was used to calculate the cell densities from harvested cell suspensions on the subsequent days of culturing. The population densities of BAECs during this culture period were used to form a growth curve, and identify when cultures had recovered from their initial lag phases of growth in order to introduce continuous transmural media perfusion.

4.3.4 Cell Culture with Transwell Permeable Supports

4.3.4.1 Transwell insert membranes. Transwell inserts containing a polyester (PET) membrane were used. The membrane area was 1.12 cm^2. Each pore on the membrane was 0.4 μm in diameter and the membrane pore density was 4.0e6 pores/cm^2.

4.3.4.2 Coating PET membranes cultures with Fibronectin. BAEC cultures were inoculated on membranes that were pre-coated with FN diluted to 30 μg/mL with MEM. 224 μL of diluted FN was pipetted onto the apical side of the Transwell insert membrane. FN coated Transwell inserts in companion plates were incubated for 2 hours and then excess FN was removed.

4.3.4.3 Cell culture media for Transwell Permeable Supports. The recommended Transwell insert to companion well volume ratio was 1:3, respectively, with 0.5mL of culture media contained in the Transwell insert and 1.5mL of culture media contained in the companion well. To culture cells with 10FB-MEM, the defined media was placed in both compartments.

4.3.4.4 BAEC and BASMC plating densities, locations, and total culture times. BAEC and BASMC cultures were inoculated with a 1:1 plating density ratio of 1.25e5 cells/cm^2. BAECs in monoculture and coculture formats were always the apical culture on the Transwell membrane. BASMCs in coculture formats were inoculated on the bottom surface of the companion well. The total BASMC culture time in cocultures was 2 days. The total BAEC culture time in monoculture and coculture arrangements was 5 days.

4.3.4.5 BAEC and BASMC monocultures and cocultures.

<u>4.3.4.5.1 BAEC monocultures</u>

A BAEC culture was inoculated on an apical FN coated Transwell membrane, supplied with 10FB-MEM, and incubated for a total of 5 days. Endothelial L_p was measured for paired static and continuous 10FB-MEM perfusion cultures.

4.3.4.5.2 BAEC and BASMC cocultures

When BASMCs were cocultured with an existing BAEC culture, the total coculture, BASMC culture, and BAEC culture times were 2, 2, and 5 days, respectively. A BAEC culture was inoculated on an apical FN coated Transwell membrane, supplied with 10FB-MEM, and incubated for 3 days. Then a BASMC culture was inoculated in a separate companion well and allowed to settle and attach to this surface during a 30 minute incubation period. The Transwell insert containing the BAEC culture was then paired with the companion well containing the BASMC culture. The coculture was supplied with 10FB-MEM and incubated for 2 more days. Cocultures were dissociated on day 5 in order to measure endothelial L_p.

4.3.4.6 Monoculture and coculture notations and formats. The apical location of the Transwell membrane will be denoted as (a) and the bottom surface of the companion well is denoted as (c). BAEC culture inoculums are abbreviated as (EC), and BASMC culture inoculums are abbreviated as (SMC). Monoculture formats are described by [Location (Inoculum)]. Coculture formats are described by [Location (First Inoculum); Location (Second Inoculum)]. Monoculture and coculture notations and formats are presented in Figure 4.1.

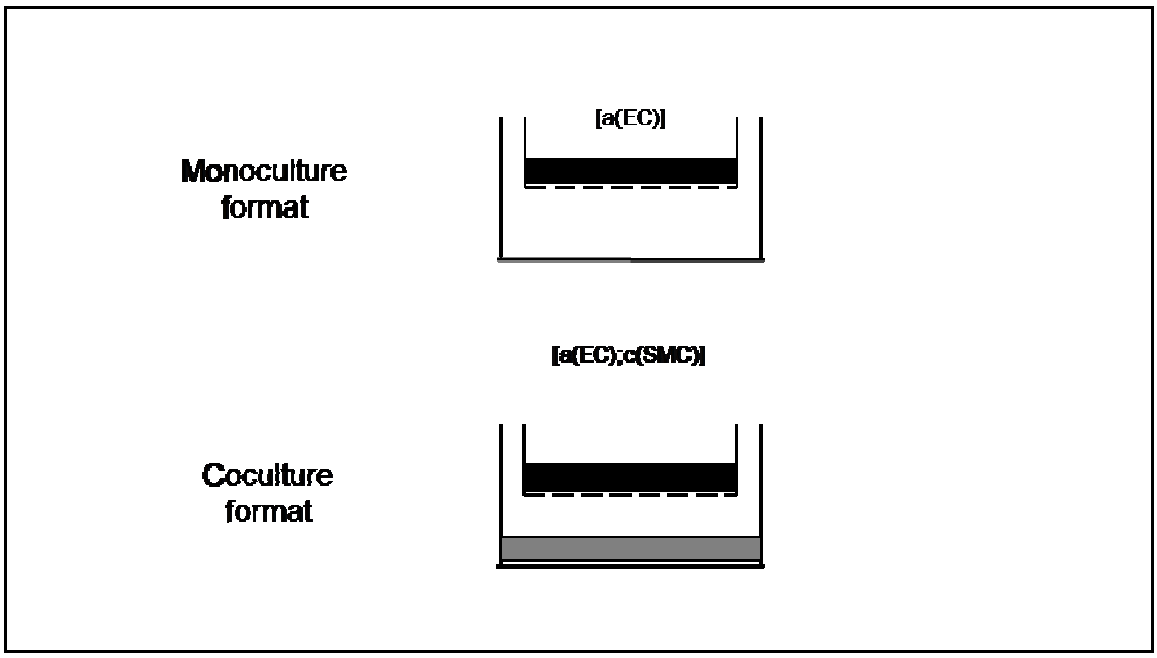

Figure 4.1. Schematic of BAEC and BASMC monoculture and coculture formats on Transwell membranes and companion wells. The horizontal dashed line indicates the location of the porous Transwell membrane. The black band indicates the location of BAEC cultures. The grey band indicates the location of BASMC cultures. The monoculture format is [a(EC)], and the coculture format is [a(EC);c(SMC)].

4.3.4.7 Media perfusion cultures. A 6 cartridge peristaltic pump system with a 0.1 to 600 r.p.m. drive range and a 5:1 gear ratio was used to pump media across each of 6 Transwell inserts cultures from 6 respective companion wells that were reserved with culture media. The peristaltic pump tubing (PharMed) was connected to polyetheretherketone (PEEK) tubing with adapters, and extended to the center position above each well. The PEEK tubing directed to each Transwell inserts was connected to additional peristaltic tubing that could be retained by the Transwell insert wall (Figure 4.2).

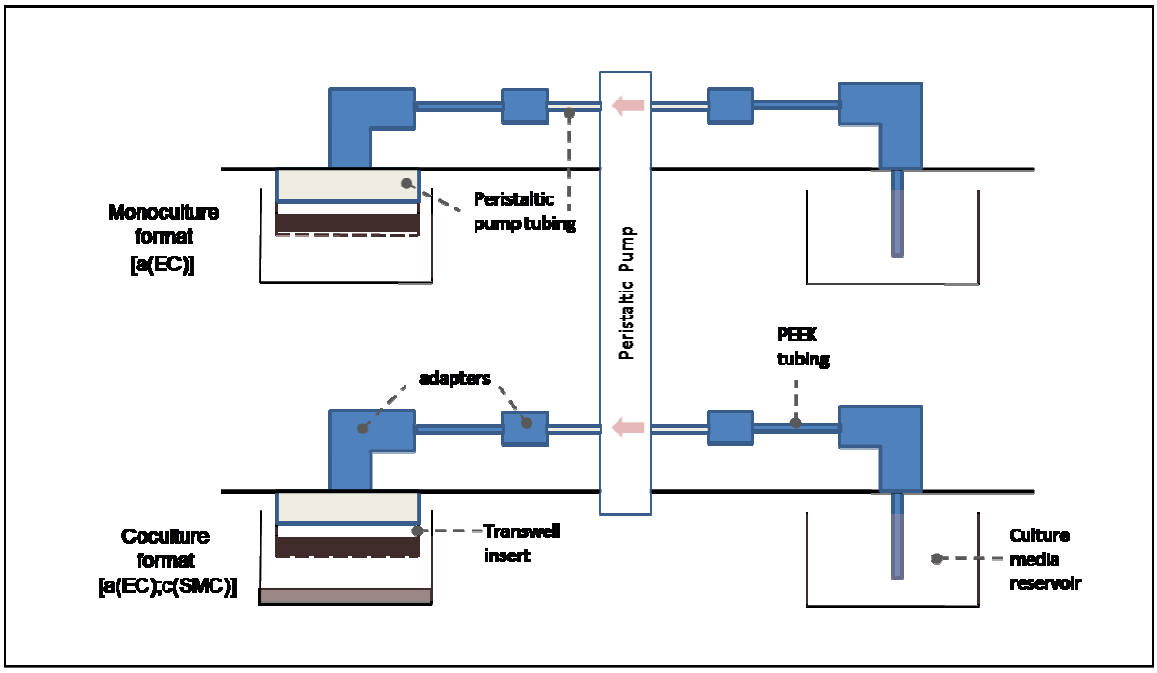

Figure 4.2. Schematic of flow circuit for transmural media perfusion across Transwell insert cultures. A peristaltic pump drives media from the culture media reservoir across the Transwell insert.

The pump system was calibrated using the manufacturer's recommendations and custom flow rates of 6.048e-6 and 1.232e-6 mL/s were used to directly correlate to membrane fluid fluxes (J_v) of 5.4e-6 and 1.1e-6 cm/s, respectively, across a constant Transwell membrane area of 1.12 cm^2. The J_v value of 5.4e-6 cm/s was typical of previous L_p experiments with membranes exposed to a 10 cmH_2O pressure differential[4]. The lower value is typical of physiological transmural water fluxes in arteries[21]. J_v of 1.1e-6 cm/s correlated to the lowest flow rate (1.232 mL/s) that could be achieved with our pumping system.

To avoid high bursting pressures from developing inside the flow circuit during sterilization, the tubing components were disconnected and submerged in distilled and deionized water while being autoclaved for 30 minutes at 110^0C. Next, in a laminar flow hood, excess water was vacuum aspirated, and each component was carefully assembled. Contact with the entry sites of

the inner diameters for each tubing component, where culture media is expected to flow, was meticulously avoided during assembly in order to prevent the potential for media contamination. The assembled system was then sprayed with ethanol and irradiated with ultraviolet light for 20 minutes. Using a sterile 12 well companion plate, each of the 6 channels of the system was then primed with 3 mL of warm and buffered 10FB-MEM that was pumped from 6 respective companion wells.

Next, a total of 6 Transwell insert cultures, which were on day 3 of static media culturing, were each exposed to a continuous supply of warm and buffered 10FB-MEM with the primed peristaltic pump system. Media was perfused across cultures from the apical to basal direction to simulate the normal direction of transmural perfusion. The hydrostatic pressure difference between the Transwell culture well media (2 mL) and the separate companion well media (4 mL), which was reserved for pumping, was 0.53 cmH_2O. Transwell membrane media fluxes of either 5.4e-6 or 1.1e-6 cm/s were prescribed for the remaining 48 hours of culture. The total culture time for perfused media cultures and controls (static media cultures) was 5 days.

4.3.4.8 Calculating L_p of Transwell cultures. Fluid flux (J_v) across Transwell insert cultures was measured in pairs with a bubble tracking apparatus and those measurements were then used to calculate L_p. Both the bubble tracking apparatus and the equations for calculating L_p have been described previously[4] and are explained briefly here. Following the prescribed monoculture and coculture times, the Transwell insert was transferred to the bubble tracking apparatus. E-MEM was added above and below the Transwell culture insert to eliminate the presence of an osmotic pressure gradient that develops across the membrane culture. An air bubble was then injected into a capillary glass tube that was connected to the basal fluid compartment of Transwell. The displacement of the air bubble meniscus was tracked over time

with the apparatus' photodetector while effluent E-MEM was driven through the flow circuit. The L_p calculation for each culture was reduced to the ratio of the E-MEM fluid flux, J_v, across the Transwell insert culture and the hydrostatic pressure gradient, $\Delta P = 10$ cmH_2O, driving the transmembrane fluid flow (Equation 1).

$$L_p = J_v / \Delta P \qquad \text{(Eqn. 1)}$$

The units for J_v were cm/s and the units of L_p were $cm/s/cmH_2O$. Each measurement was repeated 6 times.

4.3.4.9 Statistical analysis of L_p. Hydraulic conductivity measurements for each culture format are presented as the mean L_p +/- the standard error of the mean (SEM). A Student's *t*-test with a two-tailed distribution was used to determine the significance level, p, between paired L_p measurements. Hydraulic conductivity measurements for paired BAEC monocultures, and paired cocultures were considered statistically significant if $p < 0.05$.

4.4 Results

4.4.1 Static and Continuous Media Perfusion Culture L_p

4.4.1.1 BAEC monocultures. The L_p measurements of BAEC monoculture controls cultured for 5 days in static media were paired with L_p measurements of BAEC monocultures that were supplied with 48 hours (day 3 to 5) of continuous media perfusion at flow rates of either 5.4e-6 cm/s (Figure 4.3) or 1.1e-6 cm/s (Figure 4.4). In Figure 4.3, 48 hours of continuous perfusion of 10FB-MEM at a flow rate of 5.4e-6 cm/s lead to a 50% higher, but not significant, EC L_p compared to controls. In Figure 4.4, EC L_p measurements following 48 hours of 1.1e-6 cm/s media perfusion was nearly identical to EC L_p of controls.

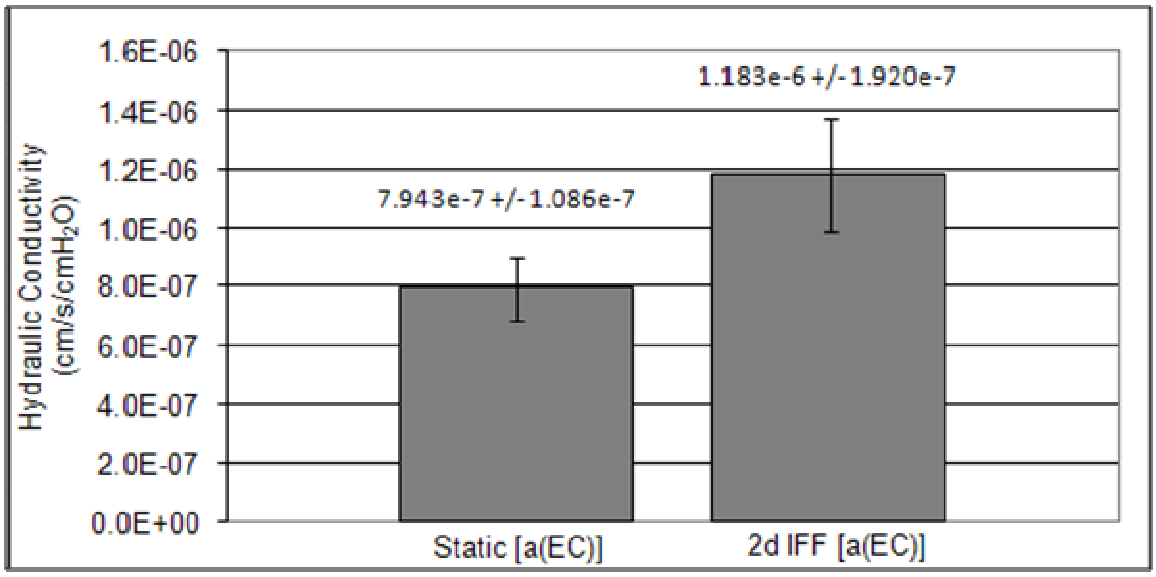

Figure 4.3. Hydraulic conductivity of 5 day apical EC ([a(EC)]) monocultures following culture in static 10FB-MEM or with 2 days of IFF of 10FB-MEM at a constant fluid flux of 5.4e-6 cm/s. The L_p (mean +/- SEM) for static and 2d IFF [a(EC)] were 7.943e-7 +/- 1.086e-7 cm/s/cmH_2O and 1.183e-6 +/- 1.920e-7 cm/s/cmH_2O, respectively. n = 6.

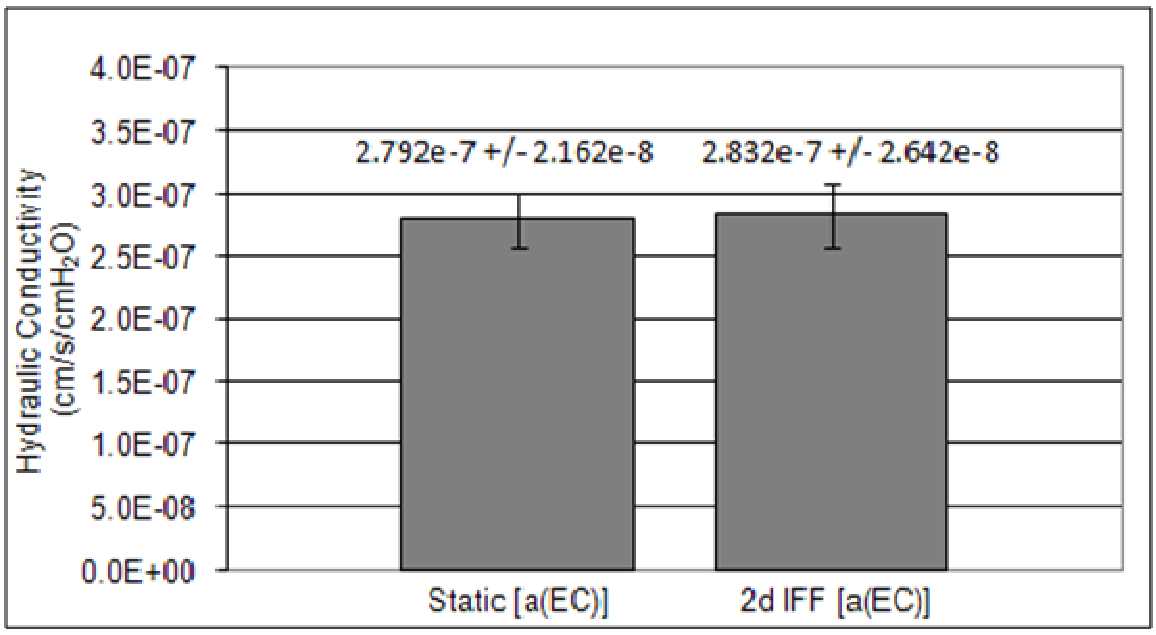

Figure 4.4. Hydraulic conductivity of 5 day apical EC ([a(EC)]) monocultures following culture in static 10FB-MEM or with 2 days of IFF of 10FB-MEM at a constant fluid flux of 1.1e-6 cm/s. The L_p (mean +/- SEM) for static and 2d IFF [a(EC)] were 2.792e-7 +/- 2.162e-8 cm/s/cmH_2O and 2.832e-7 +/- 2.642e-8 cm/s/cmH_2O, respectively. n = 6.

4.4.1.2 BAEC and BASMC cocultures. The L_p measurements of ECs from static media cocultures (control) supplied with 10FB-MEM were paired with L_p measurements of ECs from cocultures that were exposed to 48 hours of continuous media perfusion at a flow rate of 5.4e-6 cm/s (Figure 4.5). Figure 4.5 shows that EC L_p from [a(EC);c(SMC)] cocultures following 48 hours (day 3 to 5) of continuous media perfusion was similar to EC L_p measurements from control cocultures.

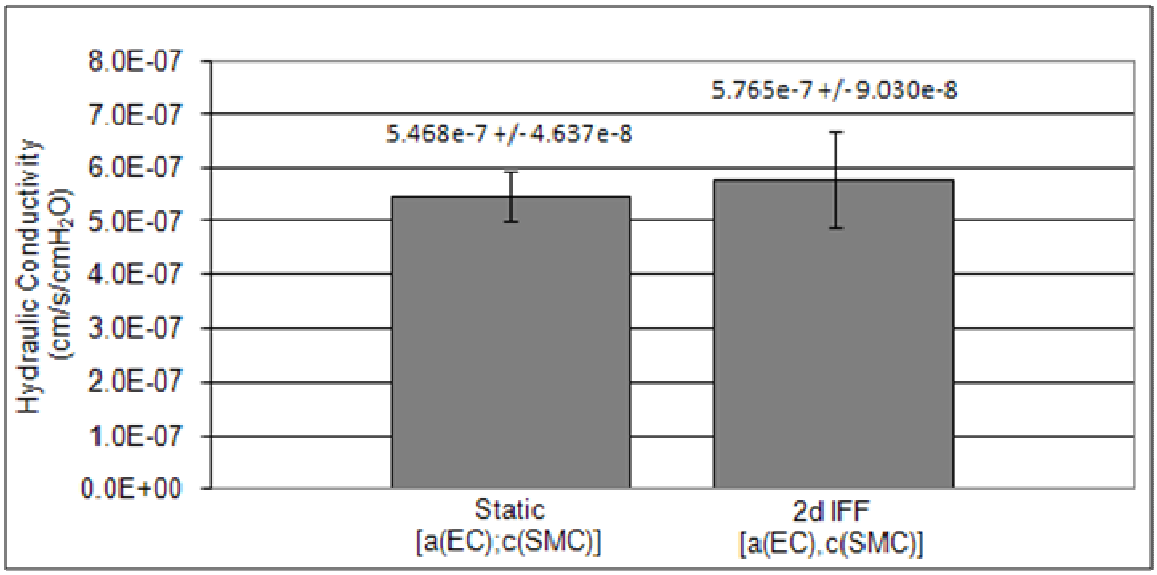

Figure 4.5. Hydraulic conductivity of [a(EC);c(SMC)] cocultures following culture in static 10FB-MEM or with 2 days of IFF of 10FB-MEM at a constant fluid flux of 5.4e-6 cm/s. The L_p (mean +/- SEM) for static and 2d IFF [a(EC);c(SMC)] were 5.468e-7 +/- 4.637e-8 cm/s/cmH_2O and 5.765e-7 +/- 9.030e-8 cm/s/cmH_2O, respectively. n = 6.

4.4.1.3 Bubble displacements. Air bubble displacements representative of each culture condition are shown in Figure 4.6. The culture condition [a(EC)] with 48 hours of 10FB-MEM perfusion at 5.4e-6 cm/s shows the largest bubble displacement during the one hour (3600 sec) L_p measurement period.

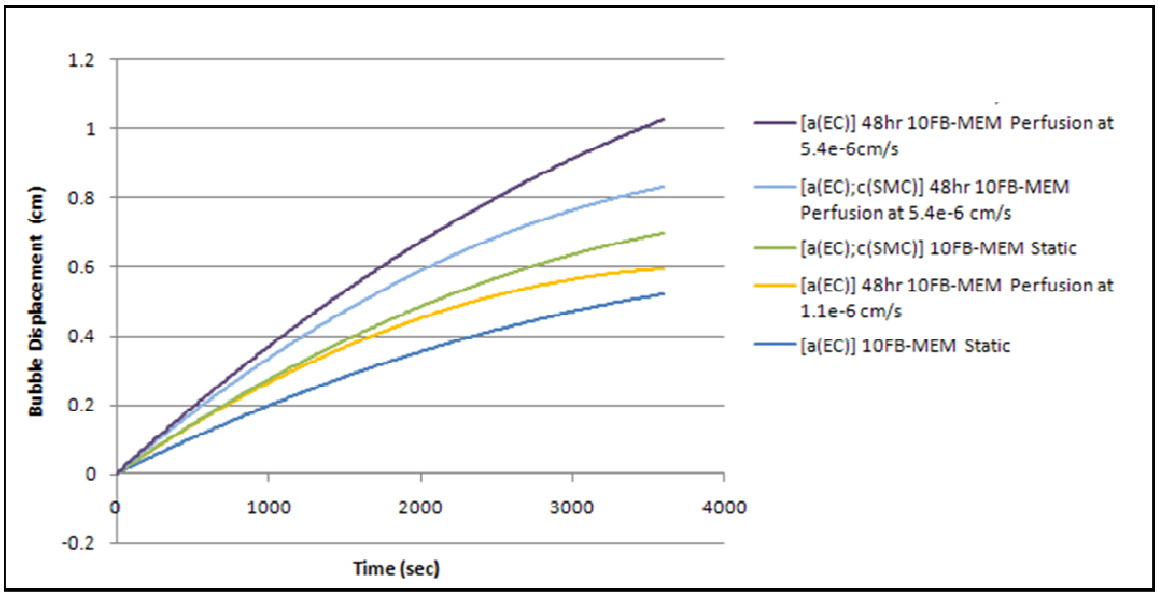

Figure 4.6. Representative bubble displacements for each culture condition during the one hour period of measuring L_p. Static media cultures include [a(EC)] 10FB-MEM, and [a(EC);c(SMC)] 10FB-MEM. 48 hour perfusion media cultures include [a(EC)] 10FB-MEM with 5.4e-6 and 1.1e-6 cm/s fluid fluxes, and [a(EC);c(SMC)] 10FB-MEM with a 5.4e-6 cm/s fluid flux.

4.5 Discussion

The lowest settings of our pumping apparatus produced a continuous media perfusion across cultures at a membrane fluid flux value of 1.1e-6 cm/s that is similar to arterial values[21]. The higher membrane fluid flux value of 5.4e-6 cm/s for continuous media perfusion is characteristic of higher perfusion fluxes often observed *in-vitro*[4]. To impose even higher membrane fluid fluxes would require significant investments into the design of our current peristaltic pumping system. There was a 50% increase in EC L_p that was not significant, compared to the L_p of static EC cultures with 10FB-MEM, when 10FB-MEM was continuously supplied to EC cultures for 48 hours at a fluid flux of 5.4e-6 cm/s (Figure 4.3). However, EC L_p following 48 hours of 10FB-MEM perfusion at a fluid flux of 1.1e-6 cm/s was nearly identical to EC L_p in paired static media cultures (Figure 4.4). We elected to employ a coculture model of ECs and SMCs with shared cell culture media (Figure 4.1). Aortic coculturing through shared media has been shown to influence the function of each cell type[3, 8, 22, 23]. This type of coculture gave us the flexibility to introduce continuous perfusion across ECs alone (Figure 4.2) and then import the separated EC culture into the bubble tracking apparatus on day 5 for measuring EC L_p. Figure 4.5 shows that ECs from cocultures which were exposed to 48 hours of media perfusion at a membrane fluid flux of 5.4e-6 cm/s had a similar L_p value compared to ECs from static media cocultures.

While every effort was made to ensure repeatability in our experiments, it is possible for confounding errors to propagate from the assembly and application of this novel pumping apparatus as well as from undefined effects of membrane stretching. Earlier work[20] with Transwell EC cultures, however, showed that there were no hydrostatic pressure effects on membrane stretching. Our experiments identify that aortic endothelial cultures are capable of withstanding continuous exposure to transmural fluid perfusion. The osmotic gradient across

each Transwell culture was removed on day 5 of culturing by replacing the existing culture media with E-MEM in order to determine J_v with the bubble tracking apparatus. This apparatus identified a sealing effect[4, 13, 15, 19, 20] (reduction in L_p with time after exposure to the pressure differential) for each culture condition, including those that were predisposed to continuous media perfusion (Figure 4.6). Earlier studies[6, 20] involving up to 6 hours of media perfusion showed that there were significant increases in J_v over time as a result of stepwise increases in ΔP. Our results show that continuous transmural media perfusion for 48 hours does not significantly alter EC L_p. This means that EC L_p increases upon initial exposure to transmural flow but returns to its static baseline value following continuous transmural fluid perfusion for 48 hours. This L_p trend is analogous to trends in other recent studies[12, 16, 24] which show that transient (shorter time) increases in EC transport properties, in response to fluid shear stress on the EC surface, return to baseline levels after longer exposures.

4.6 References

1. Barker S.G., A. Talbert, S. Cottam, P.A. Baskerville, and J.F. Martin. Arterial intimal hyperplasia after occlusion of the adventitial vasa vasorum in the pig. *Arterioscler. Thromb. and Vasc. Biol.* 13:70-77, 1993.
2. Chang Y.S., J.A. Yaccino, S. Lakshminarayanan, J.A. Frangos, and J.M. Tarbell. Shear-induced increases in hydraulic conductivity in endothelial cells is mediated by a nitric oxide-dependent mechanism. *Arterioscler. Thromb. Vasc. Biol.* 20: 35-42, 2000.
3. Davies P.F., G.A. Truskey, H.B. Warren, S.E. O'Connor, and B.H. Eisenhaure. Metabolic cooperation between vascular endothelial cells and smooth muscle cells in coculture: changes in low density lipoprotein metabolism. *J. Cell Biol.* 101: 871-879, 1985.
4. DeMaio L., J.M. Tarbell, R.C. Scaduto, T.W. Gardner, and D.A. Antonetti. A transmural pressure gradient induces mechanical and biological adaptive responses in endothelial cells. *Am. J. Physiol. Heart Circ. Physiol.* 286: 731-741, 2004.
5. Dull R.O., H. Jo, H. Sill, T.M. Hollis, and J.M. Tarbell. The effect of varying albumin concentration and hydrostatic pressure on hydraulic conductivity and albumin permeability of cultured endothelial monolayers. *Microvasc. Res.* 41(3): 390-407, 1991.
6. Dull R.O., I. Mecham, and S. McJames. Heparan sulfates mediate pressure-induced increase in lung endothelial hydraulic conductivity via nitric oxide/reactive oxygen species. *Am. J. Physiol. Lung Cell Mol. Physiol.* 292: L1452-L1458, 2007.
7. Dull R.O., M. Cluff, J. Kingston, D. Hill, H. Chen, S. Hoehne, D.T. Malleske, and R. Kaur. Lung heparan sulfates modulate K_{fc} during increased vascular pressure: evidence

for glycocalyx-mediated mechanotransduction. *Am. J. Physiol. Lung Cell Mol. Physiol.* 302:(9) L816-L828, 2012.

8. Fillinger M.F., L.N. Sampson, J.L. Cronenwett, R.J. Powell, and R.J. Wagner. Coculture of endothelial cells and smooth muscle cells in bilayer and conditioned media models. *J. Surg. Res.* 67: 169-178, 1997.
9. Gössl M., P.E. Beighley, N.M. Malyar, and E.L. Ritman. Role of vasa vasorum in transendothelial solute transport in the coronary vessel wall: a study with cryostatic micro-CT. *Am. J. Physiol. Heart Circ. Physiol.* 287:H2346-H2351, 2004.
10. Heistad D.D., M.L. Marcus, G.E. Larsen, and M.L. Armstrong. Role of vasa vasorum in nourishment of the aortic wall. *Am. J. Physiol. Heart Circ. Physiol.* 240:H781-787, 1981.
11. Hillsley M.V., and J.M. Tarbell. Oscillatory shear alters endothelial hydraulic conductivity and nitric oxide levels. *Biochem. Biophys. Res. Commun.* 293: 1466-1471, 2002.
12. Jo H., R.O. Dull, T.M. Hollis, and J.M. Tarbell. Endothelial albumin permeability is shear dependent, time dependent, and reversible. *Am. J. Physiol.* 260: H1992-H1996, 1991.
13. Kim M-H., N.R. Harris, and J.M. Tarbell. Regulation of hydraulic conductivity in response to sustained changes in pressure. *Am. J. Physiol. Heart Circ. Physiol.* 289: H2551-2558, 2005.
14. Lindbergh C.A. An apparatus for the culture of whole organs. *J. Exp. Med.* 62:409-431, 1935.
15. Russell S., L.M. Cancel, J.M. Tarbell, and D.S. Rumschitzki. A protein diffusion model of the sealing effect. *Chem. Engr. Sci.* 64: 4504-4514, 2009.

16. McIntire L., J. Wagner, and P. Whitson. Effect of flow on macromolecular transport across bovine brain endothelial cell monolayers. *ASME/BED Bioeng. Conf.* 29: 79-80, 1995.

17. Tada S., and J.M. Tarbell. Fenestral pore size in the internal elastic lamina affects transmural flow distribution in the artery wall. *Ann. Biomed. Engr.* 29:456-466, 2001.

18. Tada S., and J.M. Tarbell. Internal elastic lamina affects the distribution of macromolecules in the arterial wall: a computational study. *Am. J. Physiol. Heart Circ. Physiol.* 287:H905-H913, 2004.

19. Tarbell J.M. Shear stress and the endothelial transport barrier. *Cardiovasc. Res.* 87: 320-330, 2010.

20. Tarbell J.M., L. DeMaio, and M.M. Zaw. Effect of pressure on hydraulic conductivity of endothelial monolayers: role of endothelial cleft shear stress. *J. Appl. Physiol.* 87: 261-268, 1999.

21. Tarbell J.M., M.J. Lever, and C.G. Caro. The effect of varying albumin concentration of the hydraulic conductivity of the rabbit common carotid artery. *Microvasc. Res.* 35: 204-220, 1988.

22. Vouyouka A.G., Y. Jiang, and M.D. Basson. Pressure alters endothelial effects upon vascular smooth muscle cells by decreasing smooth muscle cell proliferation and increasing smooth muscle cell apoptosis. *Surg.* 136: 282-290, 2004.

23. Vouyouka A.G., S.S. Salib, S. Cala, J.D. Marsh, and M.D. Basson. Chronic high pressure potentiates the antiproliferative effect and abolishes contractile phenotype changes caused by endothelial cells in cocultured smooth muscle cells. *J. Surg. Res.* 110: 344-351, 2003.

24. Warboys C.M., R.E. Berson, G.E. Mann, J.D. Pearson, and P.D. Weinberg. Acute and chronic exposure to shear stress have opposite effects on endothelial permeability to macromolecules. *Am. J. Physiol. Heart Circ. Physiol.* 298: H1850-H1856, 2010.

25. Werber A.H., and D.D. Heistad. Diffusional support in arteries. *Am. J. Physiol. Heart Circ. Physiol.* 248:H901-H906, 1985.

BIBLIOGRAPHY

Chapter 1

1. Baetscher M., and K. Brune. An in vitro system for measuring endothelial permeability under hydrostatic pressure. *Exp. Cell Res.* 148: 541-547, 1983.
2. Bazzoni G., and E. Dejana. Endothelial Cell-to-cell junctions: molecular organization and role in vascular homeostasis. *Physiol. Rev.* 84: 869-901, 2004
3. Berk B.C. Vascular smooth muscle growth: autocrine growth mechanisms. *Physiol. Rev.* 81: 999-1030, 2001.
4. Cancel L., A. Fitting, and J.M. Tarbell. In vitro study of LDL transport under pressurized (convective) conditions. *Am. J. Physiol. Heart Circ. Physiol.* 293: 126-132, 2007.
5. Cancel L.M., and J.M. Tarbell. The role of apoptosis in LDL transport through cultured endothelial cell monolayers. Atherosclerosis 208(2): 335-341, 2010.
6. Cancel L.M., and J.M. Tarbell. The role of mitosis in LDL transport through cultured endothelial cell monolayers. Am. J. Physiol. Heart Circ. Physiol. 300(3): H769-H776, 2011.
7. Caro C.G. Discovery of the role of wall shear in atherosclerosis. *Arterioscler. Thromb. Vasc. Biol.* 29: 158-161, 2009.
8. Chiu J., L. Chen, P. Lee, C. Lee, L. Lo, S. Usami, and S. Chien. Shear stress inhibits adhesion molecule expression in vascular endothelial cells induced by coculture with smooth muscle cells. *Blood* 101: 2667-2674, 2003.
9. Davies P.F., G.A. Truskey, H.B. Warren, S.E. O'Connor, and B.H. Eisenhaure. Metabolic cooperation between vascular endothelial cells and smooth muscle cells in

coculture: changes in low density lipoprotein metabolism. *J. Cell Biol.* 101: 871-879, 1985.

10. DeMaio L., J.M. Tarbell, R.C. Scaduto, T.W. Gardner, and D.A. Antonetti. A transmural pressure gradient induces mechanical and biological adaptive responses in endothelial cells. *Am. J. Physiol. Heart Circ. Physiol.* 286: 731-741, 2004.
11. Ebnet K. Organization of multiprotien complexes at cell-cell junctions. *Histochem. Cell Biol.* 130: 1-20, 2008.
12. Fillinger M.F., L.N. Sampson, J.L. Cronenwett, R.J. Powell, and R.J. Wagner. Coculture of endothelial cells and smooth muscle cells in bilayer and conditioned media models. *J. Surg. Res.* 67: 169-178, 1997.
13. Garcia-Cardena G., J. Comander, K.R. Anderson, B.R. Blackman, and M.A. Gimbrone. Biomechanical activation of vascular endothelium as a determinant of its functional phenotype. PNAS 98: 4478-4485, 2001.
14. Heydarkhan-Hagvall S., G. Helenius, B.R. Johansson, J.Y. Li, E. Mattsson, and B. Risberg. Coculture of endothelial cells and smooth muscle cells affects gene expression of angiogenic factors. *J. Cell. Biochem.* 89: 1250-1259, 2003.
15. Hsiai T.K. Mechanosignal transduction coupling between endothelial and smooth muscle cells: role of hemodynamic forces. *Am. J. Physiol. Cell Physiol.* 294: 659-661, 2008.
16. Kim M., N.R. Harris, and J.M. Tarbell. Regulation of hydraulic conductivity in response to sustained changes in pressure. *Am. J. Physiol. Heart Circ. Physiol.* 289: 2551-2558, 2005.
17. Kumar V., A.K. Abbas, and N. Fausto. Unit II: Diseases of organ systems: blood vessels In Robbins & Cotran Pathologic Basis of Disease. 7th Edition. Saunders 2004.

18. Kurzen H., S. Manns, G. Dandekar, T. Schmidt, S. Pratzel, and B.M. Kraling. Tightening of endothelial cell contacts: a physiologic response to cocultures with smooth muscle-like 10T1-2 cells. *J. Invest. Dermatol.* 119: 143-153, 2002.

19. Lavender M.D., Z. Pang, C.S. Wallace, L.E. Niklason, and G.A. Truskey. A system for direct coculture of endothelium on smooth muscle cells. *Biomaterials* 26: 4642-4653, 2005.

20. Lee K., G.M. Saidel, and M.S. Penn. Permeability change of arterial endothelium is an age-dependent function of lesion size in apolipoprotein E-null mice. *Am. J. Physiol. Heart Circ. Physiol.* 295: 2273-2279, 2008.

21. Muller-Marschhausen K., and D. Drenckhahn. Physiological hydrostatic pressure protects endothelial monolayer integrity. *Am. J. Physiol. Cell Physiol.* 294: 324-332, 2008.

22. Ryan U.S., J.W. Ryan, and C. Whitaker. How do kinins affect vascular tone? Adv. Exp. Med. Biol. 120A: 375-391, 1979.

23. Solan A., V. Prabhakar, and L. Niklason. Engineered vessels: importance of the extracellular matrix. *Transplantation Proceedings* 33: 66-68, 2001.

24. Starry H.C., A.B. Chandler, R.E. Dinsmore, V. Fuster, S. Glagov, W. Jr. Insull, M.E. Rosenfeld, C.J. Schwartz, W.D. Wagner, and R.W. Wissler. A definition of advanced types of atherosclerotic lesions and a histological classification of atherosclerosis. Circ. 92(5): 1355-1374, 1995.

25. Stegemann J.P., H. Hong, and R.M. Nerem. Mechanical, biochemical, and extracellular matrix effects on vascular smooth muscle cell phenotype. *J. Appl. Physiol.* 98: 2321-2327, 2005.

26. Stevens T., R. Rosenberg, W. Arid, T. Quertermous, F.L. Johnson, J. Garcia, R.P. Hebbel, R.M. Tuder, and S. Garfinkel. NHLBI workshop report endothelial cell phenotypes in heart, lung and blood diseases. *Am. J. Physiol.* 281: 1422-1433, 2001.

27. Tada S., and J.M. Tarbell. Interstitial flow through the internal elastic lamina affects shear stress on arterial smooth muscle cells. *Am. J. Physiol. Heart Circ. Physiol.* 278: 1589-1597, 2000.

28. Tarbell J.M. Mass transport in arteries and the localization of atherosclerosis. *Ann. Rev. Biomed. Eng.* 5: 79-118, 2003.

29. Corning Life Sciences, Transwell permeable supports selection and use guide. CLS-CC-007W REV5.

30. Tsukita S., M. Furuse, and M. Itoh. Multifunctional strands in tight junctions. *Nature Reviews: Mol. Cell Biol.* 2: 285-293, 2001.

31. Turner M.R. Flows of liquid and electrical current through monolayers of cultured bovine arterial endothelium. *J. Physiol.* 449: 1-20, 1992.

32. Vandenbroucke E., D. Mehta, R. Minshall, and M.B. Malik. Regulation of endothelial junctional permeability. *Ann. NY Acad. Sci.* 1123: 134-145, 2008.

33. Vouyouka A.G, S.S. Salib, S. Cala, J.D. Marsh, and M.D. Basson. Chronic high pressure potentiates the antiproliferative effect and abolishes contractile phenotype changes caused by endothelial cells in cocultured smooth muscle cells. *J. Surg. Res.* 110: 344-351, 2003.

34. Vouyouka A.G., Y. Jiang, and M.D. Basson. Pressure alters endothelial effects upon vascular smooth muscle cells by decreasing smooth muscle cell proliferation and increasing smooth cell apoptosis. *Surgery* 136: 282-290, 2004.

35. Wallace C.S., J.C. Champion, and G.A. Truskey. Adhesion and function of human endothelial cells cocultured on smooth muscle cells. *Ann. Biomed. Eng.* 35: 375-386, 2007.

36. Wallace C.S., S.A. Strike, and G.A. Truskey. Smooth muscle cell rigidity and extracellular matrix organization influence endothelial cell spreading and adhesion formation in coculture. *Am. J. Physiol. Heart Circ. Physiol.* 293: 1978-1986, 2007.

37. Wang S., and J.M. Tarbell. Effect of fluid flow on smooth muscle cells in a 3-dimensional collagen gel model. *Arterioscler. Thromb. Vasc. Biol.* 20: 2220-2225, 2000.

Chapter 2

1. Aiello V.D., P.S. Gutierrez, M.J.F. Chaves, A.A.B. Lopes, M.L. Higuchi, and J.A.F. Ramires. Morphology of the internal elastic lamina in arteries from pulmonary hypertensive patients: a confocal laser microscopy study. Mod. Pathol. 16(5): 411-416, 2003.

2. Bird B.R., W.E. Stewart, and E.N. Lightfoot. "Shell momentum balances and velocity distributions in laminar flow." In: Transport Phenomena, edited by New York: John Wiley & Sons Inc., 2007, pp. 53-55.

3. Buschmann I., and W. Schaper. Arteriogenesis versus angiogenesis: two mechanisms of vessel growth. Am. J. Physiol. Physiol. 14: 121-125, 1999.

4. Cancel L.M., A. Fitting, and J.M. Tarbell. In-vitro study of LDL transport under pressurized (convective) conditions. Am. J. Physiol. Heart Circ. Physiol. 293: H126-H132, 2007.

5. Castellot, Jr. J.E., M.J. Karnovsky, and B.M. Spiegelman. Potent stimulation of vascular endothelial cell growth by differentiated 3t3 adipocytes. Cell Biol. 77(10): 6007-6011, 1980.
6. Chang Y.S., J.A. Yaccino, S. Lakshminarayanan, J.A. Frangos, and J.M. Tarbell. Shear-induced increases in hydraulic conductivity in endothelial cells is mediated by a nitric oxide-dependent mechanism. Arterioscler. Thromb. Vasc. Biol. 20: 35-42, 2000.
7. Chiu J., L. Chen, P. Lee, C. Lee, L. Lo, S. Usami, and S. Chien. Shear stress inhibits adhesion molecule expression in vascular endothelial cells induced by coculture with smooth muscle cells. Blood 101: 2667-2674, 2003.
8. Conway E.M., D. Collen, and P. Carmeliet. Molecular mechanisms of blood vessel growth. Cardiovasc. Res. 49: 507-521, 2001.
9. Davies P.F., G.A. Truskey, H.B. Warren, S.E. O'Connor, and B.H. Eisenhaure. Metabolic cooperation between vascular endothelial cells and smooth muscle cells in co-culture: changes in low density lipoprotein metabolism. J. Cell Biol. 101: 871-879, 1985.
10. DeMaio L., J.M. Tarbell, R.C. Scaduto, T.W. Gardner, and D.A. Antonetti. A transmural pressure gradient induces mechanical and biological adaptive responses in endothelial cells. Am. J. Physiol. Heart Circ. Physiol. 286: 731-741, 2004.
11. De Wit C., M. Boettcher, and V.J. Schmidt. Signaling across myoendothelial gap junctions – fact or fiction? Cell Commun. Adhes. Sep 15(3): 231-245, 2008.
12. Dull R.O., H. Jo, H. Sill, T.M. Hollis, and J.M. Tarbell. The effect of varying albumin concentration and hydrostatic pressure on hydraulic conductivity and albumin permeability of cultured endothelial monolayers. Microvasc. Res. 41(3): 390-407, 1991.

13. Duthu G.S. and J.R. Smith. In vitro proliferation and lifespan of bovine aorta endothelial cells: effect of culture conditions and fibroblast growth factor. J. Cell Physiol. 103(3): 385-392, 1980.

14. Fillinger M.F., L.N. Sampson, J.L. Cronenwett, R.J. Powell, and R.J. Wagner. Coculture of endothelial cells and smooth muscle cells in bilayer and conditioned media models. J. Surg. Res. 67: 169-178, 1997.

15. Gaballa M.A., T.E. Raya, B.R. Simon, and S. Goldman. Arterial mechanics in spontaneously hypertensive rats. Mechanical properties, hydraulic conductivity, and two-phase (solid/fluid) finite element models. Circ. Res. 71: 145-158, 1992.

16. Gartner L.P., and J.L. Hiatt. "Circulatory System." In: Color Textbook of Histology, edited by Philadelphia: Saunders Co., 2001, pp. 251-256.

17. Heberlein K., A. Straub, and B.E. Isakson. The myoendothelial junction: breaking through the matrix? Microcirculation 16(4): 307-322, 2009.

18. Heydarkhan-Hagvall S., G. Helenius, B.R. Johansson, J.Y. Li, E. Mattsson, and B. Risberg. Co-culture of endothelial cells and smooth muscle cells affects gene expression of angiogenic factors. J. Cell Biochem. 89: 1250-1259, 2003.

19. Hillsley M.V., and J.M. Tarbell. Oscillatory shear alters endothelial hydraulic conductivity and nitric oxide levels. Biochem. Biophys. Res. Commun. 293: 1466-1471, 2002.

20. Kurzen H., S. Manns, G. Dandekar, T. Schmidt, S. Pratzel, and B.M. Kräling. Tightening of endothelial cell contacts: a physiologic response to cocultures with smooth muscle-like 10 T1/2 cells. J. Invest. Dermatol. 119: 143-153, 2002.

21. Li G., M.J. Simon, L.M. Cancel, Z.D. Shi, X. Ji, J.M. Tarbell, B. Morrison 3rd, and B.M. Fu. Permeability of endothelial and astrocyte cocultures: in vitro blood brain barrier models for drug delivery studies. Ann. Biomed. Eng. 38(8): 2499-2511, 2010.

22. Pang Z., L.E. Niklason, and G.A. Truskey. Porcine endothelial cells cocultured with smooth muscle cells became procoagulant in vitro. Tissue Eng. Part A. 16(6): 1835-1844, 2010.

23. Pnueli D., and C. Gutfinger. "Exact solutions of the Navier-Stokes equations." In: Fluid Mechanics, edited by New York: Cambridge University Press, 1992, pp. 193-196.

24. Renkin E.M., and F.E. Curry. Endothelial permeability: Pathways and modulations. Ann. NY Acad. Sci. 401: 248-259, 1982.

25. Rose S.L., and J.E. Babensee. Complimentary endothelial cell/smooth muscle cell co-culture systems with alternate smooth muscle cell phenotypes. Ann. Biomed. Eng. 35: 1382-1390, 2007.

26. Ryan U.S., J.W. Ryan, and C. Whitaker. How do kinins affect vascular tone? Adv. Exp. Med. Biol. 120A: 375-391, 1979.

27. Schaper W., and I. Buschmann. Arteriogenesis, the good and bad of it. Cardiovasc. Res. 43: 835-837, 1999.

28. Tada S., and J.M. Tarbell. Interstitial flow through the internal elastic lamina affects shear stress on arterial smooth muscle cells. Am. J. Physiol. Heart Circ. Physiol. 278: H1589-H1597, 2000.

29. Tarbell J.M.. Shear stress and the endothelial transport barrier. Cardiovasc. Res. 87: 320-330, 2010.

30. Tarbell J.M., L. DeMaio, and M.M. Zaw. Effect of pressure on hydraulic conductivity of endothelial monolayers: role of endothelial cleft shear stress. J. Appl. Physiol. 87: 261-268, 1999.

31. Tarbell J.M., M.J. Lever, and C.G. Caro. The effect of varying albumin concentration of the hydraulic conductivity of the rabbit common carotid artery. Microvasc. Res. 35: 204-220, 1988.

32. van Oostrom M.C., O. van Oostrom, P.H.A. Quax, M.C. Verhaar, and I.E. Hoefer. Insights into the mechanisms behind arteriogenesis: what does the future hold? J. Leukocyte Biol. 84: 1379-1391, 2008.

33. Ziegler T., R.W. Alexander, and R.M. Nerem. An endothelial cell-smooth muscle cell co-culture model for use in the investigation of flow effects in vascular biology. Ann. Biomed. Eng. 23: 216-225, 1995.

Chapter 3

1. Aiello V.D., P.S. Gutierrez, M.J.F. Chaves, A.A.B. Lopes, M.L. Higuchi, and J.A.F. Ramires. Morphology of the internal elastic lamina in arteries from pulmonary hypertensive patients: a confocal laser microscopy study. Mod. Pathol. 16(5): 411-416, 2003.

2. Ainslie K.M., J.S. Garanich, R.O. Dull, and J.M. Tarbell. Vascular smooth muscle cell glycocalyx influences shear stress-mediated contractile response. J. Appl. Physiol. 98: 242-249, 2005.

3. Borg-Capra C., M. Fournet-Bourguignon, P. Janiak, N. Villeneuve, J. Bidouard, J. Vilaine, and P.M. Vanhoutte. Morphological heterogeneity with normal expression but

altered function of G proteins in porcine cultured regenerated coronary endothelial cells. Br. J. Pharmacol. 122: 999-1008, 1997.

4. Cancel L.M., A. Fitting, and J.M. Tarbell. In-vitro study of LDL transport under pressurized (convective) conditions. Am. J. Physiol. Heart Circ. Physiol. 293: H126-H132, 2007.
5. Castellot, Jr. J.E., M.J. Karnovsky, and B.M. Spiegelman. Potent stimulation of vascular endothelial cell growth by differentiated 3t3 adipocytes. Cell Biol. 77(10): 6007-6011, 1980.
6. Chang Y.S., J.A. Yaccino, S. Lakshminarayanan, J.A. Frangos, and J.M. Tarbell. Shear-induced increases in hydraulic conductivity in endothelial cells is mediated by a nitric oxide-dependent mechanism. Arterioscler. Thromb. Vasc. Biol. 20: 35-42, 2000.
7. Chiu J., L. Chen, P. Lee, C. Lee, L. Lo, S. Usami, and S. Chien. Shear stress inhibits adhesion molecule expression in vascular endothelial cells induced by coculture with smooth muscle cells. Blood 101: 2667-2674, 2003.
8. Civelek M., K. Ainslie, J.S. Garanich, and J.M. Tarbell. Smooth muscle cells contract in response to fluid flow via a Ca+-independent signaling mechanism. J. Appl. Physiol. 93: 1907-1917, 2002.
9. DeMaio L., J.M. Tarbell, R.C. Scaduto, T.W. Gardner, and D.A. Antonetti. A transmural pressure gradient induces mechanical and biological adaptive responses in endothelial cells. Am. J. Physiol. Heart Circ. Physiol. 286: 731-741, 2004.
10. De Wit C., M. Boettcher, and V.J. Schmidt. Signaling across myoendothelial gap junctions – fact or fiction? Cell Commun. Adhes. Sep 15(3):231-245, 2008.

11. Dull R.O., H. Jo, H. Sill, T.M. Hollis, and J.M. Tarbell. The effect of varying albumin concentration and hydrostatic pressure on hydraulic conductivity and albumin permeability of cultured endothelial monolayers. Microvasc Res 41(3): 390-407, 1991.
12. Duthu G.S. and J.R. Smith. In vitro proliferation and lifespan of bovine aorta endothelial cells: effect of culture conditions and fibroblast growth factor. J. Cell Physiol. 103(3): 385-392, 1980.
13. Fillinger M.F., L.N. Sampson, J.L. Cronenwett, R.J. Powell, and R.J. Wagner. Coculture of endothelial cells and smooth muscle cells in bilayer and conditioned media models. J. Surg. Res. 67: 169-178, 1997.
14. Gartner L.P., and J.L. Hiatt. "Circulatory System." In: Color Textbook of Histology, edited by Philadelphia: Saunders Co., 2001, pp. 251-256.
15. Heberlein K., A. Straub, and B.E. Isakson. The myoendothelial junction: breaking through the matrix? Microcirculation 16(4): 307-322, 2009.
16. Heydarkhan-Hagvall S., G. Helenius, B.R. Johansson, J.Y. Li, E. Mattsson, and B. Risberg. Co-culture of endothelial cells and smooth muscle cells affects gene expression of angiogenic factors. J. Cell Biochem. 89: 1250-1259, 2003.
17. Hillsley M.V., and J.M. Tarbell. Oscillatory shear alters endothelial hydraulic conductivity and nitric oxide levels. Biochem. Biophys. Res. Commun. 293: 1466-1471, 2002.
18. Kurzen H., S. Manns, G. Dandekar, T. Schmidt, S. Pratzel, and B.M. Kräling. Tightening of endothelial cell contacts: a physiologic response to cocultures with smooth muscle-like 10 T1/2 cells. J. Invest. Dermatol. 119: 143-153, 2002.

19. Lavender M.D., Z. Pang, C.S. Wallace, L.E. Niklason, and G.A. Truskey. A system for direct co-culture of endothelium on smooth muscle cells. Biomaterials 26: 4642-4653, 2005.

20. Li G., Simon M.J., Cancel L.M., Shi Z.D., Ji X., Tarbell J.M., Morrison B. 3rd, and Fu B.M. Permeability of endothelial and astrocyte cocultures: in vitro blood brain barrier models for drug delivery studies. Ann. Biomed. Eng. 38(8): 2499-2511, 2010.

21. Pang Z., Niklason L.E., and Truskey G.A. Porcine endothelial cells cocultured with smooth muscle cells became procoagulant in vitro. Tissue Eng. Part A. 16(6): 1835-1844, 2010.

22. Patel N.A., C.E. Chalfant, M. Yamamoto, J.E. Watson, D.C. Eichler, and D.R. Cooper. Acute hyperglycemia regulates transcription and posttranscriptional stability of PKCbetaII mRNA in vascular smooth muscle cells. FASEB J. 13: 103–113, 1999.

23. Rose S.L., and J.E. Babensee. Complimentary endothelial cell/smooth muscle cell co-culture systems with alternate smooth muscle cell phenotypes. Ann. Biomed. Eng. 35: 1382-1390, 2007.

24. Ryan U.S., J.W. Ryan, and C. Whitaker. How do kinins affect vascular tone? Adv. Exp. Med. Biol. 120A:375-391, 1979.

25. Stary H.C., B. Chandler, R.E. Dinsmore, V. Fuster, S. Glagov, W. Insull Jr., M.E. Rosenfeld, C.J. Schwartz, W.D. Wagner, and R.W. Wissler. A definition of advanced types of atherosclerotic lesions and a histological classification of atherosclerosis: a report from the committee on vascular lesions of the council on atherosclerosis, American Heart Association. Circulation 92: 1355-1374, 1995.

26. Tada S., and J.M. Tarbell. Interstitial flow through the internal elastic lamina affects shear stress on arterial smooth muscle cells. Am. J. Physiol. Heart Circ. Physiol. 278: 1589-1597, 2000.
27. Tarbell J.M. Shear stress and the endothelial transport barrier. Cardiovasc. Res. 87: 320-330, 2010.
28. Tarbell J.M., L. DeMaio, and M.M. Zaw. Effect of pressure on hydraulic conductivity of endothelial monolayers: role of endothelial cleft shear stress. J. Appl. Physiol. 87: 261-268, 1999.
29. Ziegler T., R.W. Alexander, and R.M. Nerem. An endothelial cell-smooth muscle cell co-culture model for use in the investigation of flow effects in vascular biology. Ann. Biomed. Eng. 23:216-225, 1995.

Chapter 4

1. Barker S.G., A. Talbert, S. Cottam, P.A. Baskerville, and J.F. Martin. Arterial intimal hyperplasia after occlusion of the adventitial vasa vasorum in the pig. *Arterioscler. Thromb. and Vasc. Biol.* 13:70-77, 1993.
2. Chang Y.S., J.A. Yaccino, S. Lakshminarayanan, J.A. Frangos, and J.M. Tarbell. Shear-induced increases in hydraulic conductivity in endothelial cells is mediated by a nitric oxide-dependent mechanism. *Arterioscler. Thromb. Vasc. Biol.* 20: 35-42, 2000.
3. Davies P.F., G.A. Truskey, H.B. Warren, S.E. O'Connor, and B.H. Eisenhaure. Metabolic cooperation between vascular endothelial cells and smooth muscle cells in coculture: changes in low density lipoprotein metabolism. *J. Cell Biol.* 101: 871-879, 1985.

4. DeMaio L., J.M. Tarbell, R.C. Scaduto, T.W. Gardner, and D.A. Antonetti. A transmural pressure gradient induces mechanical and biological adaptive responses in endothelial cells. *Am. J. Physiol. Heart Circ. Physiol.* 286: 731-741, 2004.
5. Dull R.O., H. Jo, H. Sill, T.M. Hollis, and J.M. Tarbell. The effect of varying albumin concentration and hydrostatic pressure on hydraulic conductivity and albumin permeability of cultured endothelial monolayers. *Microvasc. Res.* 41(3): 390-407, 1991.
6. Dull R.O., I. Mecham, and S. McJames. Heparan sulfates mediate pressure-induced increase in lung endothelial hydraulic conductivity via nitric oxide/reactive oxygen species. *Am. J. Physiol. Lung Cell Mol. Physiol.* 292: L1452-L1458, 2007.
7. Dull R.O., M. Cluff, J. Kingston, D. Hill, H. Chen, S. Hoehne, D.T. Malleske, and R. Kaur. Lung heparan sulfates modulate K_{fc} during increased vascular pressure: evidence for glycocalyx-mediated mechanotransduction. *Am. J. Physiol. Lung Cell Mol. Physiol.* 302:(9) L816-L828, 2012.
8. Fillinger M.F., L.N. Sampson, J.L. Cronenwett, R.J. Powell, and R.J. Wagner. Coculture of endothelial cells and smooth muscle cells in bilayer and conditioned media models. *J. Surg. Res.* 67: 169-178, 1997.
9. Gössl M., P.E. Beighley, N.M. Malyar, and E.L. Ritman. Role of vasa vasorum in transendothelial solute transport in the coronary vessel wall: a study with cryostatic micro-CT. *Am. J. Physiol. Heart Circ. Physiol.* 287:H2346-H2351, 2004.
10. Heistad D.D., M.L. Marcus, G.E. Larsen, and M.L. Armstrong. Role of vasa vasorum in nourishment of the aortic wall. *Am. J. Physiol. Heart Circ. Physiol.* 240:H781-787, 1981.

11. Hillsley M.V., and J.M. Tarbell. Oscillatory shear alters endothelial hydraulic conductivity and nitric oxide levels. *Biochem. Biophys. Res. Commun.* 293: 1466-1471, 2002.

12. Jo H., R.O. Dull, T.M. Hollis, and J.M. Tarbell. Endothelial albumin permeability is shear dependent, time dependent, and reversible. *Am. J. Physiol.* 260: H1992-H1996, 1991.

13. Kim M-H., N.R. Harris, and J.M. Tarbell. Regulation of hydraulic conductivity in response to sustained changes in pressure. *Am. J. Physiol. Heart Circ. Physiol.* 289: H2551-2558, 2005.

14. Lindbergh C.A. An apparatus for the culture of whole organs. *J. Exp. Med.* 62:409-431, 1935.

15. Russell S., L.M. Cancel, J.M. Tarbell, and D.S. Rumschitzki. A protein diffusion model of the sealing effect. *Chem. Engr. Sci.* 64: 4504-4514, 2009.

16. McIntire L., J. Wagner, and P. Whitson. Effect of flow on macromolecular transport across bovine brain endothelial cell monolayers. *ASME/BED Bioeng. Conf.* 29: 79-80, 1995.

17. Tada S., and J.M. Tarbell. Fenestral pore size in the internal elastic lamina affects transmural flow distribution in the artery wall. *Ann. Biomed. Engr.* 29:456-466, 2001.

18. Tada S., and J.M. Tarbell. Internal elastic lamina affects the distribution of macromolecules in the arterial wall: a computational study. *Am. J. Physiol. Heart Circ. Physiol.* 287:H905-H913, 2004.

19. Tarbell J.M. Shear stress and the endothelial transport barrier. *Cardiovasc. Res.* 87: 320-330, 2010.

20. Tarbell J.M., L. DeMaio, and M.M. Zaw. Effect of pressure on hydraulic conductivity of endothelial monolayers: role of endothelial cleft shear stress. *J. Appl. Physiol.* 87: 261-268, 1999.

21. Tarbell J.M., M.J. Lever, and C.G. Caro. The effect of varying albumin concentration of the hydraulic conductivity of the rabbit common carotid artery. *Microvasc. Res.* 35: 204-220, 1988.

22. Vouyouka A.G., Y. Jiang, and M.D. Basson. Pressure alters endothelial effects upon vascular smooth muscle cells by decreasing smooth muscle cell proliferation and increasing smooth muscle cell apoptosis. *Surg.* 136: 282-290, 2004.

23. Vouyouka A.G., S.S. Salib, S. Cala, J.D. Marsh, and M.D. Basson. Chronic high pressure potentiates the antiproliferative effect and abolishes contractile phenotype changes caused by endothelial cells in cocultured smooth muscle cells. *J. Surg. Res.* 110: 344-351, 2003.

24. Warboys C.M., R.E. Berson, G.E. Mann, J.D. Pearson, and P.D. Weinberg. Acute and chronic exposure to shear stress have opposite effects on endothelial permeability to macromolecules. *Am. J. Physiol. Heart Circ. Physiol.* 298: H1850-H1856, 2010.

25. Werber A.H., and D.D. Heistad. Diffusional support in arteries. *Am. J. Physiol. Heart Circ. Physiol.* 248:H901-H906, 1985.